DIAGENESIS OF THE BELL CANYON AND CHERRY CANYON FORMATIONS (GUADALUPIAN), COYANOSA FIELD AREA, PECOS COUNTY, TEXAS

by

Katherine Ann Kanschat

A Thesis Submitted to the Faculty of the

DEPARTMENT OF GEOSCIENCES

In Partial Fulfillment of the Requirements
For the Degree of

MASTER OF SCIENCE

In the Graduate College

THE UNIVERSITY OF ARIZONA

1 9 8 1

STATEMENT BY AUTHOR

This thesis has been submitted in partial fulfillment of requirements for an advanced degree at The University of Arizona and is deposited in the University Library to be made available to borrowers under rules of the Library.

Brief quotations from this thesis are allowable without special permission, provided that accurate acknowledgement of source is made. Requests for permission for extended quotation from or reproduction of this manuscript in whole or in part may be granted by the head of the major department or the Dean of the Graduate College when in his judgment the proposed use of the material is in the interests of scholarship. In all other instances, however, permission must be obtained from the author.

SIGNED: Katherine A. Kanschat

APPROVAL BY THESIS DIRECTOR

This thesis has been approved on the date shown below:

J. F. Schreiber, Jr. 12/8/81

J.F. Schreiber, Jr.
Professor of Geosciences

Date

ACKNOWLEDGEMENTS

I would like to thank the Mobil Oil Corporation for allowing me the opportunity to work on this project, an idea originally incepted by C. K. Petter and supervised by E. H. McGlasson of Mobil Producing Texas and New Mexico in Houston. In addition I would like to express my appreciation for the financial support and use of facilities extended to me by Mobil during the course of the thesis.

Dr. J. F. Schreiber, Jr., Dr. W. R. Dickinson and E. H. McGlasson critically read the manuscript and offered helpful suggestions for its improvement. In particular, special thanks are extended to Dr. J. F. Schreiber, Jr. for the numerous discussions and constant encouragement provided, and the patience displayed as the project progressed.

I am grateful for the discussions with D. W. Kirkland, S. A. Dixon and T. McKee at Mobil's Field Research Laboratory in Dallas, which provided insight into various aspects of sedimentation and sandstone diagenesis. In addition, numerous individuals in the production and exploration departments of Mobil Producing Texas and New Mexico provided me with necessary background information on the Coyanosa field.

Technical assistance was offered by a number of individuals. In particular I would like to acknowledge W. Bilodeau who assisted me with many long hours of x-ray diffraction analyses at the University of Arizona and J. J. Porter, who helped with SEM-EDEX analyses at Mobil's Field Research Laboratory in Dallas. D. Sage, with Mobil in Midland, obtained core material displayed in this report.

The assistance and encouragement provided by L. E. Archibald and D. B. Silver is greatly appreciated. Finally, I thank Jack for his constant understanding and patience.

TABLE OF CONTENTS

		Page
	LIST OF ILLUSTRATIONS	viii
	LIST OF TABLES	xii
	ABSTRACT	xiii
1.	INTRODUCTION	1
	Purpose and Scope of Study	1
	Area Under Investigation	3
	Previous Investigations	8
	Regional Setting	16
	Stratigraphy of the Guadalupian Series	18
	Tectonic Interpretation	24
2.	A REVIEW OF THE COYANOSA FIELD	27
3.	LITHOLOGY OF THE BELL CANYON AND CHERRY CANYON FORMATIONS	36
	General Statement	36
	Stratigraphic Relationships within the Bell Canyon Formation	37
	Stratigraphic Relationships within the Cherry Canyon Formation	40
	Siltstones of the Bell Canyon and Cherry Canyon Formations	41
	Texture	41
	Composition	47
	Sedimentary Structures	50
	Sandstones of the Bell Canyon and Cherry Canyon Formations	53
	Texture	54
	Composition	57
	Sedimentary Structures	59
4.	DEPOSITIONAL MECHANISMS	63
	Previous Investigations	63
	Depositional Model Supported in this Study	64
	Supporting Evidence for Depositional Model	66
	Textural Relationships	66
	Sedimentary Structures	67

5. PETROGRAPHY OF THE BELL CANYON AND CHERRY CANYON FORMATIONS 68

General Statement 68
Methods Employed 69
Allogenic Components 72
Quartz 72
Feldspar 75
Rock Fragments 77
Other Detrital Components 78
Classification 81
Provenance Implications 85
Diagenetic Fabrics 89
Quartz and Feldspar Overgrowths 89
Cements 95
Calcium Carbonate 95
Dolomite 97
Anhydrite 98
Halite 99
Authigenic Clays 99
Chlorite 100
Illite 107
Discussion 113
Pyrite 117
Other Diagenetic Features 117

6. DIAGENESIS OF THE BELL CANYON AND CHERRY CANYON FORMATIONS 120

Diagenetic Sequence of Fabric and Feature Development 120
Regional Trends in Clay Diagenesis 125
General Statement 125
Elemental Trends in Chlorite Composition 125
Trends in Clay Type 127
Lithologic Affinities 135
Diagenetic Fabric Associations 135
Concluding Remarks 136

7. IMPACT OF DIAGENESIS ON RESERVOIR PROPERTIES . . 138

Introduction 138
Porosity 139
Permeability 144
Recognition of Authigenic Clay Growth on Subsurface Logs 152
Clay Treatment Programs 153

Clay Treatment Presently Employed in the Coyanosa Field Area 157

8. CONCLUSIONS 158

APPENDIX I: DETAILED CORE AND CORE CHIP SECTIONS WITH ACCOMPANYING X-RAY DIFFRACTION TRACES AND DIAGENETIC FEATURES . . . 162

REFERENCES 189

LIST OF ILLUSTRATIONS

Figure		Page
1.	Location Map	4
2.	Location of Core Material Used in the Study	5
3.	Major Tectonic Features of the Permian Basin	17
4.	Stratigraphic Relationships of Middle to Upper Permian Units in the Delaware Basin	19
5.	Initial Production and Distribution of Guadalupian Reservoirs in the Coyanosa Field Area	29
6.	Structure Map of the Top of the Brushy Canyon Formation	31
7.	Structure Map of the Top of the Cherry Canyon Formation	32
8.	Isopach Map of the Cherry Canyon Formation	33
9.	Isopach Map of the Bell Canyon Formation	34
10.	Stratigraphic Relationships within the Upper Bell Canyon and Upper Cherry Canyon Formations as Represented on Sonic-Gamma-Ray Subsurface Logs (Mobil, Sibley #B-1)	38
11.	Thin Section Photomicrographs of Textural Relationships within Bell Canyon and Cherry Canyon Siltstones	42
12.	Photographs of Sedimentary Structures Observed in Bell Canyon Siltstone Core Sections	51
13.	Thin Section Photomicrographs of Textural Relationships within Bell Canyon and Cherry Canyon Sandstones	55

14. SEM Photomicrographs of Textural Relationships within Bell Canyon Sandstones 56

15. Photographs of Sedimentary Structures Observed in Bell Canyon and Cherry Canyon Sandstone Core Sections 60

16. Photographs of Convoluted Bedding and Cementation Patterns Observed in Bell Canyon and Cherry Canyon Sandstone Core Sections . . . 61

17. Depositional Model Proposed for Bell Canyon and Cherry Canyon Sandstones and Siltstones 65

18. SEM Photomicrographs of Detrital Feldspar Alteration 76

19. Thin Section Photomicrographs of Detrital Carbonate Clasts 79

20. SEM Photomicrographs of Detrital Micas 80

21. Classification of Bell Canyon and Cherry Canyon Sandstones and Siltstones 82

22. Comparison of Average Upper Guadalupian Sandstone Compositions 84

23. Tectonic Provenance Plots (Q-F-L, Qm-F-Lt) of Bell Canyon and Cherry Canyon Sandstone Samples 87

24. Tectonic Provenance Plots (Qp-Lv-Ls, Qm-P-K) of Bell Canyon and Cherry Canyon Sandstone Samples 88

25. Thin Section Photomicrographs of Quartz Overgrowths and Carbonate Cements 90

26 SEM Photomicrographs of Quartz and Feldspar Overgrowths and Calcite Cements 91

27. Thin Section Photomicrographs of Calcite, Dolomite and Anhydrite Cements, and Detrital Grain Embayment 92

28. SEM Photomicrographs of Calcite, Dolomite, Anhydrite and Halite Cements 93

29. SEM Photomicrographs of Authigenic Chlorite Varieties 101

30. SEM Photomicrographs of Authigenic Illite . . . 110

31. Clay Fraction Obtained from Bell Canyon Sandstone Displaying Authigenic Expandable Chlorite and Illite 114

32. Clay Fraction Obtained from Bell Canyon Sandstone Displaying Authigenic Slightly-Expandable Chlorite, Illite and Mixed-Layer Illite-Chlorite 115

33. Clay Fraction Obtained from Bell Canyon Shaly Siltstone 116

34. Relative Ordering of Diagenetic Fabric and Feature Development 121

35. SEM Photomicrographs of Detrital Grain and Diagenetic Fabric Relationships 122

36. Characteristics of Diagenetic Clay Zones Identified in the Coyanosa Field Area . . . 128

37. Clay Fractions Obtained from Bell Canyon and Cherry Canyon Sandstones Displaying Extremes in Structural Ordering of Authigenic Clays 129

38. Comparison of Depth-Related Diagenetic Clay Zonation as Recognized by Various Authors 132

39. Relationship Between Diagenetic Clay Development and Tectonic Events Associated with the Bell Canyon and Cherry Canyon Formations within the Coyanosa Field Area 134

40. Relationship Between Porosity and Degree of Cementation in Selected Bell Canyon and Cherry Canyon Sandstone Samples 141

41. Decrease in Porosity as a Result of Depth-Related Compaction 143

42. Relationship Between Porosity and Permeability for the Wells Examined in the Coyanosa Field Area 145

43. Plot of Average Laboratory-Derived Permeabilities versus Clay Zone Occurrences for Wells Examined in the Coyanosa Field Area 147

44. Relationship Between Permeability and Water Saturation for Selected Wells Used in the Present Study 148

45. Plot of Average Laboratory-Derived Water Saturations versus Clay Zone Occurrences for Wells Examined in the Coyanosa Field Area 150

46. SEM Photomicrographs of Authigenic Clay Distribution within Bell Canyon Sandstones 155

LIST OF TABLES

Table		Page
1.	Core Material Incorporated in the Present Coyanosa Field Study	6
2.	Summary of Delaware Mountain Group Investigations	9
3.	Textural Parameters of Selected Bell Canyon and Cherry Canyon Samples Determined from Thin Section Analysis.	44
4.	Mineralogical Composition of Selected Bell Canyon and Cherry Canyon Samples from Thin Section Point Counting Analysis	71
5.	Heavy Mineral Analysis of Selected Bell Canyon and Cherry Canyon Samples	73
6.	Semi-Quantitative Determination of Clay Composition from X-Ray Diffraction Analysis of Selected Bell Canyon and Cherry Canyon Samples	102
7.	Determination of Relative Iron and Magnesium Content of Chlorites from Selected Bell Canyon and Cherry Canyon Samples by Semi-Quantitative X-Ray Diffraction Analysis	105
8.	Determination of Relative Iron and Magnesium Content of Illites from Selected Bell Canyon and Cherry Canyon Samples by Semi-Quantitative X-Ray Diffraction Analysis	111

ABSTRACT

The Bell Canyon and Cherry Canyon Formations of the Delaware Mountain Group represent deep-water channel sandstones and mantling siltstones which had been deposited during the Middle Permian (Guadalupian) within the confines of the Delaware basin. Stratified saline fluid density currents, swept in from surrounding evaporitic shelf areas, provided the mechanism of transport for the sandstones and siltstones.

Examination of textural relationships within the two formations, as they are observed in the Coyanosa field, Pecos County, West Texas, reveals well-sorted, rounded, tractively-transported, very fine-grained sandstones and very thinly-laminated, frequently bioturbated, coarse-grained siltstones.

A diagenetic sequence characterized by relatively early authigenic clay growth on detrital grain surfaces, preceeding and concurrent with quartz and feldspar overgrowthing and carbonate (calcite and dolomite) precipitation, and followed by anhydrite formation is identified in the two units. Three depth-related diagenetic clay zones

have been distinguished on the basis of clay composition and morphology, both properties appearing to be interrelated. Relative amounts of chlorite, randomly mixed-layer expandable chlorite and illite-chlorite decrease with increasing overburden. Conversely, increased relative amounts of illite and improved structural ordering within chlorite and illite clay species is noted under similar circumstances.

Sandstone porosity, being well-developed and fairly consistent within the sandstone units, is primarily dependent on the extent of pore space occlusion by secondary cements. Permeability varies widely, being controlled by the degree of authigenic clay development on detrital grain surfaces. Superposition of favorable reservoir trends with structural highs provides optimum exploration targets within the Coyanosa field. Maximum well productivity is attained by the utilization of clay-conscious stimulation programs.

CHAPTER 1

INTRODUCTION

Purpose and Scope of Study

The Delaware Mountain Group, a Guadalupian age (Permian) sequence of deep-water clastics confined to the Delaware basin, West Texas, has been studied by various authors with particular emphasis on the development of regional stratigraphic and sedimentation models explaining fine-grained sandstone and siltstone depositional processes. A few authors have examined the petrography of the group, but these studies have been restricted primarily to the Bell Canyon Formation (uppermost Delaware Mountain Group) or its contained members. With the exception of Williamson (1978) and Watson (1974) petrographic endeavors have been very general and limited to outcrop samples, neglecting diagenesis and its subsequent impact on reservoir productivity. It is the purpose of this study to examine, in detail, the petrography of the Bell Canyon and Cherry Canyon Formations. The Coyanosa field was chosen because of the ready availability of subsurface data, known Delaware Mountain Group production and renewed interest in reservoir development. Attention has been concentrated on diagenesis,

particularly with respect to authigenic clay formation and the concurrent enhancement or destruction of porosity and permeability, through the utilization of the petrographic microscope, scanning electron microscope and x-ray diffraction techniques.

Specific objectives of this study include: (1) extension of regional diagenetic trends within the Bell Canyon Formation from the Coyanosa field in the southeast corner of the Delaware basin toward the north-northwest, complementing the work of Williamson (1978) and Watson (1974); inhomogeneities in the character of the Bell Canyon Formation should be detected if they exist; (2) detailed petrographic analysis of the Cherry Canyon Formation, which, to the best of the author's knowledge has not been previously attempted; (3) determination of authigenic clay zonation (both vertical and lateral) within the two formations; diagenetic clay growth constitutes the most important feature influencing reservoir productivity, particularly when considered in conjunction with well-treatment programs employed during production; incongruent clay identification results by Williamson (1978) and Watson (1974) suggest either inhomogeneities within the Bell Canyon Formation or misinterpretation of data; and (4) development of formation treatment techniques in view of the diagenetic changes that have occurred within the formations.

It should be noted that subsurface analysis of the Brushy Canyon Formation was not feasible because of the lack of available data. Also, detailed modeling of depositional systems for the Bell Canyon and Cherry Canyon Formations was not attempted due to its thorough coverage in the literature and the restricted scope of this study.

Area Under Investigation

The area of study is located in northwest Pecos County, Texas, bounded on the north and south by 31°15'30" and 31°07'30" north latitude parallels, respectively, and on the east and west by 103°00' and 103°12' west longitude meridians, respectively (Figure 1). This rectangular area occupies a position in the southeast corner of the Delaware basin where the basin begins to slope up toward the Central Basin platform. The majority of the slabbed core and core chip material was obtained from within the limits of the Coyanosa field (including North, South and West Coyanosa fields) (Figure 2). A few wells peripheral to the Coyanosa field were also examined in an attempt to establish diagenetic trends and to determine if any correlation between these trends and field productivity exists. A total of five slabbed cores, ten sets of core chips and approximately 100 gamma-ray-neutron logs were incorporated in this study (Table 1).

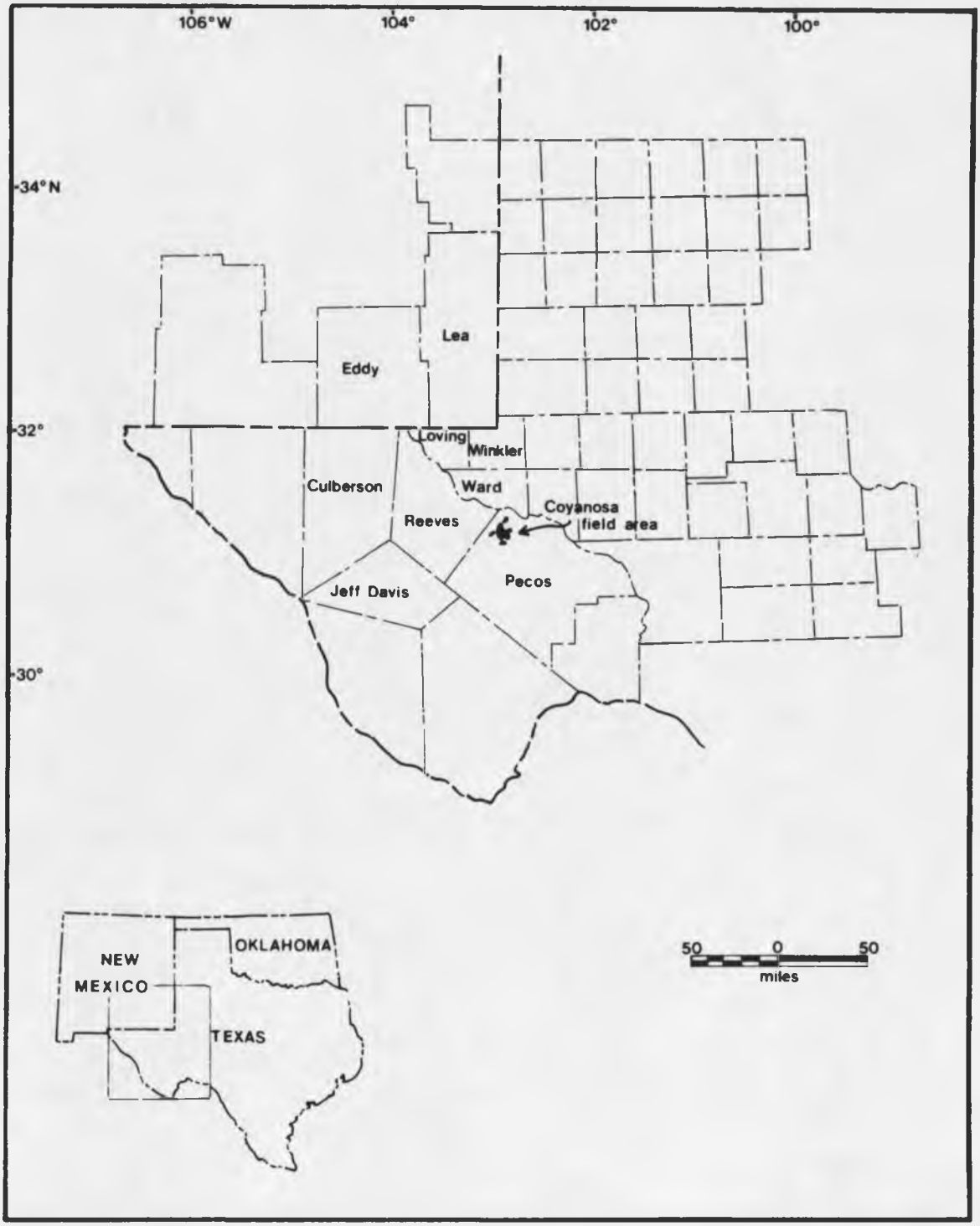

Figure 1. Location Map

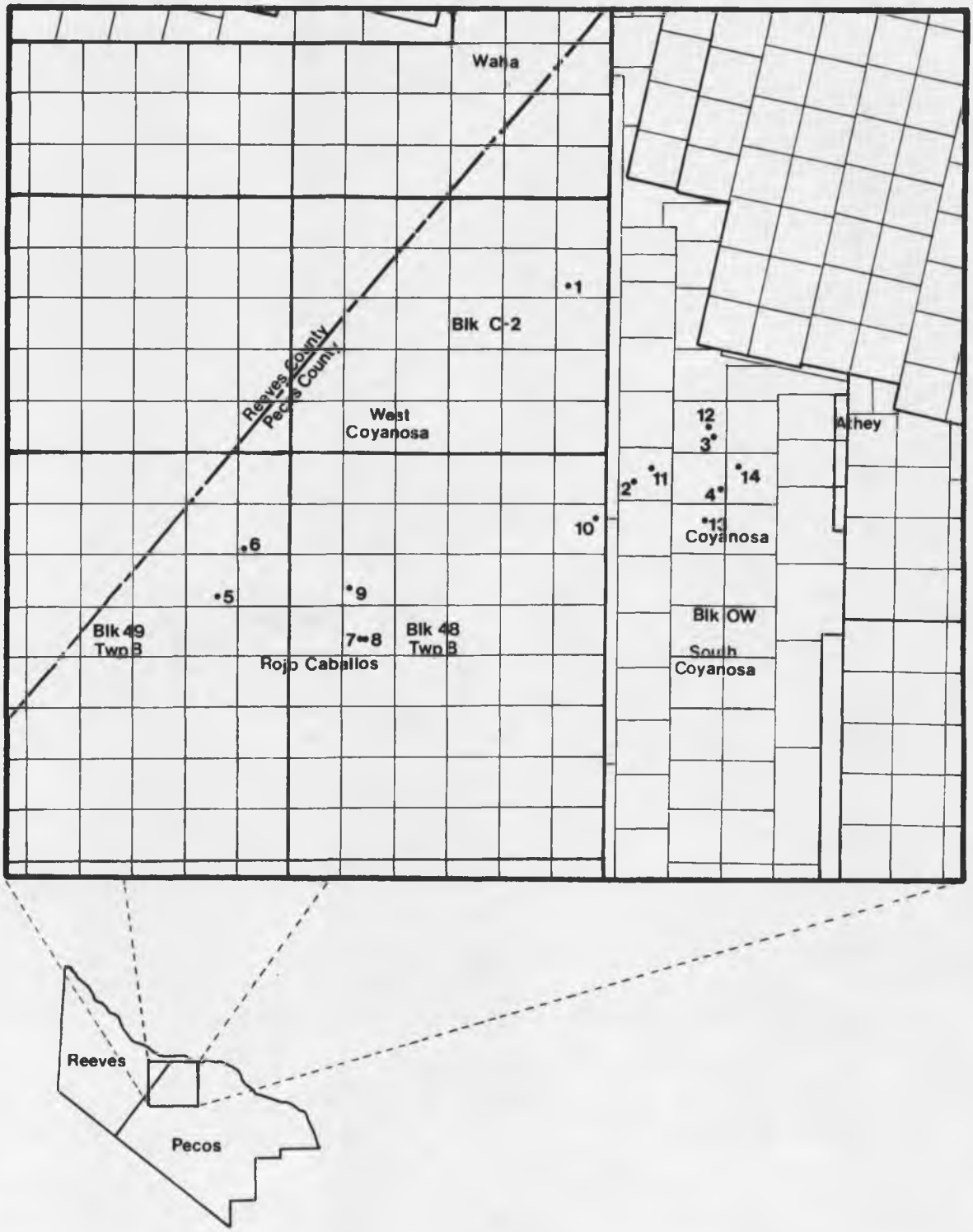

Figure 2. Location of Core Material Used in the Study. See Table 1 on the following page for well names and locations.

Table 1. Core Material Incorporated in the Present Coyanosa Field Study

Slabbed Cores

Mobil

1. Wayne Moore #10
   Section 57, Block C-2
   PSL Survey
   1320' FSL, 1320' FWL

2. Charles B. Athey #C-3
   Section 44, Block OW
   TT RR Survey
   3300' FSL, 1980' FEL

3. Charles B. Athey #4
   Section 52, Block OW
   TT RR Survey
   1980' FSL, 1980' FEL

4. Coyanosa Plant "A" SWDW #1
   Section 48, Block OW
   TT RR Survey
   2090' FSL, 721' FEL

Core Chips

Cactus Drilling

5. McCarty #1
   Section 14, Block 40-T8
   T&P RR Survey
   660' FSL, 1980' FEL

Pennzoil and Brown

6. Whissell #1
   Section 12, Block 49-T8
   T&P RR Survey
   660' FSL, 660' FWL

Mobil

7. Ivy B. Weatherby #1
   Section 20, Block 48-T8
   T&P RR Survey
   1650' FSL, 1650' FWL

Table 1. -- Continued

Mobil

8. Ivy B. Weatherby #4
Section 20, Block 48-T8
T&P RR Survey
660' FNL, 660' FWL

9. Schumaker #1
Section 17, Block 48-T8
T&P RR Survey
1980' FSL, 660' FWL

10. State Ivey #1
Section 12, Block 48-T8
T&P RR Survey
1320' FNL, 1320' FWL

11. Athey Unit #1
Section 44, Block OW
TT RR Survey
1980' FNL, 1980' FEL

12. Charles B. Athey #1
Section 52, Block OW
TT RR Survey
2130' FNL, 1980' FEL

13. Sibley #1-B
Section 45, Block OW
TTRR Survey
1980' FNL, 1980' FEL

14. J.O. Neal #2
Section 47, Block OW
TT RR Survey
1320' FNL, 1320' FWL

Prior to examination of subsurface information, a field investigation of the Delaware Mountain Group, as it appears in outcrop in the Guadalupe Mountains, Culberson County, Texas and Eddy County, New Mexico, was conducted in order to obtain an appreciation for the depositional environment associated with the units.

Previous Investigations

The Guadalupian Delaware Mountain Group has been the subject of numerous investigations, particularly with regard to mechanisms of deposition for the contained Bell Canyon, Cherry Canyon and Brushy Canyon Formations. Initial studies of the Delaware Mountain Group concentrated on basic stratigraphic identification and correlation while later work involved the development of regional sedimentation models to explain depositional patterns observed in outcropping sections. Subsequent studies considered the subsurface expression and extension of these depositional systems, often accompanied by detailed petrographic descriptions of the formations. Most recent work has examined these deep-water clastic units with regard to their associated reservoir properties. This can be attributed to the renewed interest in developing the hydrocarbon potential of these once economically marginal reservoir units. Table 2 summarizes these investigations.

Table 2. Summary of Delaware Mountain Group Investigations

Author(s)	Date	Contribution
G.G. Richardson	1904	Inception of the Captain and Delaware Mountain Formations in the Trans-Pecos area, Texas.
P.B. King	1934	Redefined the Delaware Mountain Formation and removed the Bone Spring Limestone as a member in the Guadalupe Mountian area.
P.B. King	1942	Raised the Delaware Mountain Formation to group status. Recognized three distinct formations - Bell Canyon, Cherry Canyon and Brushy Canyon based on lithologic and faunal changes. Within the Bell Canyon formation five distinct limestone members were designated and described (Guadalupe Mountains).
P.B. King	1948	Limestone members of the Bell Canyon exposed in the southern Guadalupe Mountains and Delaware Mountains were described in detail. General descriptions of the clastic units also were included. Basin-shelf margin-shelf transition recognized.
N.D. Newell and others	1953	Studied the depositional environment of the Permian reef complex. First to suggest deposition of basinal clastic units by turbidity currents. Wind transport suggested to explain fine texture and even distribution of non-channel sands.

Table 2. -- Continued

Author(s)	Date	Contribution
J.P.D. Hull, Jr.	1957	Performed grain size, textural and petrographic analyses on Bell Canyon, Cherry Canyon and Brushy Canyon Formations. Hypothesized that sequences of clastic limestone, laminated sandstone and massive sandstone were controlled by cyclic subsidence (changing sea level or constant sea level, tectonic subsidence) with resultant sand distribution in the basin by turbidity currents.
C.F. Dodge	1958	Suggested using the Ford Member, a continuous, mappable, laminated shaly sandstone and black shale horizon in the Delaware basin, as a means of detecting deep structural relief.
M.W. Nottingham	1960	Suggested turbidity currents as a depositional mechanism for the Bell Canyon Formation. Revised Haynie's classification of the Ramsey and Ford Members after examining subsurface data from the North Mason and El Mar fields.
P.T. Hayes	1964	Described in detail the stratigraphic relationships of the Guadalupian facies as they are exposed in the Guadalupe Mountains. Also invoked a turbidity current origin for the Delaware Mountain Group basinal clastics.
J.E. Adams	1965	Proposed a stratigraphic-tectonic model for the development of the Delaware basin. Believed turbidity currents accounted for deposition of Guadalupian basinal clastics.

Table 2. -- Continued

Author(s)	Date	Contribution
W.F. Grauten	1965	Suggested that the incongruent fluid relationships (gas, oil, water) observed within the upper Bell Canyon sandstone members are a result of differential entrapment of these fluids in sublenses within a continuous sandstone body.
S.C. Harrison	1966	Described depositional mechanics of the Cherry Canyon Formation. Advocated that the Cherry Canyon consists of deep-sea fan and fringe deposits which were introduced into the basin through submarine canyons, similar to the model proposed for sediment dispersal in modern continental-borderland basins off the California coast. A glacially-controlled eustatic model is invoked to explain basinal alternations of carbonate and clastic members.
L.C. St. Germaine	1966	Described depositional mechanics of the Brushy Canyon Formation. Depositional model proposed similar to that of Harrison (1966).
R.H. Beck	1967	Described depositional mechanics of the Cherry Canyon Formation. Depositional model proposed similar to that of Harrison (1966).
A.D. Jacka and others	1967	Clastic deposits of Guadalupian age identified as ancient deep-sea fans, consisting of channel, levee, overbank and fringe deposits. Invoked glacially-controlled eustatics to explain carbonate deposition and reef growth during periods

Table 2. -- Continued

Author(s)	Date	Contribution
		of high sea level; clastic transport and deposition during periods of low-standing sea level. Also suggested that saline density or suction currents were possibly main agents of sediment transport.
S.S. Oriel and others; E.D. McKee and S.S.Oriel	1967	Presented reviews of the Permian stratigraphic and tectonic elements, and generalized sedimentation patterns within the Permian basin.
R.P. McNeal and T.D. Mooney	1968	Examined oil composition and its relationship to lithologic and stratigraphic units within the Delaware Mountain Group and overlying Ochoan units.
B.A. Silver and R.G. Todd	1969	Favored a glacially-controlled eustatic origin for the sea level changes which resulted in the cyclicity of the basinal sediments (alternating thin carbonates and thick clastics). Transport of clastics into the basin accomplished by turbidity currents.
J.G. Elam	1972	Proposed that sea level changes, resulting in cyclicity of Guadalupian sediments, may also have tectonic controls as a result of differential vertical uplift and accompanying subsidence of the Delaware basin.

Table 2. -- Continued

Author(s)	Date	Contribution
J.M. Hills	1972	Discussed regional sedimentation patterns during the Late Paleozoic in the Permian basin.
F.F. Meissner	1972	Recognized cyclicity in Guadalupian age deposits which was attributed to glacially-controlled eustatics. This cyclic sedimentation was believed to be characteristic of all Middle Permian strata deposited on the cratonic shelf of west-central United States.
W.S. Motts	1972	Studied reef and back-reef equivalents of the Bell Canyon Formation and suggested that saline density currents were important factors in Bell Canyon deposition.
J.C. Harms	1974	Examined the Brushy Canyon Formation at the outcrop level finding evidence that dispelled a deep turbidity current explanation for deposition of the clastic units. Features identified within the Brushy Canyon Formation suggested deposition by saline and cold density currents with surrounding shelf areas providing the dense water masses.
W.G. Watson	1974	Examined the Ramsey Member of the Bell Canyon Formation in Geraldine Ford field with regard to petrography, palynology and sedimentation patterns. Attributed accumulations of Ramsey Sandstone to quick deposition by grain-flow deposits. The presence of interbedded organic laminae occurred as a result of slow deposition of siltstone units and annual planktonic production.

Table 2. -- Continued

Author(s)	Date	Contribution
M.W. Payne	1976	Recognized three lithologic units within the Bell Canyon Formation after examination of outcrop and subsurface data. These included (1) lutite composed of organic pelagic shale; (2) laminite composed of laminated coarse-grained siltstone with organic material concentrated in laminae; (3) arenite composed of fine-grained sands infilling linear submarine channels with deposition occurring primarily as a result of fluid density currents with turbidity currents subordinate.
C.R. Williamson	1978	Examined the Bell Canyon Formation in both outcrop and subsurface in the northern half of the Delaware basin. Channel erosion and sediment transport in the basin resulted from long-lived fluid density underflows which were subject to many irregular fluctuations. Detailed petrographic and diagenetic analysis, isotope studies of pore fluids and examination of reservoir parameters (porosity and permeability) performed in an attempt to understand constraints of reservoir productivity.
R.R. Berg	1979	Suggested turbidity origin for Bell Canyon and Brushy Canyon Formations after examination of subsurface data from the northern half of the Delaware basin. Channel sands appear to be restricted to earlier erosional submarine channels with no overbank deposits being formed. Channel sands were subsequently enclosed by laminated,

Table 2. -- Continued

Author(s)	Date	Contribution
		very fine-grained sandstone and siltstone that had been transported by wind and deposited from suspension to form widespread sheets.
R.G. Bozanich	1979	Examined the Bell Canyon and Cherry Canyon Formations in the eastern Delaware Basin and suggested that laminated siltstones and organic-rich shales were deposited from suspension. Channel sands were deposited by erosive, bottom-hugging, fluid density currents.
D.W. Cromwell	1979	Described the Cherry Canyon Formation in the Indian Draw Delaware field as being deposited from numerous major and minor successive turbidity flows which infilled existent deep-water submarine channels.
J.A. Faber	1980	Proposed that deposition of the Cherry Canyon Formation was accomplished by fluid density currents originating in the evaporitic back-reef shelf areas. Hydrocarbon traps are structurally controlled with size, shape and orientation of the reservoir determined by stratigraphic relationships within the Delaware basin.

Regional Setting

The Delaware basin, an asymmetrical block-faulted basin, is one of a number of north-northeast trending, sub-parallel, secondary tectonic features occurring within the Permian basin (Figure 3). It is contained in the southern extension of the Great Plains Physiological Province, being bisected by the Pecos River into the Pecos Valley section to the west-southwest and the High Plains section to the east-northeast. The Pecos Valley section is characterized by an eastward-sloping, maturely-dissected plain of low relief developed on differentially eroded formations of Late Permian age. The High Plains section is primarily a little-eroded expanse of unconsolidated and semi-consolidated Cenozoic deposits and local outcrops of Upper Permian and Triassic rock units.

The Guadalupe and Delaware Mountians, manifestations of Basin and Range activity, rim the basin on the west and northwest. The Apache and Davis Mountains, which represent ridges within the larger Diablo Platform, continue the border along the southwest. The southern end of the Delaware Basin is separated from the Val Verde basin by extension of the buried Capitan reef and Sheffield channel. The reef remains buried, closely paralleling the Central Basin platform, which confines the basin to the east. The

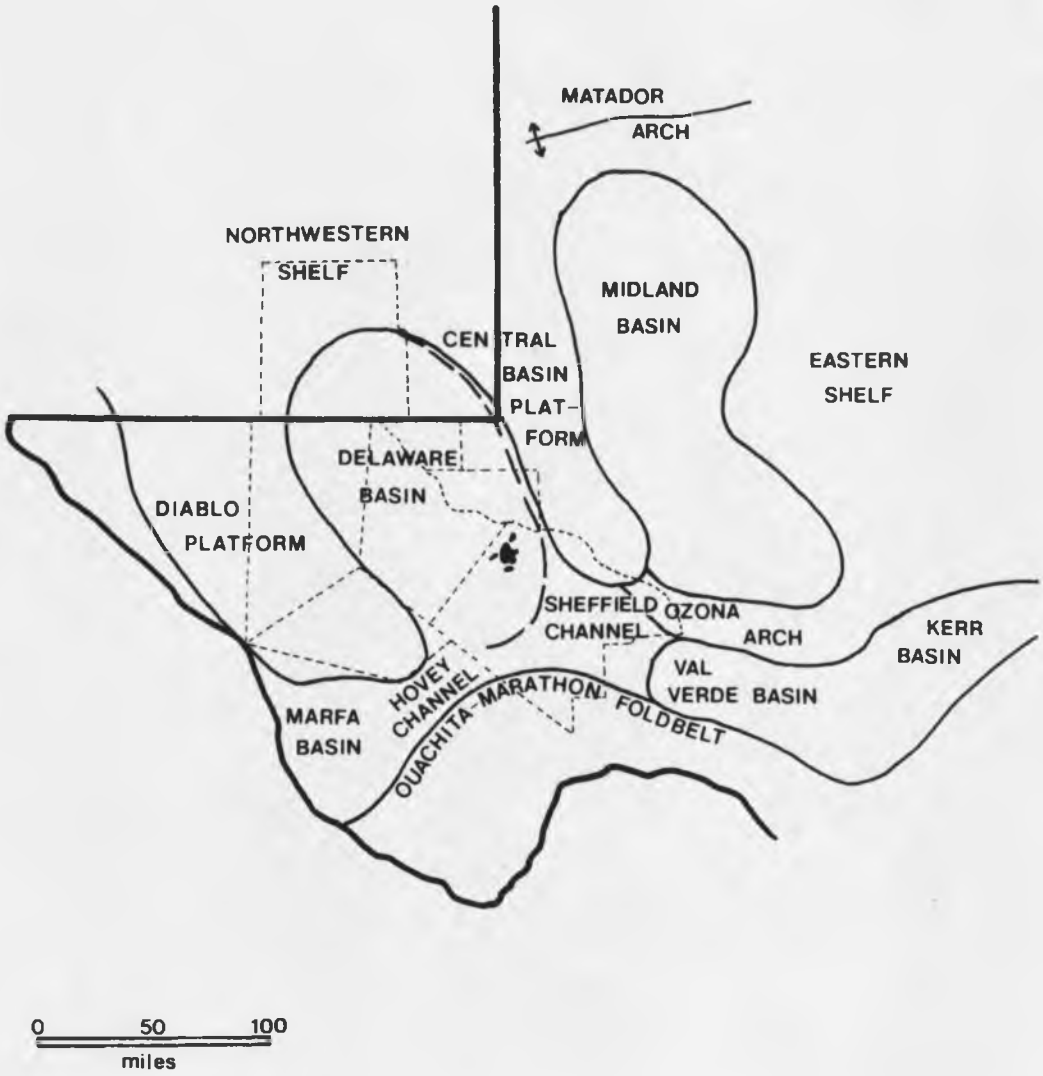

Figure 3. Major Tectonic Features of the Permian Basin

buried and exposed Capitan reef and the broad Northwestern shelf completes the enclosure of the Delaware basin to the north.

The basin is not a structurally complex feature. Aside from the numerous and locally occurring hydrocarbon-trapping anticlines that have been identified throughout the basin, high-angle reverse or steeply dipping normal fault zones border the western and eastern edges of the basin.

Stratigraphy of the Guadalupian Series

The complexity of stratigraphic relationships between units of the Guadalupian Series is reflected by marked lateral facies changes existent at that time (Figure 4). Depositional topography can be subdivided into three major time-transgressive settings - the basin, shelf-margin and shelf to express the facies' transition. Physical correlation is best between basin and shelf-margin facies, becoming less reliable between shelf-margin and shelf components.

Underlying the Guadalupian Series in all three settings is the Leonardian Bone Spring Limestone, which is comprised of thin-bedded, dark, bituminous limestone, dark mudstone, light gray sandstone and dark chert nodules and beds (King, 1948). Within the basin, the Bone Spring Lime-

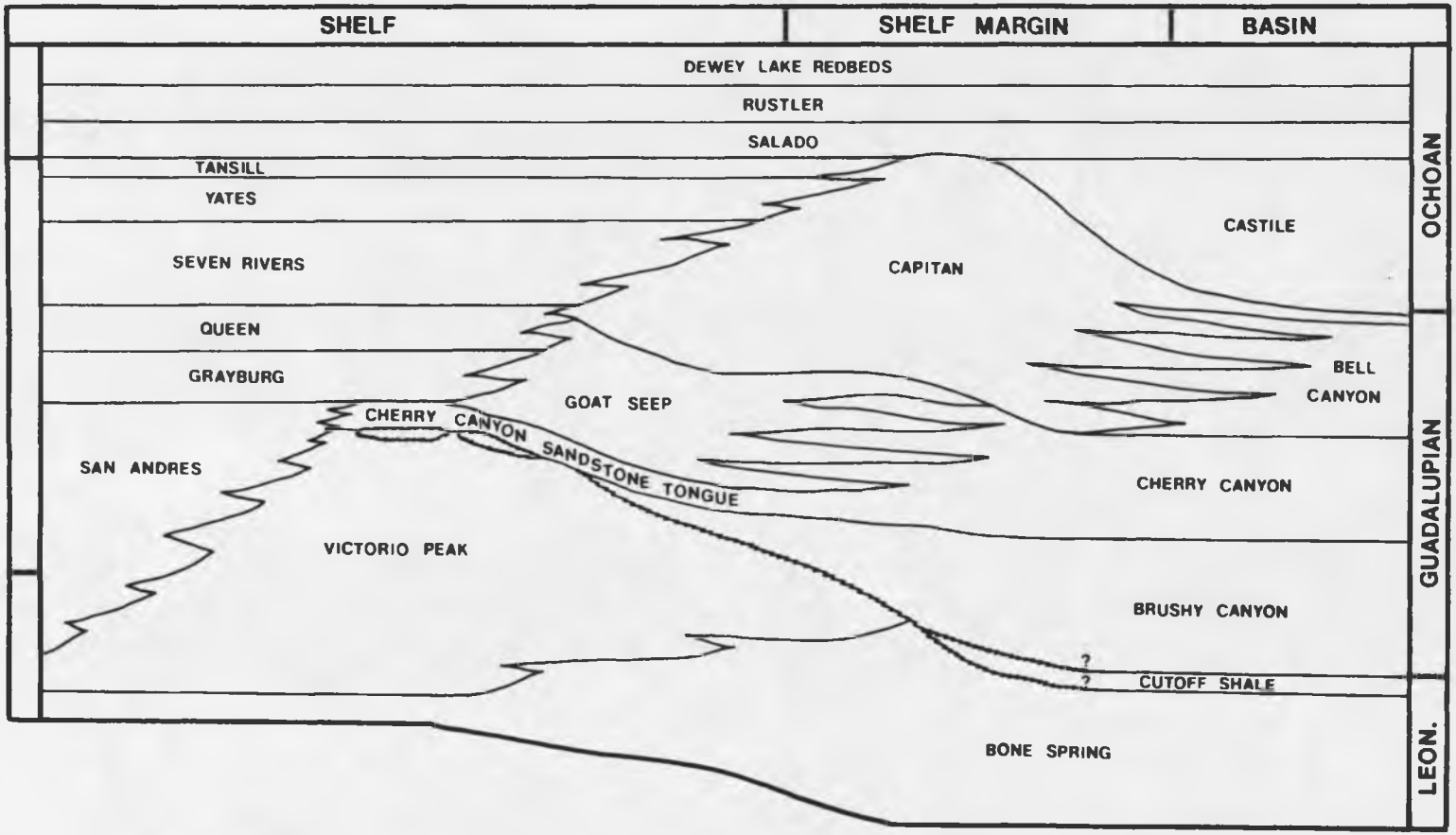

Figure 4. Stratigraphic Relationships of Middle to Upper Permian Units in the Delaware Basin (Adapted from King, 1948; Harms, 1974; Williamson, 1978)

stone is thickest and contains more terrigenous material than surrounding shelf and shelf-margin areas. At the Leonardian shelf-margin the upper part of the Bone Spring Limestone grades laterally into the Victoria Peak Limestone (King, 1965), a light-colored, thick-bedded, fossiliferous limestone with minor occurrences of chert and sandstone. Shelfward a transition into thin-bedded, sparsely fossiliferous dolomite takes place. This unit has been identified as the Yeso Formation and the lowest part of the San Andres Limestone by Boyd (1958) and Hayes (1964). Succeeding the Victorio Peak along the western basin margin is the Cutoff Shale, a thin-bedded, dark limestone, mudstone and thin-bedded, fine-grained sandstone (King, 1965). Oriel and others (1967) refer to this shale as the Pipeline Shale Member. It appears that this shale may transcend the Leonardian-Guadalupian boundary where it occurs in the shelf and the shelf-margin facies.

The Guadalupian Series, as it occurs in the Delaware basin, is represented by the Delaware Mountain Group, a predominantly deep-water clastic unit comprised of fine-grained, laminated and massive sandstones but also including dark mudstone, limestone, chert and occasionally bentonite beds. Thickness of this group exceeds 5500 feet in the basin center, thinning to 3000 to 4000 feet along the basin margin and less than 2000 feet on the adjacent Central Basin platform (Oriel and others, 1967). The

Delaware Mountain Group is subdivided into three formations (King, 1942), the oldest being the Brushy Canyon Formation which uncomformably overlies the Cutoff Shale along the basin margin. The Brushy Canyon is composed predominantly of finely-laminated siltstone and coarsely-laminated to massive sandstone with a massive boulder or cobble conglomerate occurring in basal sections. This conglomerate is comprised of clasts lithologically similar to the underlying Cutoff Shale (Harms, 1974). The Brushy Canyon Formation cannot be traced in outcrop to shelf equivalents, thus any correlation must be regarded with some degree of caution. Boyd (1958) correlated the Brushy Canyon with the middle part of the San Andres Limestone of the shelf region, which is predominantly dolomite with local occurrences of basal limestone and chert. Vertrees and others (1964) and Silver and Todd (1969) correlated the Brushy Canyon Formation with the lower or middle San Andres, while Meissner (1972) correlated it with uppermost San Andres and lower Artesia Group.

Conformably overlying the Brushy Canyon Formation within the Delaware basin is the Cherry Canyon Formation, also containing deep-water, fine-grained sandstones and siltstones with interbedded mudstones and carbonates. In the shelf-margin facies the lower Cherry Canyon Formation is represented by the thin Cherry Canyon sandstone tongue that unconformably overlies the Cutoff Shale. Shelfward

this tongue passes into patch reefs and detrital limestone banks of the upper San Andres Limestone. Middle and upper portions of the basinal Cherry Canyon Formation interfinger with the Goat Seep Limestone, a carbonate reef facies, in shelf-margin regions. Shelf equivalents include the Grayburg and Queen Formations of the Artesia Group, both being primarily dolomite with subordinate amounts of anhydrite and reddish fine-grained sandstone and siltstone (Hayes, 1964). The Artesia Group is believed to represent restricted lagoonal deposits (Newell and others, 1953; Boyd, 1958). Others have suggested a supratidal flat or sabkha origin for these deposits (Kerr and Thomson, 1963; Meissner, 1972).

The Bell Canyon Formation, the youngest formation within the Delaware Mountian Group basinal facies is almost lithologically identical to the Cherry Canyon Formation, consisting mainly of fine-grained sandstones and siltstones. It also contains five thin limestone marker beds, the most significant being the uppermost Lamar Limestone Member (King, 1942). Three clastic members (Ramsey, Ford and Olds Members) have also been defined by Nottingham (1960) to describe oil reservoirs in the basin subsurface. The Bell Canyon interfingers with the Capitan Limestone, a prominent reef facies of the shelf-margin region. Shelfward the Capitan grades into the Seven Rivers, Yates and Tansill Formations of the Artesia Group, representing dolomite, red

sandstone and siltstone, and dolomite, anhydrite and halite, respectively. These units become increasingly evaporitic toward the shelf interior (Meissner, 1972).

Evaporite deposition predominated during Ochoan time, resulting in extremely thick (approximately 5000 feet) accumulations of anhydrite, halite, dolomite, limestone, reddish siltstone and sandstone, and gypsum (Oriel and others, 1967). Formations representing the Upper Permian Ochoan Series include, in ascending order, the Castile, Salado and Rustler Formations, and Dewey Lake Redbeds. The Castile Formation, restricted to the Delaware basin, appears to grade reefward into laminated limestone and uppermost Capitan carbonate (Jones, 1954; Newell and others, 1953), although the two units are not time-equivalent. The Castile is unusual in that it is composed of seasonally varved anhydrite (Anderson and others, 1972) that seems to suggest extremely rapid deposition of the beds over a relatively short period of time. These seasonal accumulations may have been initiated concurrently with late Bell Canyon deposition of laminated siltstones and sandstones (Kirkland, 1980). The remaining formations do not recognize the previous basin, shelf-margin and shelf facies boundaries.

Tectonic Interpretation

The Delaware basin evolved out of the early Paleozoic Tobosa basin (Adams, 1965) as a result of compressive stresses generated in the Ouachita-Marathon foldbelt to the south during the Late Mississippian. Prior to this time, the Tobosa basin was a broad sag open to marine incursion from the south. Walper (1976) has proposed that the Tobosa basin (or as it is sometimes referred to, the Delaware aulacogen) formed as a consequence of rifting activities during the Late Precambrian or Early Paleozoic. Evidence consisting of basaltic dikes, sills and interbedded flows associated with sequences of clastic and carbonate rocks lends support to this hypothesis (see Walper, 1976 for detailed discussion).

As the continental margin subsided following rifting, transgression occurred toward the north-northwest, covering the Tobosa basin with shallow-water carbonates. Deeper-water deposition was confined to the continental margin, presently outlined by the Ouachita-Marathon foldbelt. Collision of an Afro-South American plate upon the North American continent during the Late Mississippian along this suture belt initiated foredeep basins in the south (Marfa, Val Verde and Kerr Basins). Thick clastic sequences subsequently accumulated in these basins.

The Delaware and Midland basins became separate and distinct features as compressive stresses, transmitted into the continental interior upon collision, reactivated boundary faults running longitudinally along the basins' margins. The Central Basin platform and Diablo platform represent large block-faulted uplifts which concurrently developed as a result of this stress system.

During the Late Pennsylvanian and Early Permian, the Delaware and Midland basins were characterized by rapid subsidence. However, sediment capture by the foredeep basins to the south and reef development surrounding the Delaware and Midland basins resulted in the development of starved basin conditions during the Late Pennsylvanian (Adams, 1965). Isostatic response to this subsidence was reflected in increased uplift in the adjacent Central Basin and Diablo platforms. Thrusting in the Marathon region reached a climax late in the Virgilian (King, 1977) overriding sediments deposited in the southern margins of the foredeep basins. This was followed by a later orogenic pulse along the thrust front in early Wolfcampian time. Erosion of this orogenic belt and associated uplifted foredeep basin deposits resulted in an increased supply of clastics to the cratonic Delaware basin during late Wolfcampian and early Leonardian epochs. Middle Permian (Guadalupian) time signaled the beginning of broad regional subsidence within the entire Permian basin with wide-

spread clastic and carbonate deposition occurring over both basin and platform areas. Cessation of tectonic activity permitted the progradation of carbonate banks and reefs outward from submarine fault scarps which in turn restricted marine circulation in the deepening Delaware basin. Fine-grained clastic sediments were carried into the basin by submarine channel systems, accumulating in thickness up to 5000 feet. These sediments, representing the Delaware Mountain Group, are believed to have originated from the Pedernal uplift and Ancestral Rockies located in New Mexico.

By Ochoan time increased marine restriction resulted in the deposition of thick evaporite sequences, which eventually marked the end of active basin sedimentation.

Stability prevailed during the Early to Middle Triassic with broad arching and erosion of the east, south and west perimeters of the Permian basin becoming dominant during the Late Triassic - Early Jurassic (Horak, 1973). Deposition of approximately 2000 feet of continental redbeds and shallow marine rocks consequently occurred within the Delaware basin. Quiescence again reigned from middle to late Cenozoic time, immediately after which Basin and Range faulting, vulcanism and collapse cut across the western Delaware basin.

CHAPTER 2

A REVIEW OF THE COYANOSA FIELD

The Coyanosa field is a large multipay oil and gas field located in the southeast corner of the Delaware basin in western Pecos County, Texas. The dimensions of the field are approximately 5 miles by 7 miles along a northwesterly trend, paralleling the axis of the encompassing Delaware basin, and Central Basin platform to the east.

The Coyanosa field, as it is referred to in this study, is actually an aggregation of three smaller contiguous fields - Coyanosa, West Coyanosa and South Coyanosa, the latter two representing later extensions to the main Coyanosa field.

The Coyanosa field produces from ten reservoirs representing the Ordovician, Devonian, Mississippian, Pennsylvanian and Permian Systems. Gas and gas condensate production occurs in all reservoirs while oil production is restricted primarily to Guadalupian age reservoirs (Bell Canyon and Cherry Canyon Formations). Pre-Guadalupian reservoirs, comprised of fractured Ellenburger dolomite and Devonian chert, Mississippian limestone and Wolfcamp age conglomerate, account for a major percentage of total esti-

mated reserves for the field which have been calculated to be 175 million barrels of oil equivalent (McGlasson and Haseltine, 1971).

Guadalupian age Bell Canyon and Cherry Canyon massive sandstones were recognized as reservoirs as early as 1965, but their full potential was not appreciated until the late 1970's when favorable economic conditions encouraged their development (Figure 5). Annual statistics published by the Petroleum Information Corporation reveal that Guadalupian reservoirs, penetrated by 26 wells, accounted for 52 percent of all oil produced in the Coyanosa field during 1979 (271,713 bbl/525,432 bbl total) and 35 percent of oil produced since 1961. Gas production in these reservoirs amounted to a mere 0.02 percent of all production in the field for the year (14,572 MCF/59,606,105 MCF total).

The structure defining the limits of Coyanosa field production was initiated during the Middle Ordovician, accentuated from Late Mississippian until very Early Permian and finally stabilized by Early Permian (Wolfcampian). This is concordant with tectonic movements which established the Delaware basin, as outlined in the introduction. This structure displays its greatest relief at the close of the Pennsylvanian, becoming increasingly subdued with subsequent Permian sedimentation. Little structural closure appears on Guadalupian structural horizons, but a definite regional anticlinal nosing (incomplete structural

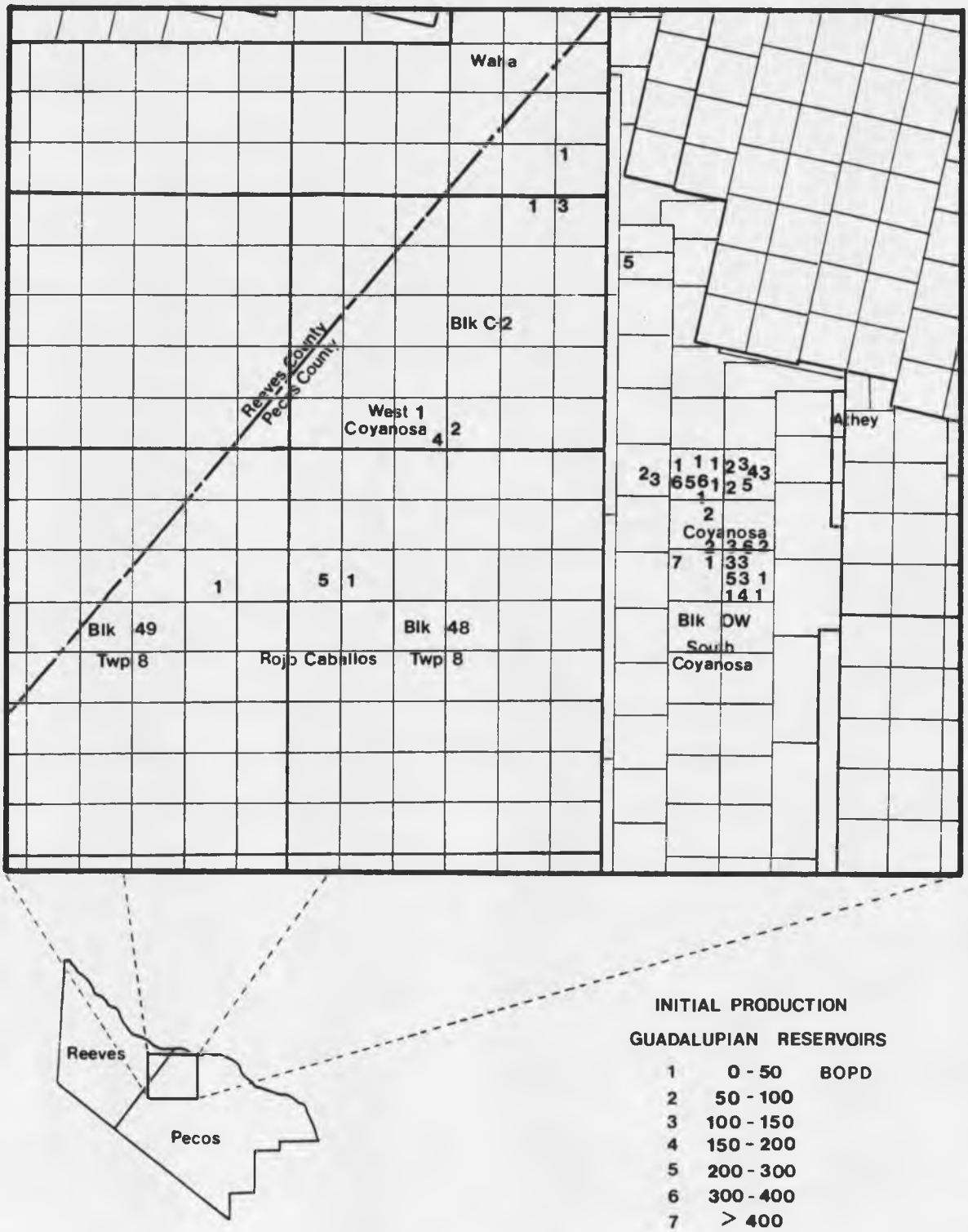

Figure 5. Initial Production and Distribution of Guadalupian Reservoirs in the Coyanosa Field Area

closure) toward the west-northwest can be discerned. Locally, within the Coyanosa field, several small anticlinal closures (less than 100 feet) and nosings occur, superimposed on the regional high.

Hydrocarbon entrapment within the Guadalupian reservoirs has been primarily controlled by these local anticlinal features. Additional stratigraphic and hydrodynamic restrictions have further confined the reservoir fluids. Examination of Brushy Canyon and Cherry Canyon structure maps (Figures 6 and 7) and Cherry Canyon and Bell Canyon isopach maps (Figures 8 and 9), particularly with regard to South Coyanosa, West Coyanosa and northwest Coyanosa fields where Guadalupian production is concentrated, reveal some interesting relationships. The present structural highs confining production are overlain, in most cases, by relatively thicker sequences of Guadalupian clastics containing the massive, very fine-grained reservoir sandstones. These sandstones represent the more porous and permeable clastic units which were deposited in submarine channel systems. This occurred as a result of density stratification of saline, sediment-laden currents that were swept into the basin from evaporitic shelf areas that lay to the east. These, in turn, were blanketed by siltstones and shales settling out of suspension. The relatively greater thickness of the units suggests that their deposition followed topographic lows on the basin bottom, a relationship anti-

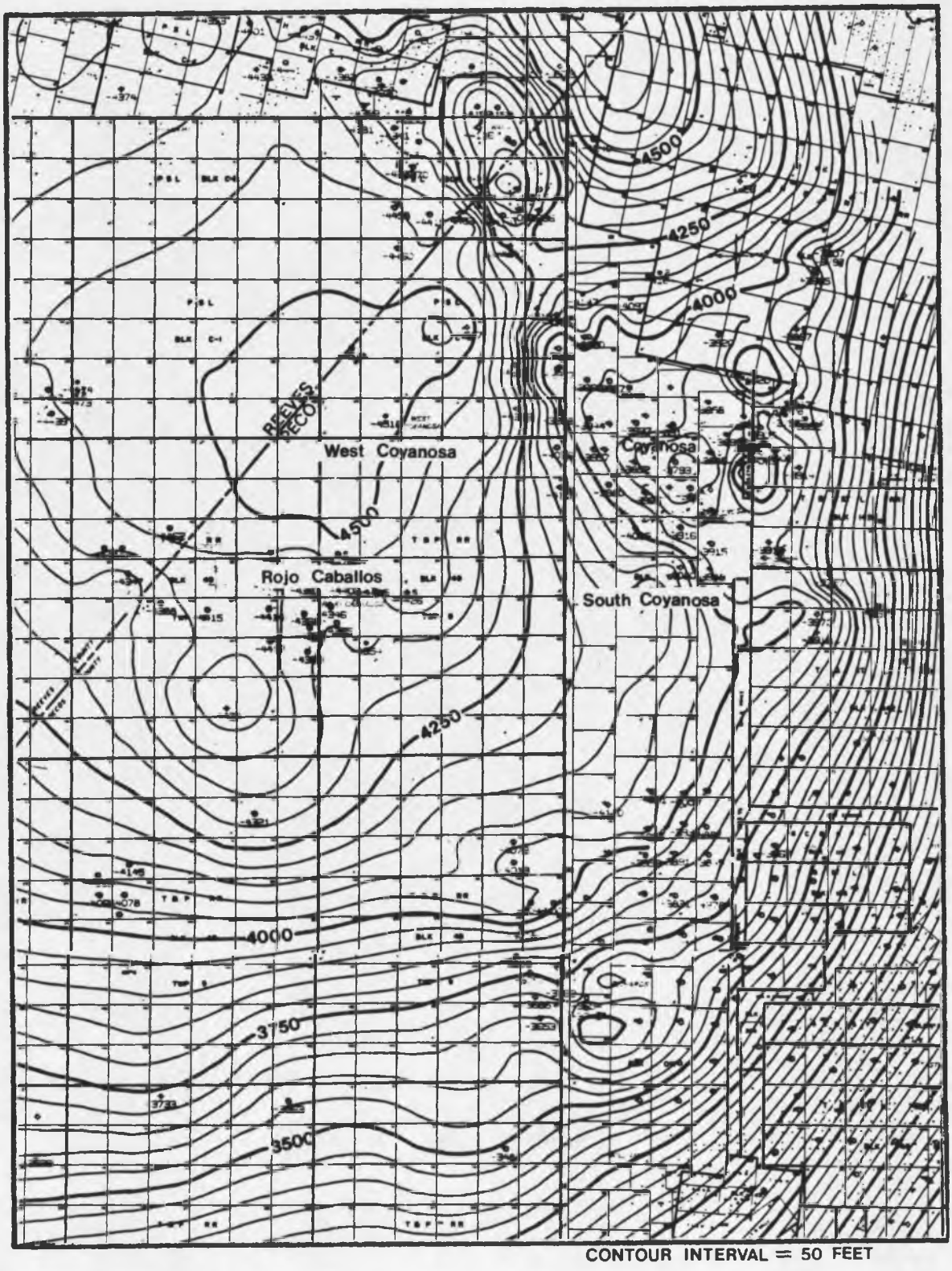

Figure 6. Structure Map of the Top of the Brushy Canyon Formation

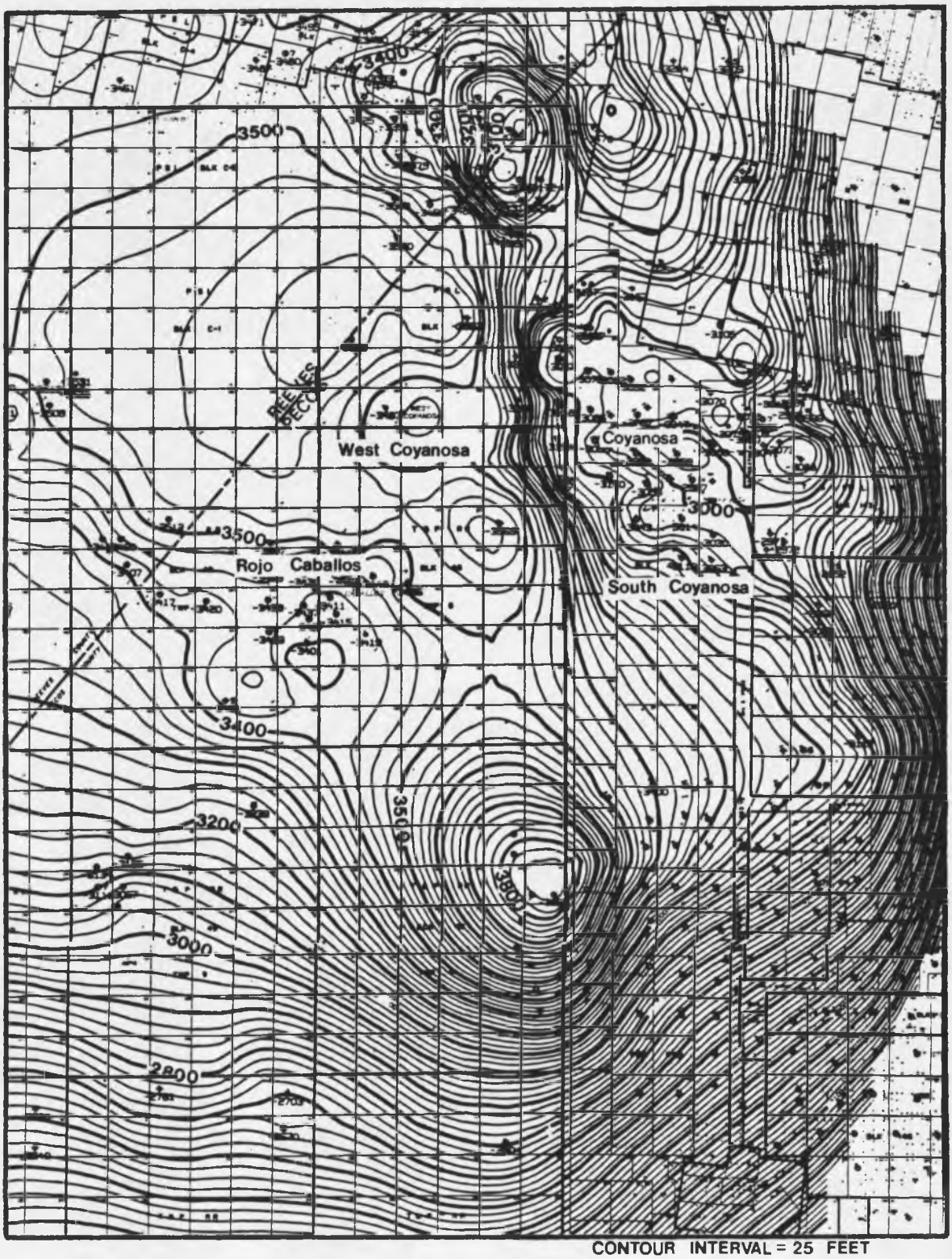

Figure 7. Structure Map of the Top of the Cherry Canyon Formation

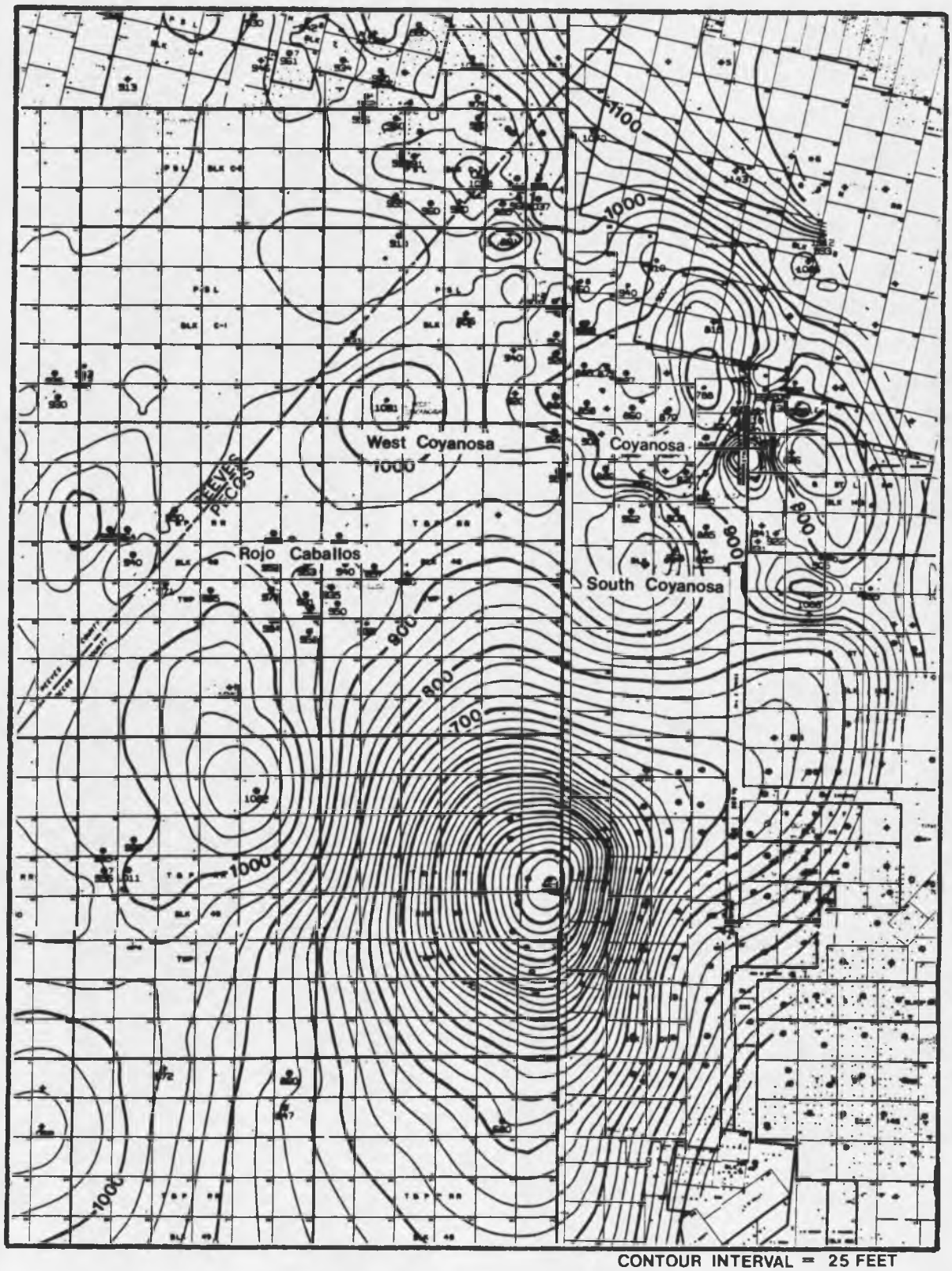

Figure 8. Isopach Map of the Cherry Canyon Formation

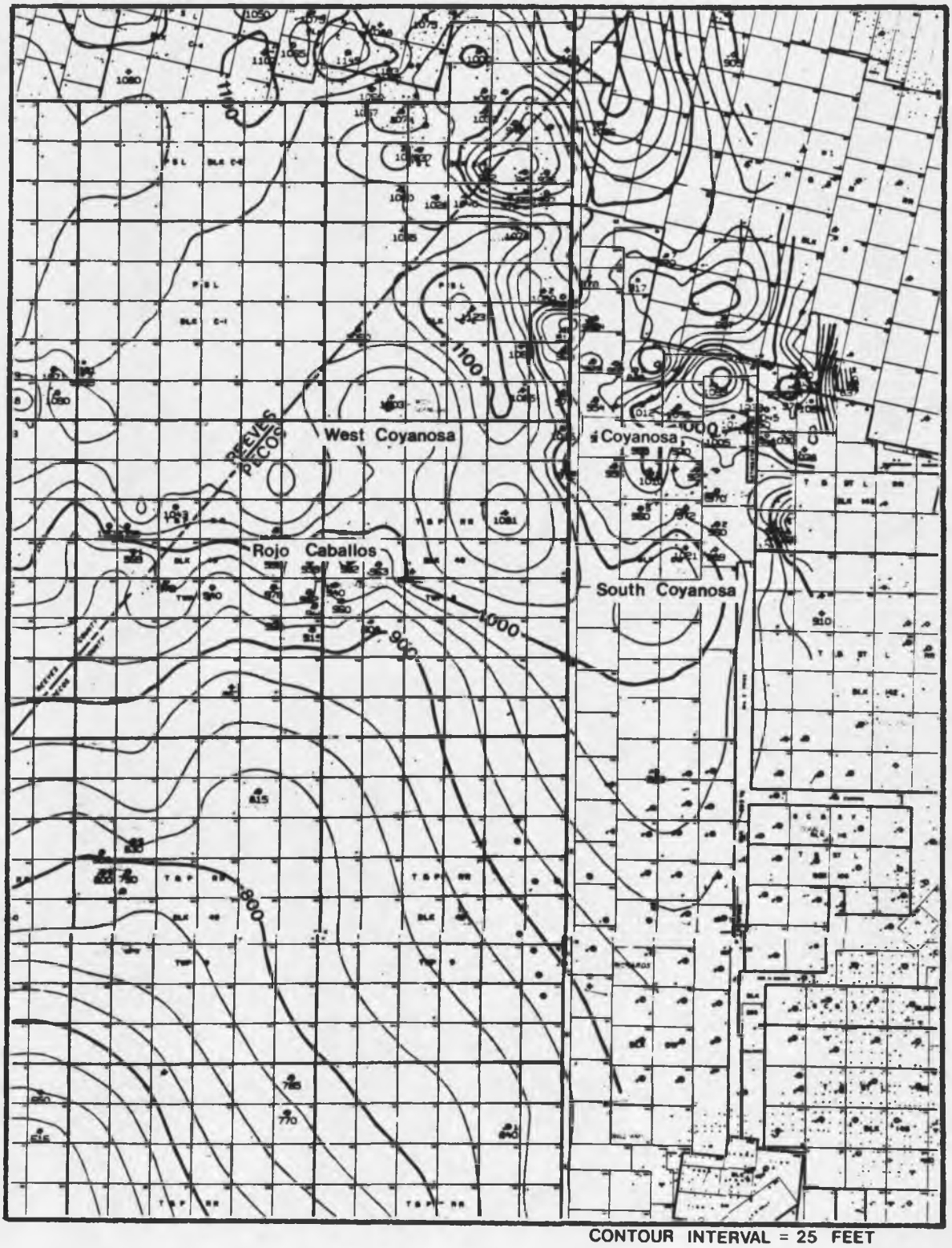

Figure 9. Isopach Map of the Bell Canyon Formation

cipated with gravity-propelled density flows. Hydrocarbons generated in the enclosing organic-rich siltstones and shales (Grauten, 1965) migrated into the massive channel sands and were subsequently trapped by permeability barriers established between the lithologic units. Further entrapment was accomplished by local anticlinal structures which developed contemporaneous with or after sandstone deposition and prior to hydrocarbon generation and migration. These protuberances were possibly created by draping and folding of thick sedimentary sequences over the regional upwarp. Thus, structure appears to be the overriding control on hydrocarbon emplacement within the Guadalupian reservoirs in the Coyanosa field with better definition of the fields accomplished by permeability contrasts, irreducible water saturations and lithologic variations.

CHAPTER 3

LITHOLOGY OF THE BELL CANYON AND CHERRY CANYON FORMATIONS

General Statement

The Bell Canyon and Cherry Canyon Formations are comprised primarily of alternating sequences of siltstone and very fine-grained sandstone units representing fluctuations in depositional flow regime. The thinly-laminated siltstones and interbedded organic-rich shales seem to suggest deposition from suspension preceding and/or concurrent with periods of intense bioturbation. These processes were accompanied by the formation of secondary minerals (pyrite) and organic material indicative of stagnant, reducing conditions. The massive sandstone units, conversely, appear to have been deposited by erosive, bottom-hugging fluid density currents resulting in a geometry akin to submarine channel systems. Also included, to a lesser extent, are intervening thin shale and carbonate units which act as excellent marker horizons throughout the basin. Because of the similarity of these lithologic units within the Bell Canyon and Cherry Canyon Formations, observations and descriptions incorporated in this study will pertain to both

formations unless a situation warrants that a distinction be made.

Material examined in this study includes four slabbed cores and ten sets of core chips obtained from the Coyanosa field and surrounding areas representing eleven Bell Canyon and eight Cherry Canyon sections. Because of the sampling bias incurred by coring only those sections of economic interest, neither formation is completely represented in the subsurface. By careful extrapolation of observations from available core material, examination of subsurface well logs and analogy with information obtained from the literature, reasonable descriptions and interpretations concerning the two formations have been construed.

Stratigraphic Relationships within the Bell Canyon Formation

Core sampling has been restricted to the uppermost productive sandstone units contained in the two formations. In the Bell Canyon Formation this stratigraphic interval contains, in descending order, the Lamar, Ramsey, Ford and Olds Members. Detailed descriptions of these members have been provided by Nottingham (1960), Grauten (1965) and Watson (1974). This study will recognize member boundaries as they have been defined by Watson (1974). Figure 10 displays the stratigraphic subdivisions of the Bell Canyon and Cherry Canyon Formations, the latter of which will be described in the following section.

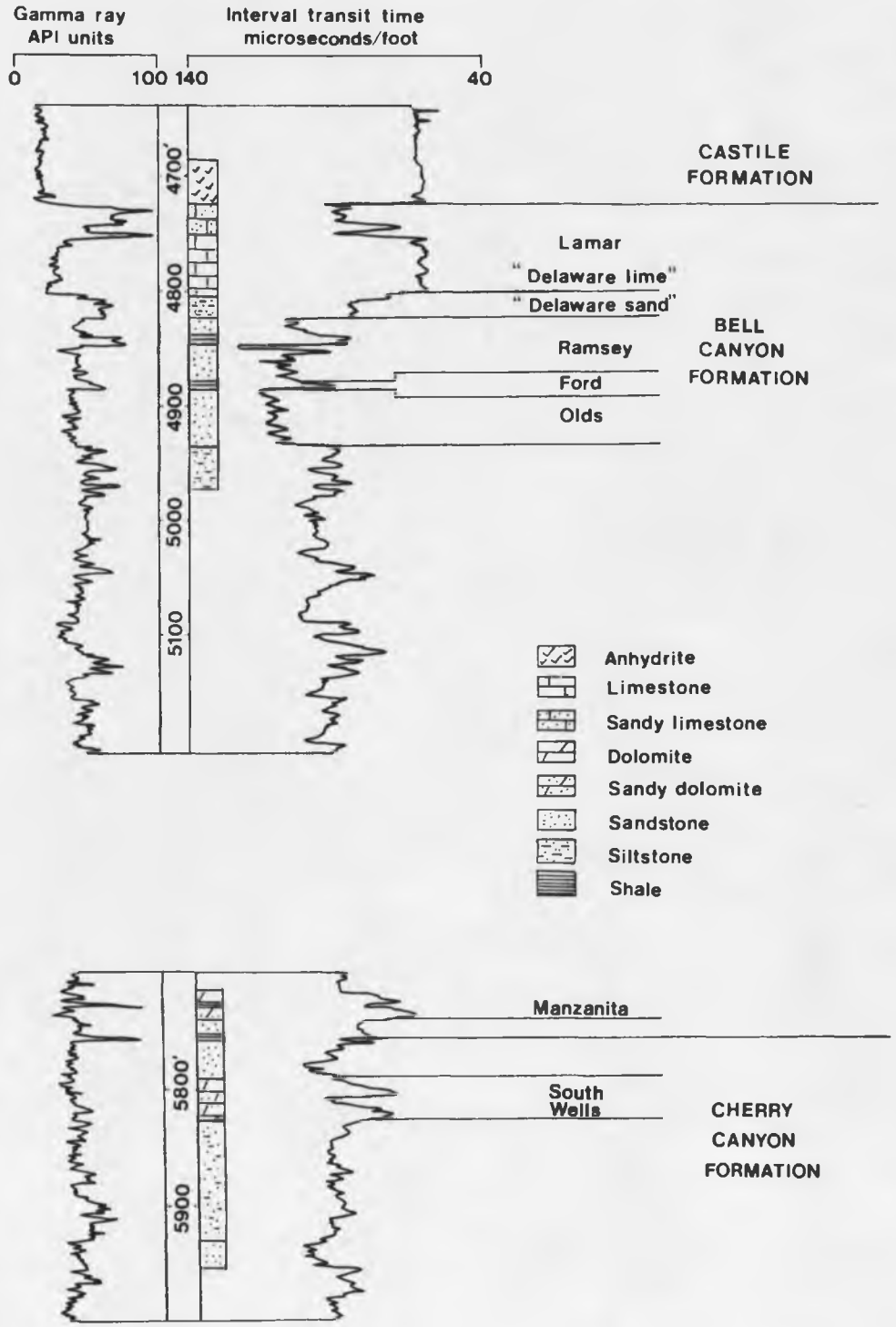

Figure 10. Stratigraphic Relationships within the Upper Bell Canyon and Upper Cherry Canyon Formations as Represented on Sonic-Gamma-Ray Subsurface Logs (Mobil, E.P. Sibley #B-1)

The Lamar Member is a very prominent marker bed characterized by a sequence of dark calcareous shales overlying and transitional into dark grey, argillaceous limestones of variable thickness (up to 20 meters in wells nearest the basin margin). In southwest Reeves and Pecos Counties the Lamar attains its maximum thickness of approximately 30 meters, deviating from the consistent 6 to 10 meter thicknesses recognized in other portions of the basin. Lithologic character appears to have been controlled by basin position with interior regions displaying increased shaliness and organic content, while basin margins reflect increased carbonate components.

The Ramsey Member lies beneath Lamar and is commonly divided into two lithologic units - a dark to medium grey, laminated, shaly siltstone which is at times interlaminated with thin, black to dark grey, clayey layers, and a light grey to greenish-grey, clean, very fine-grained, massive sandstone containing scattered interlaminations of shaly siltstone and thin, dark, organic-rich layers. The shaly siltstone intervals are characterized by average porosities of 13 percent, permeabilities of 1 md and uniform thicknesses across the basin. These siltstones encompass the relatively more permeable and porous massive sandstone units of extremely variable thicknesses, providing a perme-

ability barrier to hydrocarbons that may be contained in the sandstones.

The Ford Shale Member, underlying the Ramsey sandstones, consists predominantly of thin black shale enclosing a slightly thicker shaly siltstone, net thickness generally not exceeding 3 meters. It is not as well-developed in the eastern and southeastern sections of the basin and is thus difficult to distinguish as a marker bed on subsurface logs in the Coyanosa field area. It generally marks the lower limit of shallow Delaware Mountain Group exploration, although deeper penetration has revealed productive intervals within the underlying Olds Sandstone, a laminated and clean sandstone similar to the Ramsey member.

Stratigraphic Relationships within the Cherry Canyon Formation

The Cherry Canyon has not received the attention that the Bell Canyon has, although it probably contains the greater number of potentially productive massive sandstone intervals. There has been no formal stratigraphic nomenclature attached to the sandstone units and reference to them varies among subsurface geologists. Typical designations include an alphabetical or numerical sequence. Lithologically these massive sandstones and associated siltstones are very similar to those described in the Ramsey Member. The intervening and numerous limestones have been designated primarily as a consequence of their

use as marker beds throughout the basin. The uppermost sandstone interval of interest in this study is confined by the Manzanita Limestone above and the South Wells Limestone below. Figure 10 displays these relationships.

Siltstones of the Bell Canyon and Cherry Canyon Formations

The siltstones can be divided into three distinguishable units; (1) dark to light grey, very thinly-laminated, coarse siltstone, (2) dark to light grey, moderately to intensely-bioturbated, coarse siltstone and; (3) dark grey, very thinly-laminated, medium to fine-grained, organic-rich siltstones. These units occur interbedded with and transitional into one another and the accompanying massive sandstone members. Figures 11A through 11D display these textural relationships as viewed in siltstone core sections.

Texture

Textural parameters for the siltstone and sandstone members of the Bell Canyon and Cherry Canyon Formations were derived from the measurement of 200 grains in thin section mounts as outlined by Friedman (1958). It was necessary to follow this procedure because of the small amount of core material available for analysis in most cases. This method, which was performed in conjunction with point counting for mineralogical composition, allowed for the transformation of grain distribution measurements into sieve-

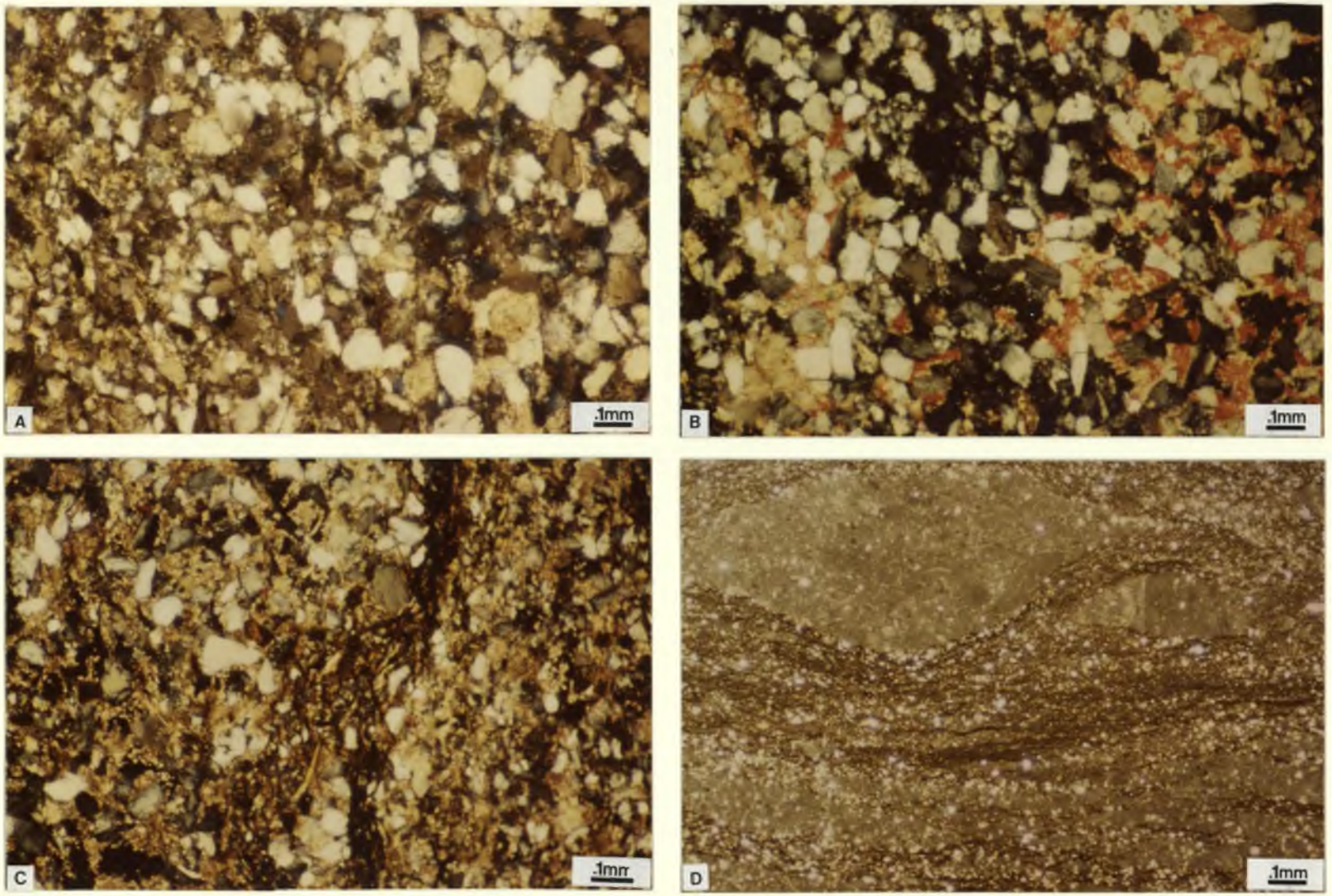

Figure 11. Thin Section Photomicrographs of Textural Relationships within Bell Canyon and Cherry Canyon Siltstones

equivalent weight terms from which mean (M_z), sorting (δI) and skewness (SK_I) were determined (Folk, 1974), (Table 3).

The fine-grained nature of the siltstones plus the overall emphasis on the massive reservoir sandstone units prevented thorough textural analysis by thin section methods, with only 5 samples out of 34 point-counted samples representing a siltstone lithology (as previously determined by megascopic examination). However, qualitative thin section estimates of textural parameters of all siltstones sampled supports quantitative analysis.

The mean grain size was determined to be 3.93 ± 0.10Ø (0.065 mm). An obvious bias was introduced by choosing siltstone samples that were coarser grained and thus amenable to point-counting procedures. In these samples approximately 40 to 60 percent of the grains measured are of the fine and very fine sand categories. Considering all the siltstones sampled, the mean grain size is probably smaller, placing them more firmly in the coarse silt category.

The sorting values (or standard deviation) range from 0.43 to 0.53Ø, averaging 0.47 ± 0.05Ø, placing these siltstones in the well-sorted to moderately well-sorted classes. Overall, these siltstones display only a slightly poorer sorting than their contiguous massive sandstones. The well-sorting displayed by these siltstones has been attributed by Newell and others (1953) to their possible

Table 3. Textural Parameters of Selected Bell Canyon and Cherry Canyon Samples Determined from Thin Section Analysis

Sample	Graphic mean (Mz)	Inclusive graphic standard deviation (δ_I)	Inclusive graphic skewness (SK_I)
Pg-80-132*	4.07 Ø	0.44 Ø	-0.21
Pg-80-147*	3.85	0.53	0.22
Pg-80-150*	4.02	0.51	0.10
Pg-80-156*	3.87	0.42	0.06
Pg-80-143*	3.86	0.44	0.21
Pg-80-40	3.41	0.47	-0.01
Pg-80-88	3.37	0.44	-0.15
Pg-80-117	3.51	0.40	0.04
Pg-80-124	3.89	0.39	0.12
Pg-80-138	3.50	0.43	0.09
Pg-80-140-1	3.86	0.47	0.05
Pg-80-155	3.49	0.38	0.13
Pg-80-172	3.28	0.41	0.12
Pg-80-173	3.36	0.41	-0.15
Pg-80-178	3.13	0.40	0.10
Pg-80-182	3.81	0.55	0.04
Pg-80-185	3.38	0.43	0.06
Pg-80-59	3.53	0.37	-0.03
Pg-80-70	3.64	0.50	-0.02
Pg-80-101	3.62	0.42	0.15
Pg-80-107	3.57	0.43	0.05
Pg-80-108	3.61	0.45	0.05
Pg-80-161	3.66	0.45	0.14
Pg-80-162	3.51	0.41	-0.06
Pg-80-163	3.74	0.42	0.00
Pg-80-165	3.70	0.53	-0.04
Pg-80-167	3.52	0.51	0.18
Pg-80-170	3.66	0.44	0.09
Pg-80-171	3.45	0.52	0.16
Pg-80-189	3.46	0.48	0.18
Pg-80-190	3.31	0.56	0.07
Pg-80-191	3.53	0.35	0.04
Pg-80-192	3.60	0.39	0.15

*Siltstone samples, all others represent sandstones

Parameters defined (Folk, 1974)

$$Mz = (\text{Ø}16 + \text{Ø}50 + \text{Ø}84)/3$$

Table 3. -- Continued

$$\delta_I = \frac{\emptyset 84 - \emptyset 16}{4} + \frac{\emptyset 95 - \emptyset 5}{6.6}$$

$$SK_I = \frac{\emptyset 16 + \emptyset 84 - 2\emptyset 50}{2(\emptyset 84 - \emptyset 16)} + \frac{\emptyset 5 + \emptyset 95 - 2\emptyset 50}{2(\emptyset 95 - \emptyset 5)}$$

Method Employed (Friedman, 1958)

Thin section quartile values (Ø5, Ø16, ..., Ø95) are derived after plotting grain size distributions on probability ordinate graph paper. These values are subsequently converted to sieve values:

$$\text{Quartile value}_{(\text{sieve})} = 0.3815 + (0.9027 \times \text{Quartile value}_{(\text{thin section})})$$

Sieve quartile values are then evaluated in terms of the textural parameters defined above.

source rocks, previously sorted Pennsylvanian sandstones of Oklahoma and Colorado. Also, comparison of basin and back-reef sandstones suggests that sorting may have been accomplished prior to sediment transport into the basin (Adams and Frenzel, 1950). Clay-size particles which would have contributed to poorer sorting had they been transported into the basin were possibly flocculated out in the hypersaline shelf environment.

Skewness measurements, averaging 0.17 ± 0.05, reveal a fine-skewed grain distribution. Contamination by another sediment source or perhaps mixing of siltstone grain sizes by bioturbation could account for this asymmetry.

Siltstone porosities average 13 percent, ranging from 2 percent to 23 percent, as determined by commercial laboratories. Permeabilities are quite low, averaging less than 1 or 2 md, although extremes of 22 md have been recorded. This "tight" character can be attributed to the fine grain size, presence of considerable detrital mica and organic material, and authigenic clay growth on grain surfaces. Although the relative impermeability of these siltstones creates a barrier to hydrocarbon migration from the enclosed massive sandstones, it has been noted (Berg, 1975; Visher, in Collins, 1975) that hydrodynamic factors also play a significant role in this entrapment.

Composition

Compositionally the sandstones and siltstones are similar, varying primarily with respect to organic matter content. Framework components of the siltstone units average 75 percent quartz (73 percent monocrystalline, 2 percent polycrystalline), 22 percent feldspar (15 percent potassium feldspar, 7 percent plagioclase) and 3 percent rock fragments (comprised predominantly of chert and sedimentary rock fragments).

Cementing agents include sparry calcite (15 to 20 percent by thin section area) with subordinate amounts of dolomite, anhydrite, authigenic clay, a matrix comprised of detrital mica, and quartz and feldspar overgrowths. Anhydrite is very rare in upper Bell Canyon sections, becoming dominant in some lower Bell Canyon and upper Cherry Canyon sections. Sparry calcite cement has a tendency to concentrate in selected laminae due to increased permeability along these horizontal planes (Figure 11B). Thus, lighter-colored laminae tend to exhibit better cementation. Dolomite, more commonly associated with the massive sandstone facies, occurs as fine-grained to very fine-grained dolomite rhombs spanning interstitial pore spaces. In addition to cementation, sparry calcite and anhydrite occur as burrow fillings and replacement minerals for rarely-occurring fossil fragments.

Detrital micaceous minerals, including muscovite, chlorite, biotite and "leached" biotite occur in significant amounts in the siltstone facies, aligned parallel to laminae planes (Figure 11C). Very fine-grained disseminated pyrite appears throughout the section, frequently associated with layers of greater organic matter content. It also occurs as secondary replacement of calcareous fossil fragments and fine, vertical, non-continuous fracture fillings. It has been suggested that the presence of pyrite within the siltstone units is associated with stagnant, non-oxygenated conditions at the sediment/water interface (Williamson, 1978). But pyrite also is found to occur within bioturbated siltstones, the organisms of which require oxygenated conditions for survival. This relationship suggests that pyrite growth did not occur until after burial of these sediments and is not related to initial depositional environment. Other accessory minerals occurring in minor amounts include leucoxene, zircon and garnet.

The organic content of the units varies with coloration; the darker the laminae, the greater the concentration. Total organic carbon measurements performed on various samples indicate marginally potential source rock in the Coyanosa field area, ranging from 0.419 to 0.025 percent organic carbon for an average of 0.187 percent (0.500 percent is generally accepted as the lower limit for potential source material). Siltstones sampled in wells periph-

eral to Coyanosa field which are situated closer to the basin interior and at greater depths indicate a total organic carbon content of approximately 0.480 percent (1.019 to 0.187 percent). This is probably a reflection of the increased shaliness of these rock units. Interbedded shale units display the greatest organic contents, averaging 0.612 percent for Coyanosa field samples and 1.755 percent for those toward the basin interior. The few carbonate samples analyzed indicate the lowest total organic content in both areas, but this may be a result of the small quantity sampled.

Analyses of acid insoluble organic matter in the Bell Canyon and Cherry Canyon Formations by Williamson (1978), Watson (1974) and Bozanich (1979) indicate a predominance of amorphous and unstructured residues comprised of marine palynomorphs. These palynomorphs are represented primarily by acritarches and minor amounts of Tasmanites. Small quantities of poorly preserved and fragmented land-derived spores and bladed coniferous pollen are also present. The palynomorphs described suggest slow sediment deposition relatively far from shore with anaerobic conditions occurring at or near the sediment/water interface (Williamson, 1978).

Sedimentary Structures

The most commonly occurring sedimentary structure within the siltstone units (see Figures 12A to 12F for examples of siltstone sedimentary structures) is extremely thin, alternating light and dark-colored, laterally continuous laminations, the thickness of which ranges from 0.1 mm to 5 mm (Figure 12D). The coloration of these laminae is the result of high organic content in the dark layers and increased sparry calcite cementation in lighter layers. In addition, the dark organic layers are generally thinner and finer-grained (medium fine silt and clay). There is no apparent textural gradation between laminations, but occasionally this feature can be observed within individual layers. The lateral continuity (as great as 15 miles) identified in some of these extremely thin laminae, particularly in the upper Bell Canyon, has been attributed to seasonal varving (Marshall, 1954). This is similar, in many respects to the sedimentation pattern observed in the Ochoan Castile Formation, a thick evaporite section directly overlying the Bell Canyon Formation (Kirkland, personal communication, 1980). The fine grain size, uniformity of laminae thicknesses and lateral continuity of these units imply that these siltstones have been deposited from suspension.

Figure 12. Photographs of Sedimentary Structures Observed in Bell Canyon Siltstone Core Sections

Bioturbation has resulted in the disruption of the majority of the thin bioturbated laminae within the Coyanosa field area. The intensity of the bioturbation varies, but in no discernible pattern. There does appear to be a correlation between siltstone layers occurring beneath and above massive sandstone units which may be a result of the oxygen-rich fluid density currents transporting the sand-size sediment. Deeper Cherry Canyon siltstones seem to have undergone relatively less bioturbation than overlying Bell Canyon units. Where bioturbated zones overlie nondisrupted units, convoluted and rippled bedding marks the contact (Figure 12F). Thus a change in current flow velocity and perhaps aeration of deep basin waters is suggested. Horizontal burrowing predominates over vertical, which one would expect in a deep-water depositional environment. A few of these burrows have been filled with sparry calcite or anhydrite cement in lower Bell Canyon and Cherry Canyon sections (Figure 12A) while most have experienced infill by contained sediment and/or fecal material (Payne, 1976). The majority of the horizontal bioturbation structures are believed to represent crawling and feeding trails (Bozanich, 1979), similar to those of Nereites which are indicative of deep-water environments (Crimes, 1970). Backfilling structures are also common in some intervals and are characteristic of the quiet water theichnogenus Zoophycus (Figure 12B).

Asymmetric ripple trains and ripple drift cross lamination occur in a few sections, generally not exceeding 1 to 2 cms in thickness and located adjacent to massive sandstone units (Figure 12C). This small-scale inclined bedding seems to suggest a change in current flow regime both prior to and proceeding massive channel sandstone deposition.

Soft sediment deformation features, including flame structures, convolute bedding and small-scale faulting have also been identified in the siltstone units. These structures are outlined by dark clayey material which has been forced upward into less cohesive fine-grained sand and coarse silt under the influence of overburden pressure.

Imbricated shale clasts and broken shale laminae reflect increases in current velocity prior to massive sandstone deposition. These disrupted zones, not exceeding 1 to 2 cms in thickness, occur in the uppermost sections of siltstone units.

Sandstones of the Bell Canyon and Cherry Canyon Formations

Light to medium grey or greenish-grey, very fine-grained, well-sorted, friable, massive sandstones characterize the reservoir sandstones of the Bell Canyon and Cherry Canyon Formations within the Coyanosa field area. This description, as with the siltstones described previously, is in accord with those provided by various authors

for these units in other locations within the Delaware basin (refer to Table 2). The consistency established within these lithologic units will facilitate reservoir potential prediction within the basin. Figures 13A, 13B, 14A and 14B display textural relationships within the sandstone units.

Texture

Twenty-eight sandstone samples were analyzed for derivation of textural parameters by thin section methods previously described (Table 3). Because of the consistency in sample composition, both mineralogical and textural, twenty-eight samples were considered adequate for reliable evaluation of parameters.

The mean grain size of massive fine-grained sandstones is 3.54 ± 0.17Ø (0.086 mm) with extremes of 3.13Ø and 3.89Ø being recorded. This places the sandstones in the very fine-grained size class. Five to 40 percent of the grains identified in these samples are of silt-size or finer. Five to 45 percent of these grains are fine sand-size or coarser. Bimodality is reflected in a few samples with 1 to 2 percent of the grains falling into the medium sand-size class (Figure 13B). This coarser fraction contains extremely well-rounded and unaltered monocrystalline quartz, potassium feldspar and detrital micritic clasts.

Sorting values (or standard deviations) range from 0.35 to 0.56Ø with an average of 0.44 ± 0.05Ø, classifying these sandstones as well-sorted.

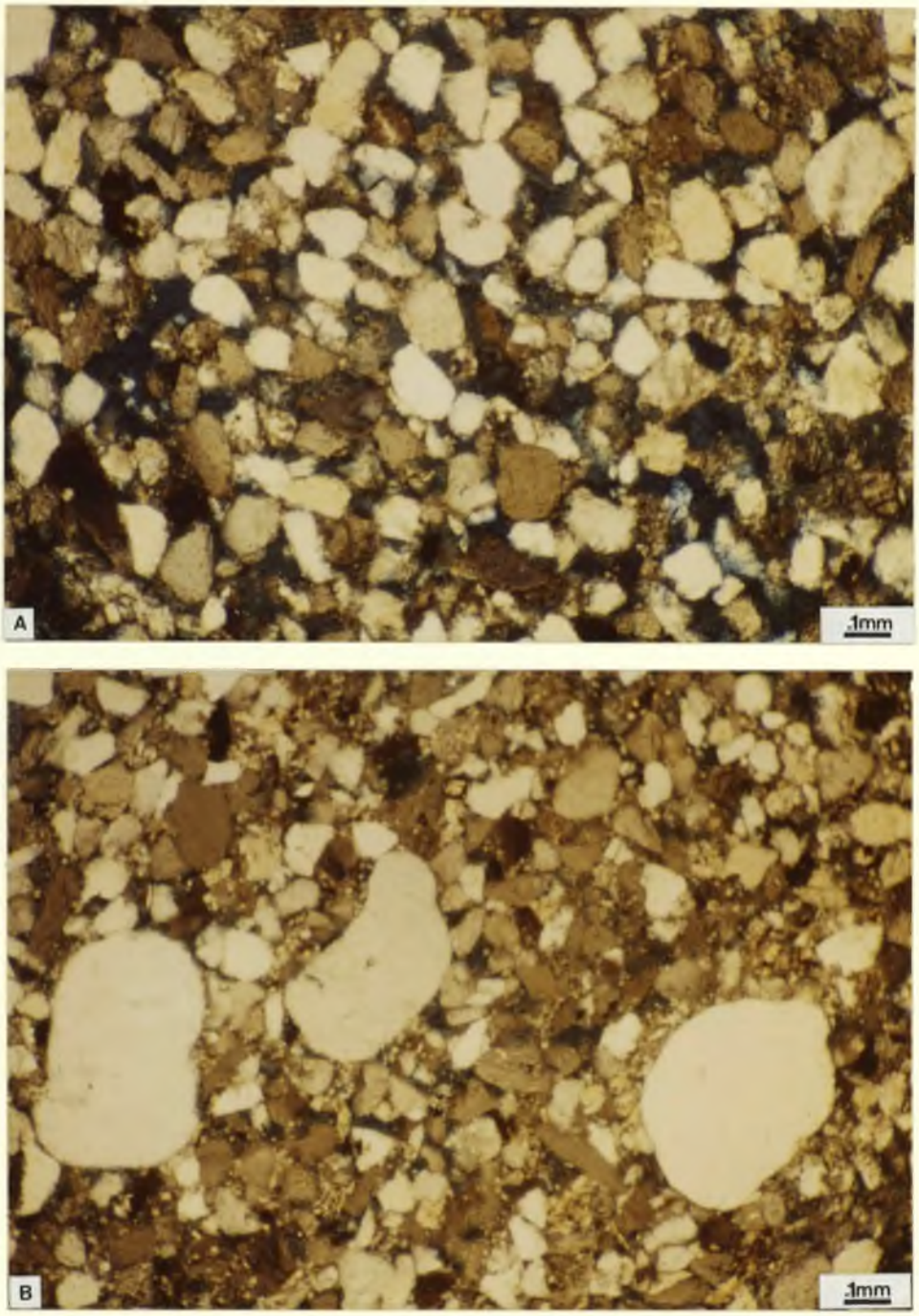

Figure 13. Thin Section Photomicrographs of Textural Relationships within Bell Canyon and Cherry Canyon Sandstones

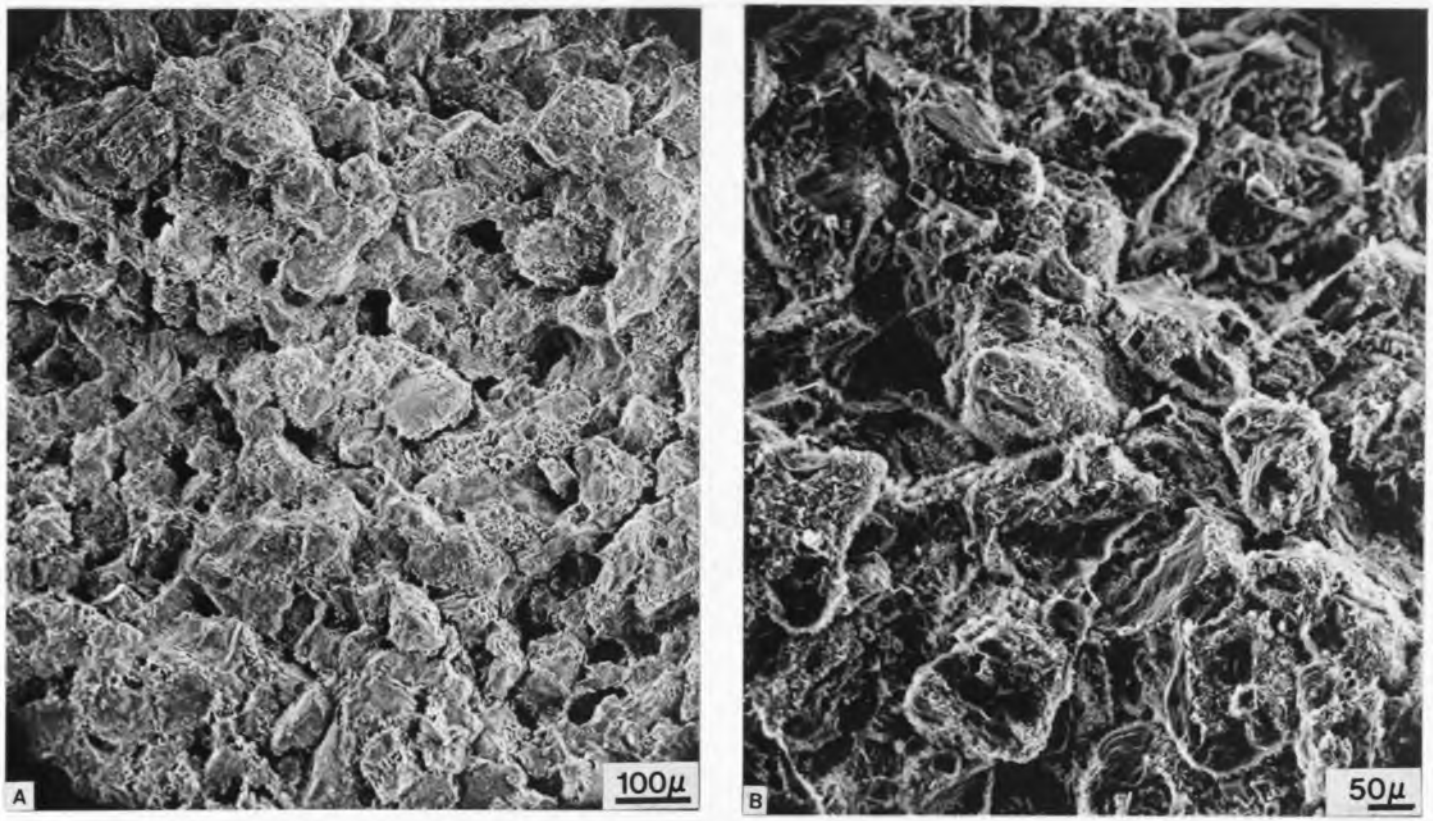

Figure 14. SEM Photomicrographs of Textural Relationships within Bell Canyon Sandstones

A. Detrital grains irregularly coated with authigenic clay growth. Pg-80-22, 4788', 100x.

B. Widely scattered, euhedral calcite rhombs projecting into well-developed intergranular pore spaces. Pg-80-D, 5073', 200x.

Skewness measurements indicate both fine and coarse-skewed end members (SK_I = -0.15 to 0.18), although the majority of the samples are nearly symmetrical in their grain distribution (SK_I = 0.05). This represents grain populations which lack significant grain contamination by extraneous sources or winnowing out of specific size classes.

Excellent porosity is indicated by values of 15 to 25 percent for most massive sandstone intervals (Figures 13A and 14A). Permeability averages 10 md, but considerably more permeable units have been identified (120 md) as have units of extremely low permeability (0.1 md). The permeability values primarily reflect the degree of authigenic clay growth and bear little relationship to porosity values. Thus, one will witness consistent porosities accompanied by widely varying permeabilities, neither of which appear dependent on the other.

Composition

Mineralogical composition is similar to that described for the siltstone units. Quartz averages 71 percent (68 percent monocrystalline, 3 to 4 percent polycrystalline); feldspar, 23 percent (15 percent potassium feldspar, 7 percent plagioclase); and rock fragments, 6 percent placing the sandstones in the subarkose category of McBride's (1963) classification system.

The extreme friability of the major portion of these sandstone units suggests a paucity of cementing agents which occupy 2 to 20 percent of sampled thin section area (Figure 14B). In addition to sparry calcite, significant amounts of dolomite, anhydrite, and quartz and feldspar overgrowths occur as cement. Of the above, magnesium and sulphate-rich cements tend to be associated with lower Bell Canyon and Cherry Canyon units. It is difficult to determine if this change in cement composition is transitional through the Bell Canyon because of the lack of cored material available from middle to lower intervals.

Detrital material contained in the sandstones includes coarse to medium sand-size micritic clasts, some of which contain relict bioclastic structures suggesting an origin in the surrounding carbonate reef bank. Most of these clasts display signs of deformation. Detrital micas represented by muscovite, chlorite, biotite and "leached" biotite, randomly occur squeezed and deformed between surrounding sand grains.

Minor amounts of other accessories include fine-grained glauconite pellets, secondary fine-grained euhedral pyrite crystals selectively rimming and replacing sand grains, leucoxene, zircon and tourmaline.

Total organic carbon measuremetns within the Coyanosa field indicate an average value of 0.250 percent, somewhat higher than the apparently more organic-rich in-

terbedded siltstones. In this situation the value does not necessarily represent source bed potential, but more likely the hydrocarbon residue that has been deposited within the massive sandstone units. Particularly high TOC values (0.459 percent) occur in sandstone units displaying good to excellent hydrocarbon shows.

Sedimentary Structures

The massive sandstones are basically structureless with the exception of random occurrences of horizontal lamination, trough cross-bedding, scour surfaces, convolute bedding and interbedded clayey layers, some of which have been disrupted into imbricated clay clasts (Figures 15A through 15E and 16A through 16E). Williamson (1978) states that this lack of structures is only apparent, particularly with regard to horizontal lamination and cross-bedding. Absence of clay-size material and well-sorting of sand grains contributes to this illusion. X-radiography performed on Williamson's core samples reveals that approximately 70 percent of the massive sand is actually structured.

Cross-bedding suggestive of bed load movement by traction is represented by extremely low to fairly high inclined laminations and beds (Figures 15A through 15E). The preservation of this high angle cross-bedding implies rapid sedimentation following development of inclination.

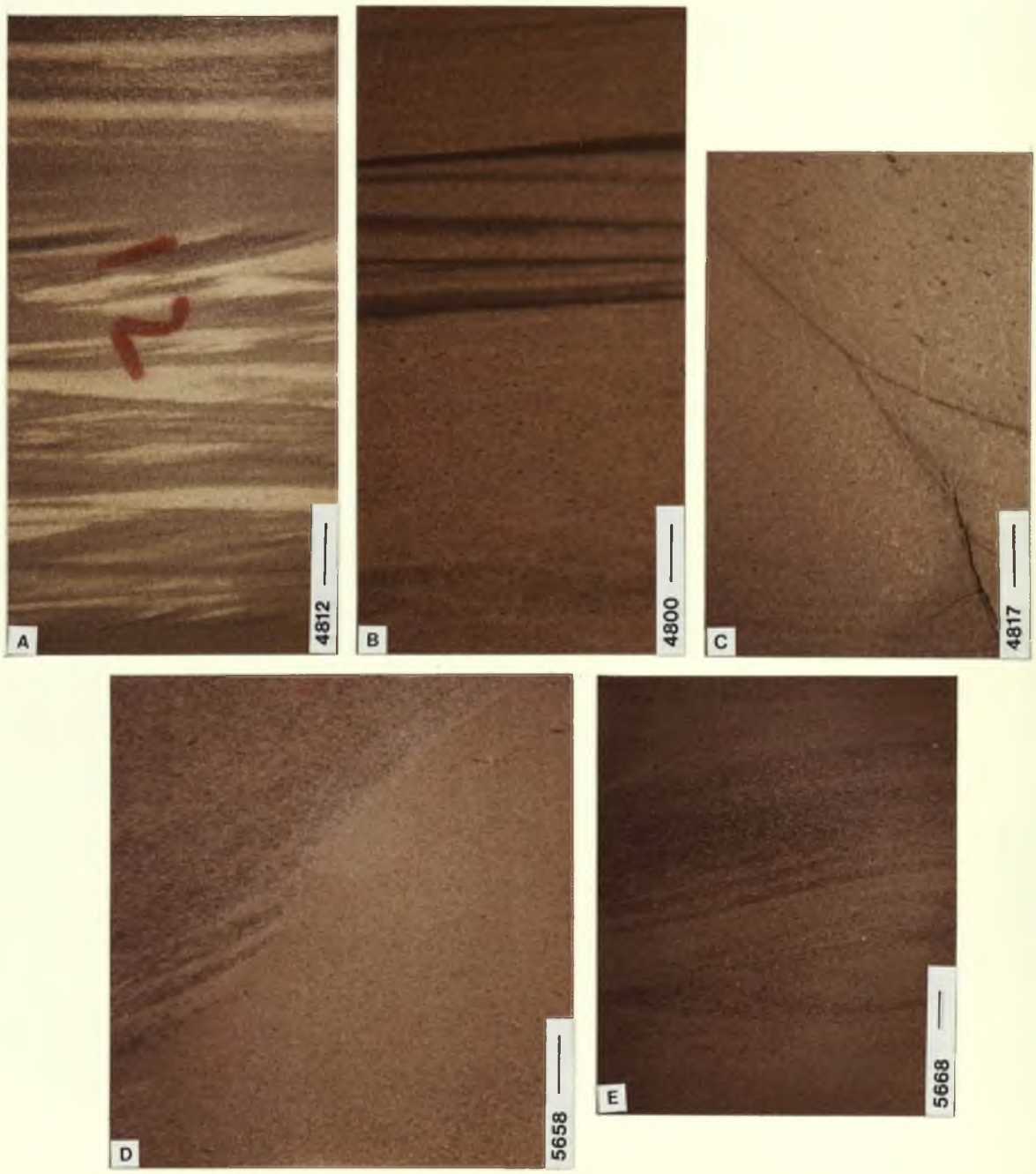

Figure 15. Photographs of Sedimentary Structures Observed in Bell Canyon and Cherry Canyon Sandstone Core Sections

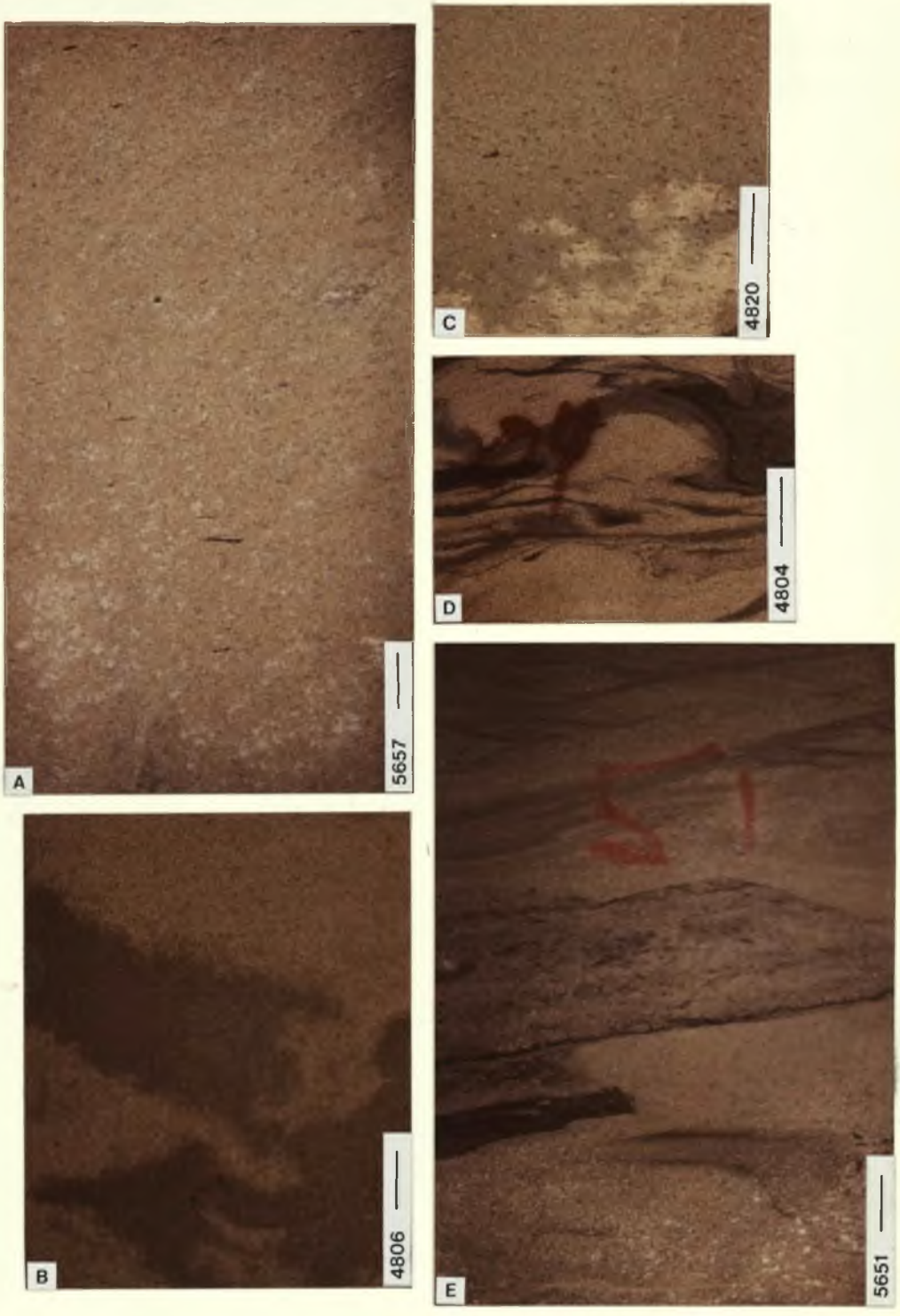

Figure 16. Photographs of Convoluted Bedding and Cementation Patterns Observed in Bell Canyon and Cherry Canyon Sandstone Core Sections

Scour surfaces are generally smooth, concave upward and infilled by slightly coarser-grained sand (Figures 15C and 15D). Other erosive processes occurring prior to and contemporaneous with initial massive sand deposition resulted in disruption of thin clayey laminae and subsequent incorporation of these clasts in lower sandstone layers (Figure 16E). Other units of clayey material are randomly interbedded throughout the sandstone units and have been deformed into convolute bedding (Figure 16D).

It should also be noted that cementation fronts (carbonate cement) can be distinguished in these sandstones on the basis of coloration and relative friability. Irregular contacts marking the fronts separate light grey, better-cemented sections from darker grey, poorer-cemented areas (Figures 16B and 16C). Anhydrite also imparts a characteristic cementation pattern to the sandstones in the form of even, light-colored mottling, delineating isolated patches of cement (Figure 16A).

CHAPTER 4

DEPOSITIONAL MECHANISMS

Previous Investigations

A number of theories have been proposed to explain the depositional mechanics of the Delaware Mountain Group siltstones and sandstones. A deep-water depositional environment for these clastics has been generally accepted since its initial inception by King (1942, 1948). Lack of shallow marine fauna, except for that which has been transported into the basin from reef margins, absence of nearshore depositional environments and sedimentary structures associated with them, and re-creation of basin paleogeography (Newell and others, 1953; Meissner, 1972; Harms, 1974) during Guadalupian time indicate water depths of approximately 1000 meters at the onset and 300 to 500 meters at the conclusion of Bell Canyon sedimentation. The major processes proposed to explain transport and deposition of clastics into the basin include turbidity currents (Jacka and others, 1968; Berg, 1979) and fluid density currents (Harms, 1974; Williamson, 1978; Bozanich, 1979). In addition to the above, aeolian transport (Berg, 1979), debris flows and submarine slides (Newell and others, 1953), and

suction currents (Jacka and others, 1968) have been invoked to account for sediment dispersal.

Depositional Model Supported in this Study

In view of the sedimentary structures and textural relationships observed in the Bell Canyon and Cherry Canyon clastic units, fluid density currents appear to be the most reasonable model proposed to explain sediment dispersal and deposition (Figure 17).

During Guadalupian time conditions existed such that evaporitic shelf areas were situated near a deep-water, semi-restricted euxinic basin, providing the fluid density contrasts necessary for sediment movement. Periods of storm activity and tidal fluctuations created buildups of dense, saline waters in shelf regions which proceeded to be swept by wind currents through shallow incisions in the surrounding reef complex (Goat Seep during Cherry Canyon deposition, Capitan during Bell Canyon). Gravity controlled subsequent movement of the dense fluids into the basin, a process which is apparent from the alignment of resultant submarine sand channels perpendicular to the surrounding reef bank. After entering the basin, density stratification of the waters occurred. Thin, dense, saline waters laden with fine and very fine-grained sand hugged the basin bottom, following topographic lows and scouring out new channels. Slight velocity changes, dependent on

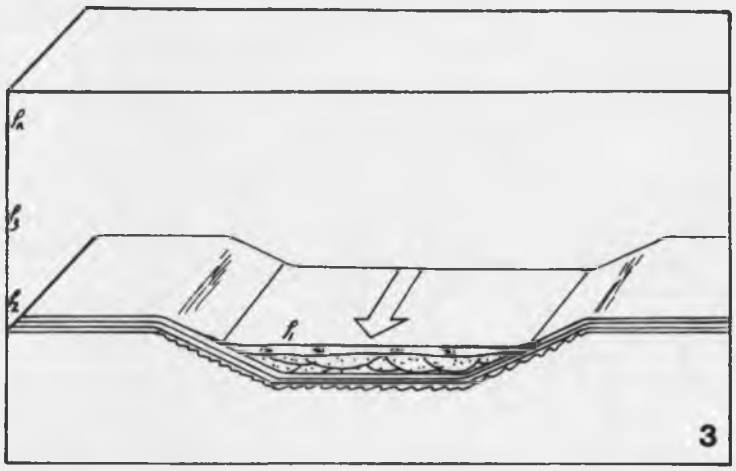

Traction deposition of sand by thin, upper-to-lower flow regime, long-lived density currents in previously scoured channels

$\rho_1 > \rho_2 > \cdots \rho_n$

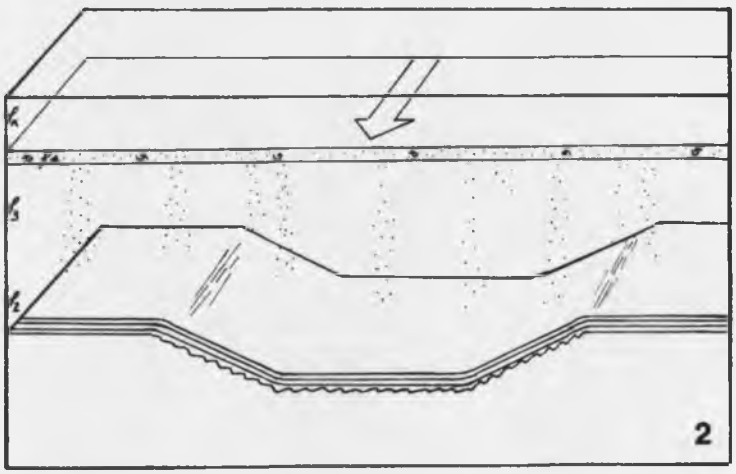

Deposition of silt by settling from intermediate density flows to form thin, uniform beds that mantle channel and adjacent surfaces

$\rho_3 > \rho_4 > \cdots \rho_n$

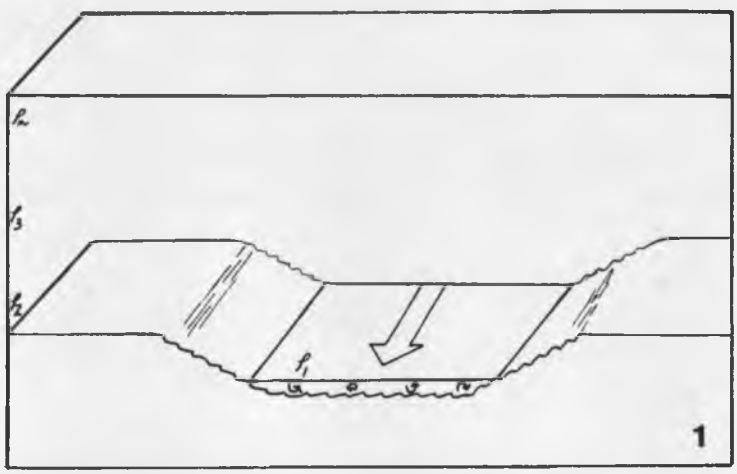

Channel scour by strong density currents flowing basinward under less dense, deep water

$\rho_1 > \rho_2 > \cdots \rho_n$

ρ = density

Figure 17. Depositional Model Proposed for Bell Canyon and Cherry Canyon Sandstones and Siltstones (adapted from Harms, 1974)

slope gradient and topography, resulted in rapid deposition of this entrained sand. Silt-size material was concurrently carried along by overlying, less dense salinity currents and was not as sensitive to slight changes in flow velocity. Deposition of siltstones occurred primarily from suspension following sand deposition. The blanket-like geometry of these siltstones (Williamson, 1978) implies that they are not overbank or levee deposits (Jacka and others, 1968; Payne, 1979). Clay-size material which is usually necessary in the stabilization of such features is also lacking. Eventually the small amount of clay and organic detritus was deposited from suspension as very thin laminations during periods of low sediment influx from shelf areas.

Supporting Evidence for Depositional Model

Textural Relationships

Lack of vertical grading in grain size within and between lithologic units is apparent in nearly all samples examined suggesting that deposition did not occur as a result of steadily waning current velocities. It also implies that grain populations were fairly well-sorted with regard to size prior to deposition resulting in the accumulation of internally homogeneous units. Lateral gradation of units is also absent in these sediments. Fluid density currents could readily account for the ex-

cellent segregation of grain sizes and uniformity of lithologic units. Although the absence of fines (clay and organic material) in suspension has been attributed to transport by currents of a non-turbid origin (Williamson, 1978; Payne, 1979), this situation could be the consequence of a source deficient in this grain size category.

Sedimentary Structures

There appears to be no vertical sequence of sedimentary structures established in the Bell Canyon and Cherry Canyon Formations. One would anticipate a Bouma-type sequence (Bouma, 1962) of structures if these were turbidite sediments. Berg (1979) and Payne (1979) have attempted to distinguish such sequences in these sediments but this author has been unable to identify similar series in core material examined. Superposition of structures and sharp lithologic contacts suggesting widely varying current velocities are more apparent.

CHAPTER 5

PETROGRAPHY OF THE BELL CANYON AND CHERRY CANYON FORMATIONS

General Statement

Approximately 200 thin sections were examined in an attempt to obtain detailed petrographic information on the lithologic units comprising the Bell Canyon and Cherry Canyon Formations. The two formations appear to be nearly identical with respect to framework constituents while authigenic components display greater variability. This disparity is probably more a reflection of relative burial depths and compositional stratification of contained reservoir waters than framework grain composition.

The Bell Canyon Formation has received the most attention with regard to detailed petrographic and diagenetic analyses. Hull (1957) performed initial laboratory investigations on the Bell Canyon and Cherry Canyon Formations, emphasizing textural relationships and mineralogy of framework and accessory grains. Subsequent Delaware Mountain Group studies stressed depositional and paleoenvironmental reconstructions for the formations with sketchy petrographic descriptions provided by thin section examination. Only two recent studies (Watson, 1974; Williamson, 1978)

have utilized other laboratory procedures in an attempt to more clearly define petrographic controls on reservoir parameters. These studies, however, have been limited to upper Bell Canyon sediments.

The following chapters supplement previous investigations and emphasize authigenic clay mineralogy and distribution, the prominent controls on reservoir parameters, particularly with regard to permeability. Hopefully some degree of clay predictability will be attained with these studies thereby facilitating reservoir production.

Methods Employed

One hundred and eighty-eight thin sections representing 12 wells were prepared by commercial laboratories for petrographic examination. This preparation included impregnation with blue epoxy to enhance pore space and add strength to the rock prior to grinding and cutting, processing in oil to preserve authigenic evaporitic constituents and staining a portion of the slide with Alizarin Red-S to detect calcite. Difficulty was encountered in obtaining complete impregnations in some thin sections because of the extremely poor permeabilities created by thick authigenic clay coats on framework grains. Thus, accurate estimation of porosity and framework grain percentages was hindered by grain plucking which occurred during grinding. It should also be noted that the fine

grain size of the sandstones and siltstones resulted in superposition of grains in thin section mounts contributing to difficulties in obtaining good optical resolution.

Thirty-four sections were selected for point-counting in order to obtain relative percentages of mineralogic components (defined by McBride, 1963 and Dickinson, 1979, Table 4) and to evaluate textural parameters as outlined by Friedman (1958). Four hundred points per slide were counted for determination of composition to ensure that at least 300 represented detrital grain counts, the minimum required for accurate clastic clssification. These thin sections were stained with sodium cobaltinitrite and amaranth solutions to distinguish potassium feldspar and sodic plagioclase, respectively.

A scanning electron microscope with attached energy dispersive x-ray spectroscopy (SEM-EDEX) was utilized in the examination of 32 samples from 11 wells. Use of the SEM-EDEX enabled greater resolution of grain relationships, pore space geometry, and authigenic fabrics and minerals. Clays were studied in particular because of their poor recognition in thin section mounts.

X-ray diffraction analysis was conducted on 46 samples. Eight samples were glycolated, three of which were heat-treated (550°C for two hours) for a more accurate identification of authigenic clay minerals present. The less than 4 micrometers fraction was separated by settling

Table 4. Mineralogical Composition of Selected Bell Canyon and Cherry Canyon Samples Derived from Thin Section Point Counting Analysis*

Sample	Quartz (Q)		Feldspar (F)		Rock fragments (L)		Cements				Miscellaneous					
	(Qm)	(Qp)	(K)	(P)	(Ls)	(Lt)	Carbonate	Anhydrite	Silica	Matrix	Carbonate Clasts	Detrital Micas	Pyrite	Zircon	Leucoxene	Porosity
Pg-80-132	74.75%	2.26%	12.62%	9.38%	0.97%	3.23%	11.75%	0.5%		4.25%		6.25%		0.25%		
Pg-80-147	68.05	7.02	16.61	5.75	2.56	9.58	11.00			7.25		2.50			0.25	
Pg-80-150	72.41	1.57	15.05	8.15	2.82	4.39	11.25			6.75	0.75	1.25		0.25		
Pg-80-156	75.93	3.09	15.43	4.63	0.93	4.02	8.00			9.50		1.50				
Pg-80-143	74.37	3.13	13.75	6.56	2.19	5.32	4.00	8.25	0.75	2.25		2.50		0.75	1.50	
Pg-80-29	71.00	5.60	19.10	1.40	2.80	8.40	6.25									11.25
Pg-80-40	68.05	3.55	13.02	11.54	3.85	7.40	2.00		0.50	0.25	0.50	0.75		0.50	0.25	11.00
Pg-80-88	75.12	3.19	17.37	0.35	3.90	7.09	8.75		0.50		2.25	1.50	0.25			16.25
Pg-80-117	66.66	6.25	11.20	10.68	5.21	11.46	1.25			0.50	0.50	0.50	0.25		0.75	
Pg-80-138	57.63	9.31	17.50	8.47	7.06	16.37	1.50	0.25		2.25	1.00	0.25		0.25	0.25	
Pg-80-140-1	67.47	6.03	16.57	5.72	4.22	10.25	8.75			5.75		1.75		0.25		
Pg-80-155	66.38	3.18	17.10	7.25	6.09	9.27	6.50			3.00	0.75	0.50		0.25		
Pg-80-172	64.78	4.71	19.18	4.08	7.23	11.94	5.75				0.50	0.75	0.25			13.00
Pg-80-173	68.72	5.08	12.30	10.96	2.94	8.02	4.00	0.25		0.75	0.50	0.25			0.25	
Pg-80-178	65.06	9.33	15.96	7.23	2.41	11.74	13.50	0.25		0.75	0.25		0.25			
Pg-80-182	63.52	8.81	14.28	8.21	5.17	13.98	6.75	1.25		6.25	0.25	1.25				
Pg-80-185	69.82	4.88	15.24	5.18	5.79	10.67	9.50	3.00		1.75	0.50	0.75				
Pg-80-124	70.36	4.18	16.77	5.99	2.69	6.87	5.75	0.25		6.00		2.50				
Pg-80-59	66.77	5.33	14.11	1.88	11.91	17.24	1.50	2.25			0.75	1.25	0.25	0.50	0.25	13.50
Pg-80-70	73.77	2.02	16.14	5.76	2.31	4.33	7.00	1.25		1.50	0.25	0.50	0.25		0.25	
Pg-80-101	73.17	1.65	14.24	1.32	9.60	11.25	5.75	1.25				1.00	1.25	0.25		15.25
Pg-80-107	72.96	1.63	10.75	12.05	2.60	4.23	2.75	3.75	0.50	3.75		0.50			0.50	11.00
Pg-80-108	70.60	2.87	14.98	9.51	2.01	4.88	6.50	1.75		2.25		1.50			0.25	
Pg-80-161	62.03	11.31	15.36	5.22	6.09	17.40	3.00		0.50	2.75	0.25	0.50	0.25	0.25		
Pg-80-162	68.33	1.39	13.89	11.94	4.44	5.83	5.00			3.25	0.25	0.25			0.50	
Pg-80-163	70.03	2.60	13.83	9.22	4.32	6.92	9.00			1.50	0.25	1.25	0.75			
Pg-80-165	70.39	3.02	13.59	11.18	1.80	4.82	7.75			5.75	1.00	1.75	0.50		0.50	
Pg-80-167	55.29	10.00	21.76	6.18	6.76	16.76	5.75			3.75		1.00	0.25			
Pg-80-170	69.92	4.06	14.09	10.57	1.35	5.41	3.00	1.50	0.50	2.25		0.25		0.25		
Pg-80-171	71.24	3.92	14.38	8.17	2.29	6.21	20.00		0.50	1.25	0.25	0.75	0.25		0.50	
Pg-80-189	71.83	0.63	16.45	8.86	2.22	2.85	17.50	1.75	0.25	0.50	0.50	0.50			0.25	
Pg-80-190	69.10	3.63	13.33	10.30	3.64	7.27	10.00	3.25	0.75	1.25		1.00	0.75	0.25	0.25	
Pg-80-191	65.77	4.76	13.39	11.61	4.46	9.22	6.50	3.75	0.75	3.50		0.25			0.25	
Pg-80-192	64.86	4.50	15.91	9.61	5.10	9.60	9.75	1.50	0.25	4.50		0.25	0.50		0.50	

*Based on 400 points counted per side

Qm = monocrystalline quartz
Qp = polycrystalline quartz including chert
K = potassium feldspar
P = sodic plagioclase
Ls = rock fragments other than chert and polycrystalline quartz and not including volcanic rock fragments
Lt = total rock fragments plus polycrystalline quartz and chert

velocity from crushed and dispersed shale, siltstone and sandstone samples. Each sample was further cleaned by centrifuging and finally air-dried on glass plates to obtain oriented clay samples. Although analysis was concentrated on the very fine-grained massive sandstone samples because of their associated reservoir potential, siltstones and shales were also examined in order to determine lithologic relationship to authigenic clay growth and to establish regional diagenetic clay zonation within the field area.

Heavy mineral separations were made on 10 sandstone samples using the heavy liquid tetrabromoethane. One hundred grains were identified from each fraction obtained (Table 5). The results of this analysis aided primarily in the determination of provenance for the Bell Canyon and Cherry Canyon Formations.

Allogenic Components

Quartz

Detrital quartz is represented primarily by subangular to rounded, slightly undulatory, moderately vacuolized monocrystalline plutonic quartz in percentages ranging from 55 to 77 percent. A few of the quartz grains contain inclusions, which are represented by rutile, tourmaline and vermicular chlorite. The presence of the latter suggests a hydrothermal vein origin for some of these

Table 5. Heavy Mineral Analysis of Selected Bell Canyon and Cherry Canyon Samples*

	Leucoxene	Apatite	Pyrite	Zircon	Tourmaline	Rutile	Hornblende	Unidentified
Pg-80-105	36	10	12	24	12	2		4
Pg-80-111	30	9	31	17	11	1		1
Pg-80-118	50	9	0	20	12	2		7
Pg-80-138	42	1	0	31	10	5		11
Pg-80-161	50	10	3	24	7	4	2	
Pg-80-189	36	3	1	40	9	5		6
Pg-80-C	42	1	0	33	8	6		10
Pg-80-G	67	2	0	12	10	2		7
Pg-80-M	47	2	0	35	3	3		10

*Based on 100 grains counted on slide

grains. A number of grains also appear embayed, yet lack other features characteristic of volcanic quartz. This irregularity in the grain surface can probably be attributed to corrosion which occurred during an earlier phase of cementation and subsequent dissolution.

A small percentage of polycrystalline quartz occurs in these samples, constituting 0.6 to 9 percent of total detrital quartz. This quartz is subangular to rounded, usually characterized by equant, interlocking, slightly undulose to undulose composite grains separated by straight boundaries, indicating a recrystallized metamorphic origin. A few of these grains display signs of more intense shearing reflected in strongly undulose composite grains, with sutured and straight boundaries occurring at points of contact.

The rounding of the grains appears to be related to grain size. Coarse to medium-grained siltstones contain a greater percentage of subangular to rounded grains while the very fine-grained massive sandstones display subrounded to well-rounded grains. This is probably indicative of slightly greater reworking of the very fine-grained sand populations as a result of tractive transport prior to deposition as channel units. The well-rounded grain fraction is primarily represented by a small percentage of medium sand grains, the presence of which results in a bimodal

sand distribution. These grains were possibly supplied from a reworked sedimentary source.

Feldspar

Feldspars account for an average of 23 percent of all detrital grains comprising the Bell Canyon and Cherry Canyon Formations. Sixty-five to 70 percent of the feldspar grains present were identified as potassium feldspar with the remaining percentage represented by sodic feldspar (plagioclase). Both tend to be indicative of a granitic plutonic source which is in accord with origins suggested for the detrital quartz.

Potassium feldspar grains (15 percent) are predominantly comprised of twinned and untwinned orthoclase and minor amounts of microcline, both of which have remained fairly unaltered. Plagioclase accounts for approximately 8 percent of the detrital grain population and is characterized by compositions ranging from An_{12} to An_{37} (albite to oligoclase). Albite twinning predominates with rarer occurrences of Carlsbad and combined Carlsbad-albite twins, and perthitic intergrowths. The plagioclases, because of their greater chemical instability, have undergone varying degrees of alteration, ranging from non-altered to nearly complete seritization along twin and cleavage planes (Figures 18A and 18B). A few of these grains have been leached so intensively that all that remains are one or two

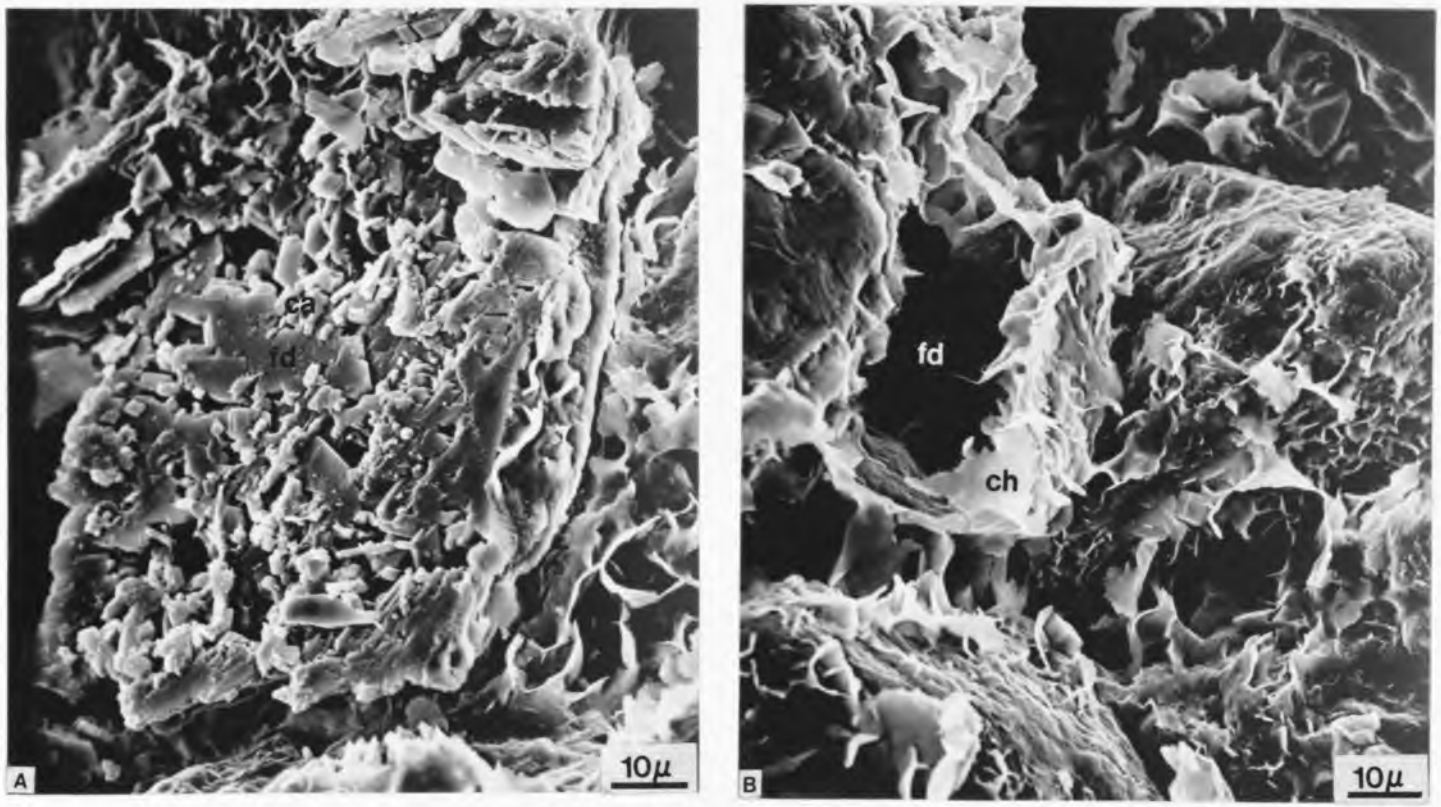

Figure 18. SEM Photomicrographs of Detrital Feldspar Alteration

A. Replacement of detrital sodic plagioclase (fd) by finely-crystalline calcium carbonate (ca). Pg-80-88, 4986', 1000x.

B. Dissolution of detrital feldspar (fd) leaving a self-supporting authigenic clay rim (ch). Illite (il) is also present in significant amounts. Pg-80-101, 5919', 1000x.

alternating twin planes. Vacuolization has occurred in a few instances, imparting a brownish "turbid" appearance to the feldspar grains. Other alteration has resulted in the replacement of feldspar by micritic calcite at grain surfaces. The occurrence of this latter alteration is restricted to massive sandstones which have incorporated micritic clasts and micrite-coated grains and grain aggregates into their framework mineralogy.

In general the feldspar grains are slightly finer grained than their quartz counterparts. However, the medium-grain size fraction of the bimodal sands contains appreciable quantities of microcline displaying better rounding than similar-sized quartz grains.

Rock Fragments

Rock fragments represent from 1 to 13 percent of the allogenic components, with the majority of the rock fragments reflecting a sedimentary or metamorphic origin. The sedimentary fragments occur in greater percentages and include chert and carbonate clasts. These carbonate clasts are characterized by thorough micritization, relatively larger size and susceptibility to deformation and subsequent dissolution at points of contact with surrounding detrital grains. A variety of these clasts have been identified including some which display relict bioclastic tex-

tures (Figure 19A) and others which enclose aggregates or individual silt-size detrital quartz (Figure 19B).

Metamorphic rock fragments consist of very fine polycrystalline grains composed of quartz, potassium feldspar and muscovite. Secondary pyrite occurs as isolated patches in a few of these grains.

Samples obtained from relatively greater depths (6000'+) contain chert and polycrystalline metamorphic fragments which have been deformed to the extent that they are indistinguishable from matrix material. The diagenetic bias that is subsequently created results in underestimation of the rock fragment percentages in these few samples.

Other Detrital Components

The micas comprise the majority of the remaining detrital minerals (Figures 20A and 20B). Muscovite and chlorite occur most frequently, amounting generally to less than a few percent. Additional biotite and "leached" biotite have also been identified in trace amounts. The siltstone facies contains the greatest percentage of detrital mica (5 to 10 percent) which occurs oriented parallel to laminations. The massive sandstone facies contains randomly interspersed and oriented mica flakes which have frequently been deformed between adjacent framework grains.

Well-rounded, bright bluish-green, very fine sand-size glauconite pellets have been noted in trace amounts in

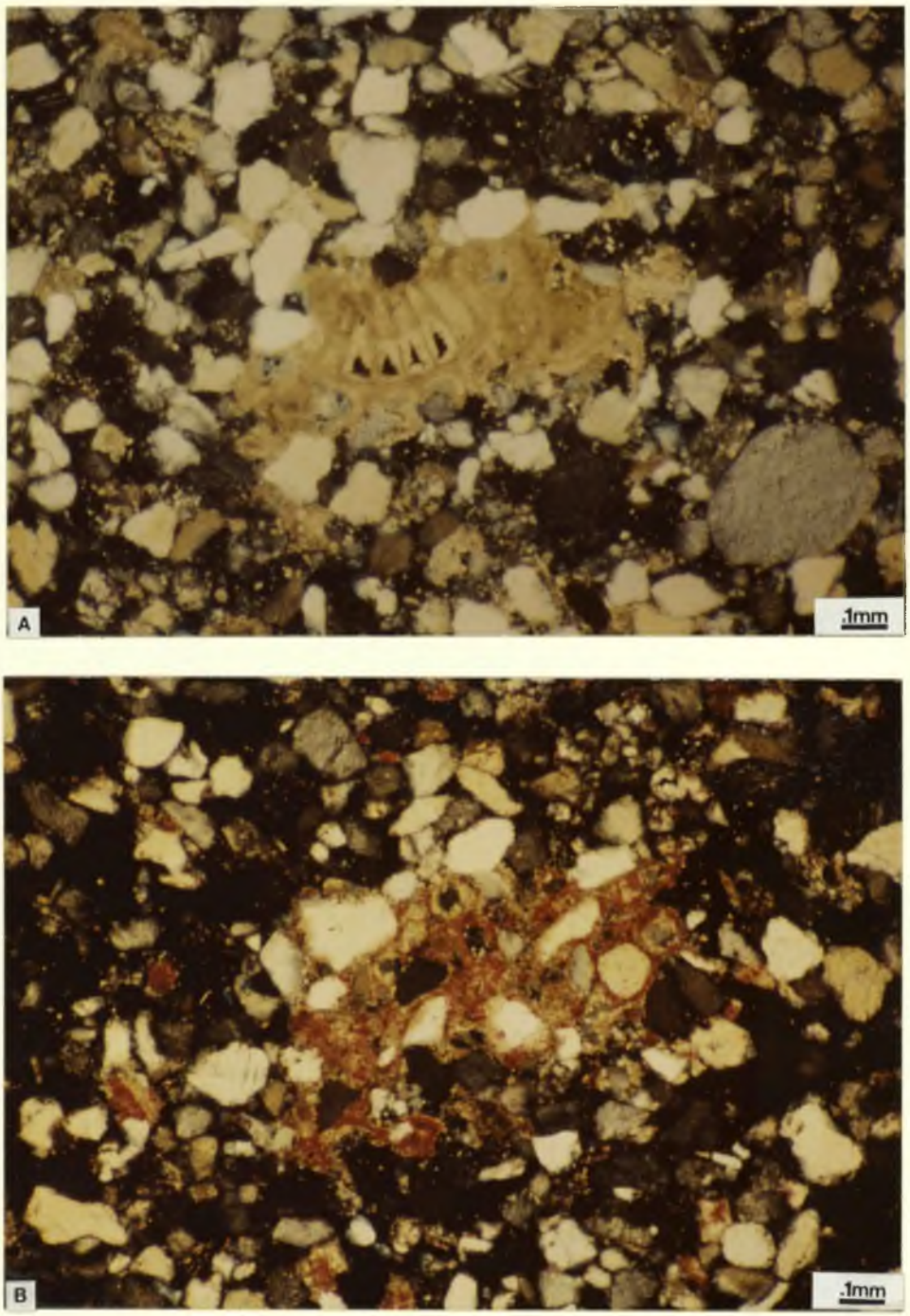

Figure 19. Thin Section Photomicrographs of Detrital Carbonate Clasts

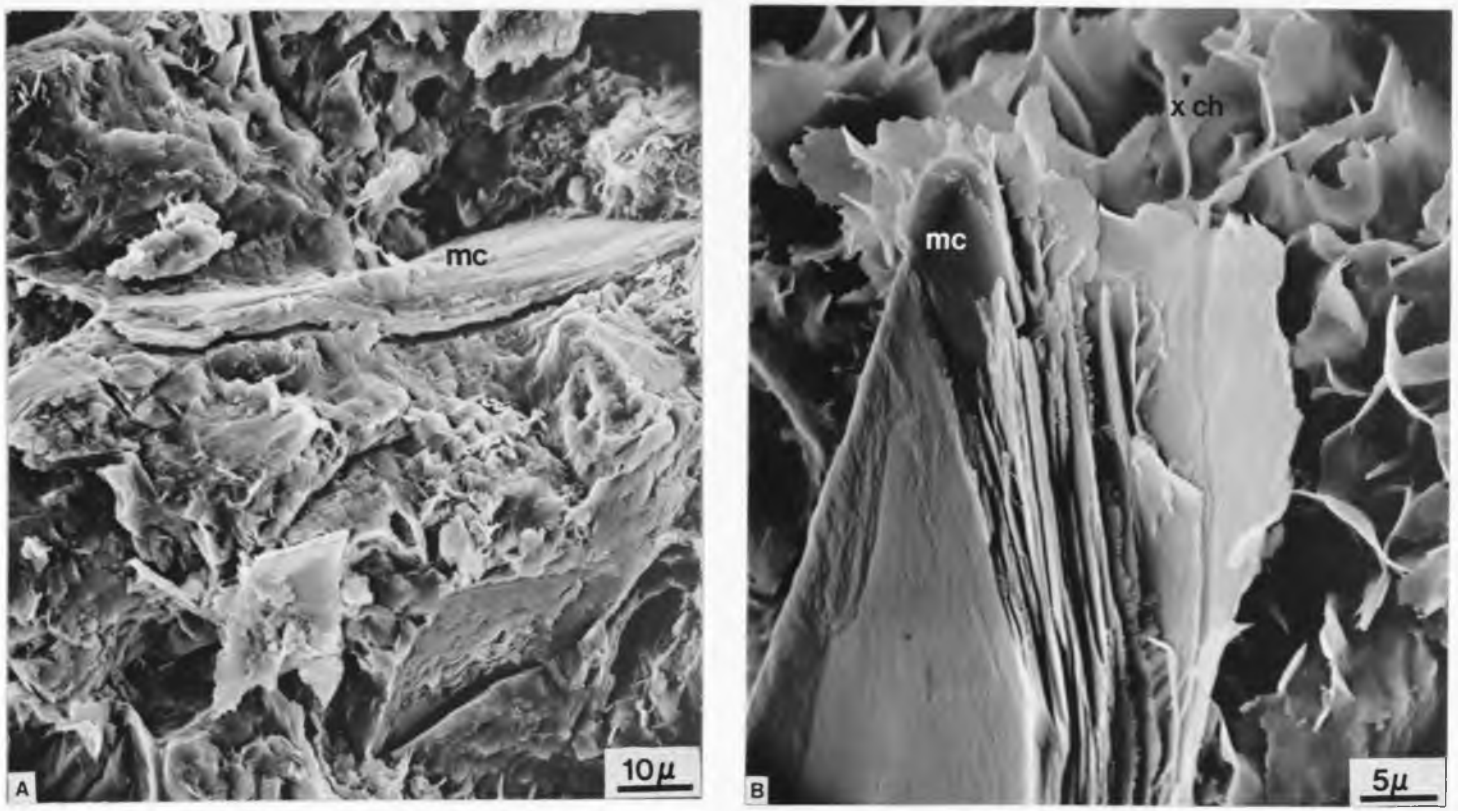

Figure 20. SEM Photomicrographs of Detrital Micas

A. Detrital mica (mc) deformed between detrital grains. Pg-80-19, 4775', 1000x.

B. Detrital mica (mc) displaying authigenic clay growth at upper end. Slight crenulation and unresolvability of individual clay flakes suggests a slightly expandable mixed-layer chlorite (xch). Pg-80-22, 4788', 2000x.

approximately one third of the samples. Their occurrence is limited to the sandstone facies indicating possible transport in from shelf areas.

The heavy mineral fraction contains a variety of opaques (authigenic pyrite and leucoxene), ultra-stable (zircon, tourmaline and rutile) and metastable (apatite, garnet and epidote) components. Table 5 lists relative percentages of these minerals.

Classification

Bell Canyon and Cherry Canyon siltstones and sandstones plot as subarkoses according to McBride's (1963) classification system (Figure 21). The end members on which this ternary plot is based include stable quartz components (Q) represented by monocrystalline, polycrystalline and microcrystalline quartz; total potassium feldspar and plagioclase (F); and unstable lithic fragments (Lt) consisting of volcanic, metamorphic and sedimentary rock fragments. Although these samples plot as a fairly uniform group, a few compositional trends can be distinguished within the assemblage. It appears that Cherry Canyon sandstone samples are, on the average, slightly more feldspathic than their Bell Canyon counterparts. In some instances the Cherry Canyon samples are included in the arkose category. This relationship may be a reflection of variability of source material and supply, transport, and

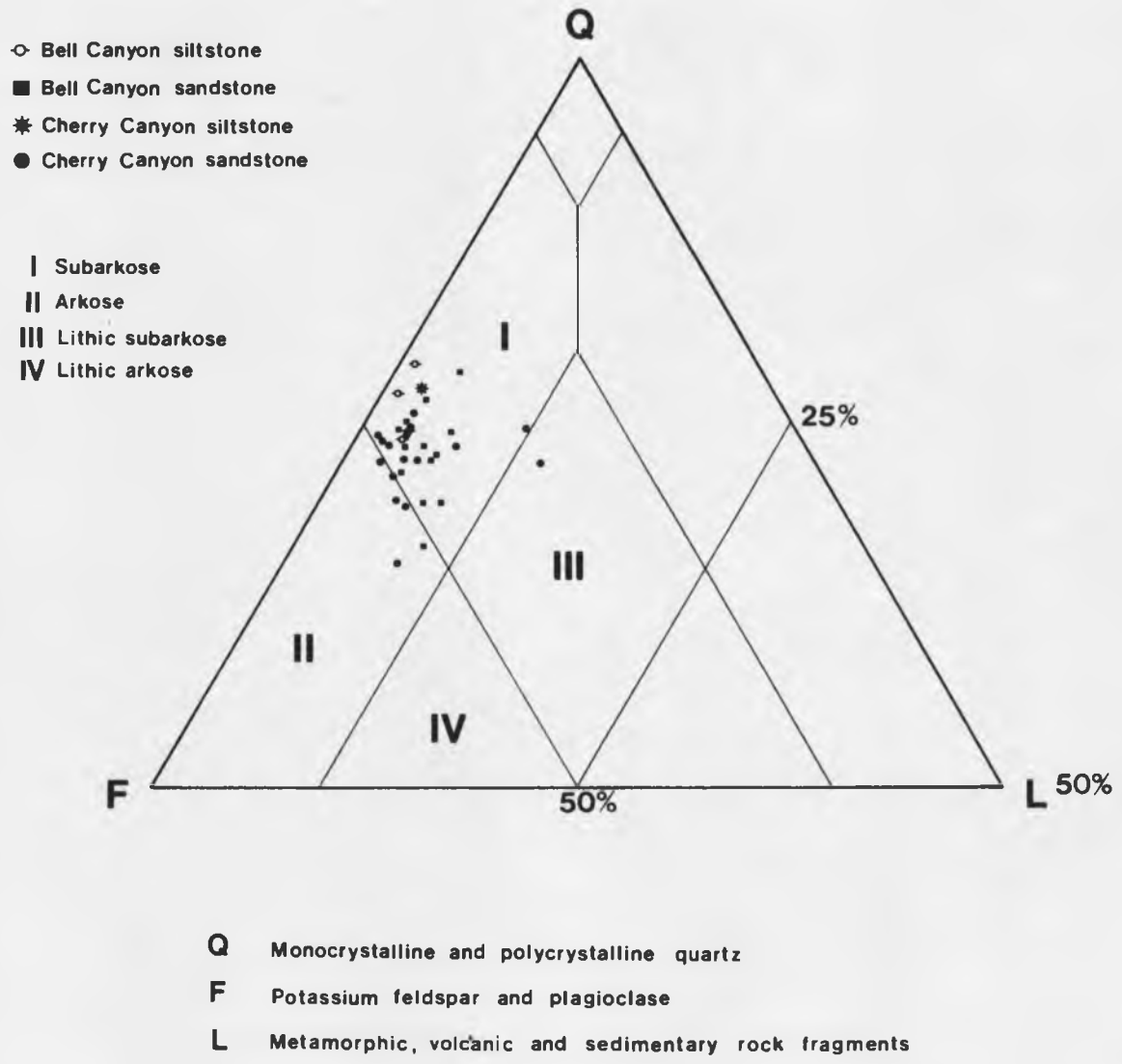

Q Monocrystalline and polycrystalline quartz

F Potassium feldspar and plagioclase

L Metamorphic, volcanic and sedimentary rock fragments

Figure 21. Classification of Bell Canyon and Cherry Canyon Sandstones and Siltstones (according to McBride, 1963). Note that only the upper 50 percent of the diagram is displayed.

intensity of weathering during Guadalupian time. Slight lithological differences can also be detected, with the few siltstones that were sampled displaying less feldspathic and lithic components than associated sandstones. This may be a consequence of the greater mineralogical instability of these components in the smaller size classes, which is also reflected, in these samples, by a relative increase in both matrix content and quantity of unidentifiable grains.

Comparison of these results with those of previous authors reveals a fairly uniform mineralogical composition for the Bell Canyon and Cherry Canyon Formations throughout the Delaware basin (Figure 22). A slight increase in feldspathic components at the expense of lithic fragments is suggested as one proceeds from the northwest corner to the eastern side of the Delaware basin. This again is probably a reflection of variability of sediment supply. The differences noted may also be attributed to inconsistencies in identification and subsequent categorization of framework grains by the various authors. For example, unless plagioclases are stained, untwinned grains can easily be mistaken for quartz, or if badly altered, they may resemble rock fragments.

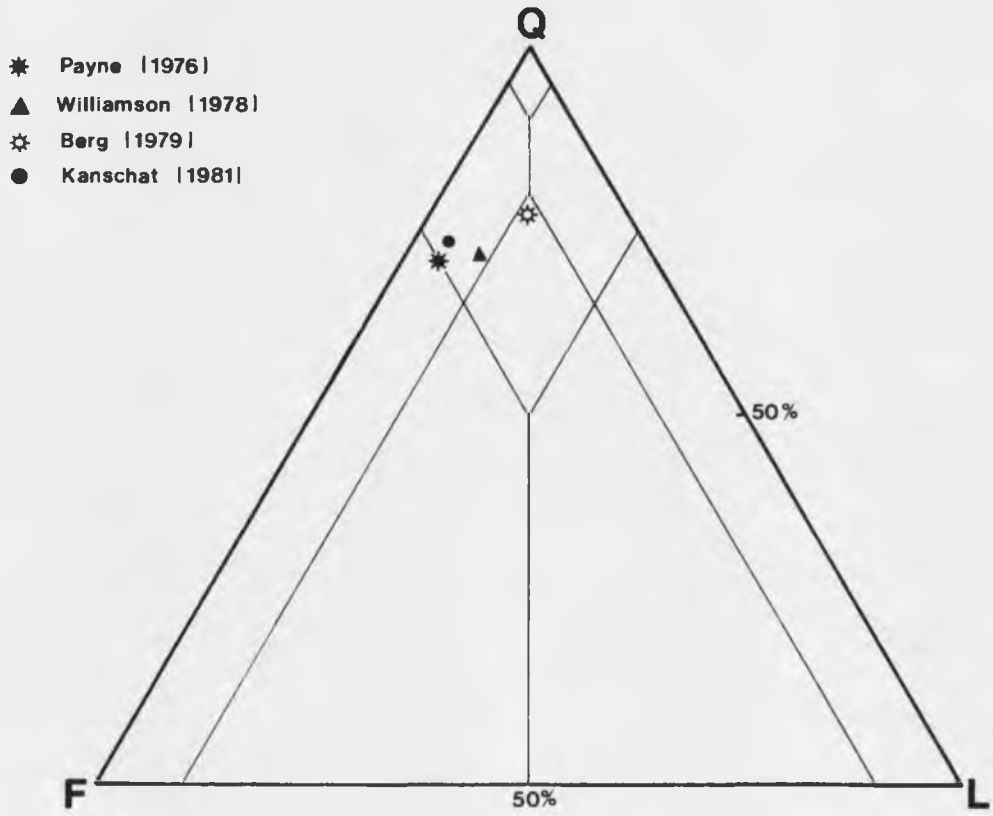

Figure 22. Comparison of Average Upper Guadalupian Sandstone Compositions. In all cases but the present study which includes Cherry Canyon samples, point count results represent Bell Canyon sandstone compositions. The classification system used is that of McBride, 1963.

Provenance Implications

Examination of framework components suggest a predominant granitic source for the Bell Canyon and Cherry Canyon units. The abundance of monocrystalline quartz and potassium feldspar, plus minor occurrences of leucoxene, supports this conclusion. Additional contribution from low-rank metamorphic sources in the form of composite quartz and metamorphic rock fragments is also noted. The presence of albitic plagioclase and detrital micas (muscovite, biotite and chlorite) indicate either source. The plutonic sources were more than likely cross-cut by a series of pegmatites as indicated by intensively vacuolized quartz containing vermicular chlorite, and rare occurrences of garnet. Well-rounded monocrystalline quartz, chert, carbonate clasts and zircon represent the small quantity of sedimentary material.

The lack of significant quantities of Guadalupian age-equivalent clastics in shelf and back-reef areas hinders the determination of the paleogeographic provenance for the two formations. The Pedernal Massif of southeastern New Mexico has been proposed (Hull, 1975; Oriel and others, 1967; Watson, 1974) as the probable source for Delaware Mountain Group deposits. However, some authors (Newell and others, 1953; Williamson, 1978) have refuted this association suggesting either reworked Pennsylvanian sands of Oklahoma and Colorado or the Ancestral Front Range

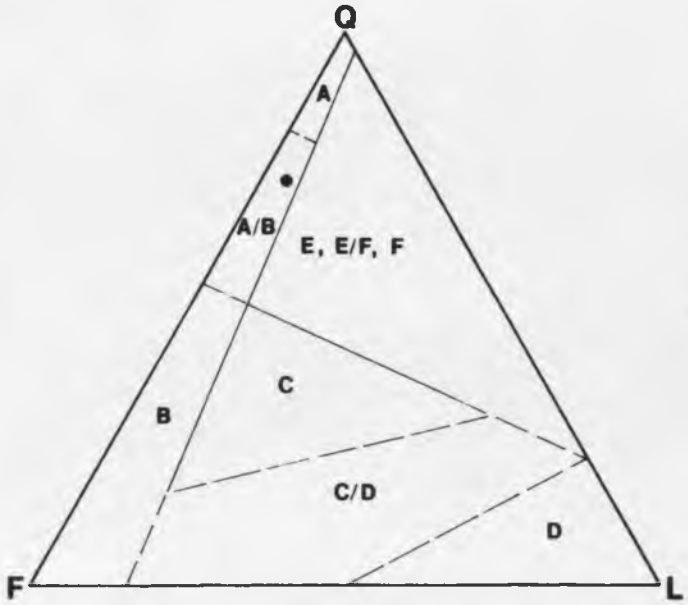

Emphasis on grain stability. Weathering, provenance relief, transport mechanism and source rock are considered

Q stable quartz
- Q_m monocrystalline quartz
- Q_p polycrystalline lithic quartz (chert)

F monocrystalline feldspar
- K potassium feldspar
- P plagioclase

L unstable polycrystalline lithic fragments
- L_v volcanic fragments
- L_s sedimentary fragments } includes metamorphosed varieties

L_t $L + Q_p$

CONTINENTAL BLOCK PROVENANCES

A - Craton interior A/B - Transitional B - Uplifted basement

MAGMATIC ARC PROVENANCES

C - Dissected C/D - Transitional D - Undissected

RECYCLED OROGEN PROVENANCES

E - Foreland uplift E/F - Collision orogen F - Subduction complex

● Average composition of Bell Canyon and Cherry Canyon samples

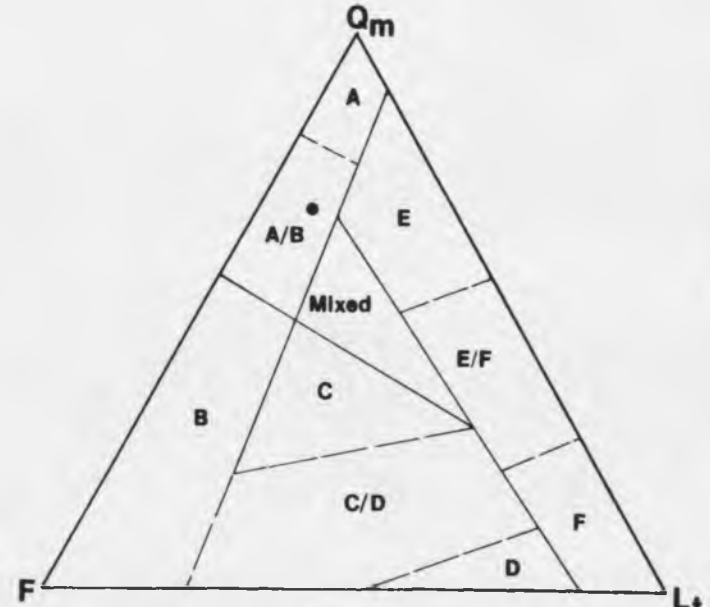

Emphasis on grain size of source rock. Fine-grained rocks yield more lithic fragments in the sand-size range

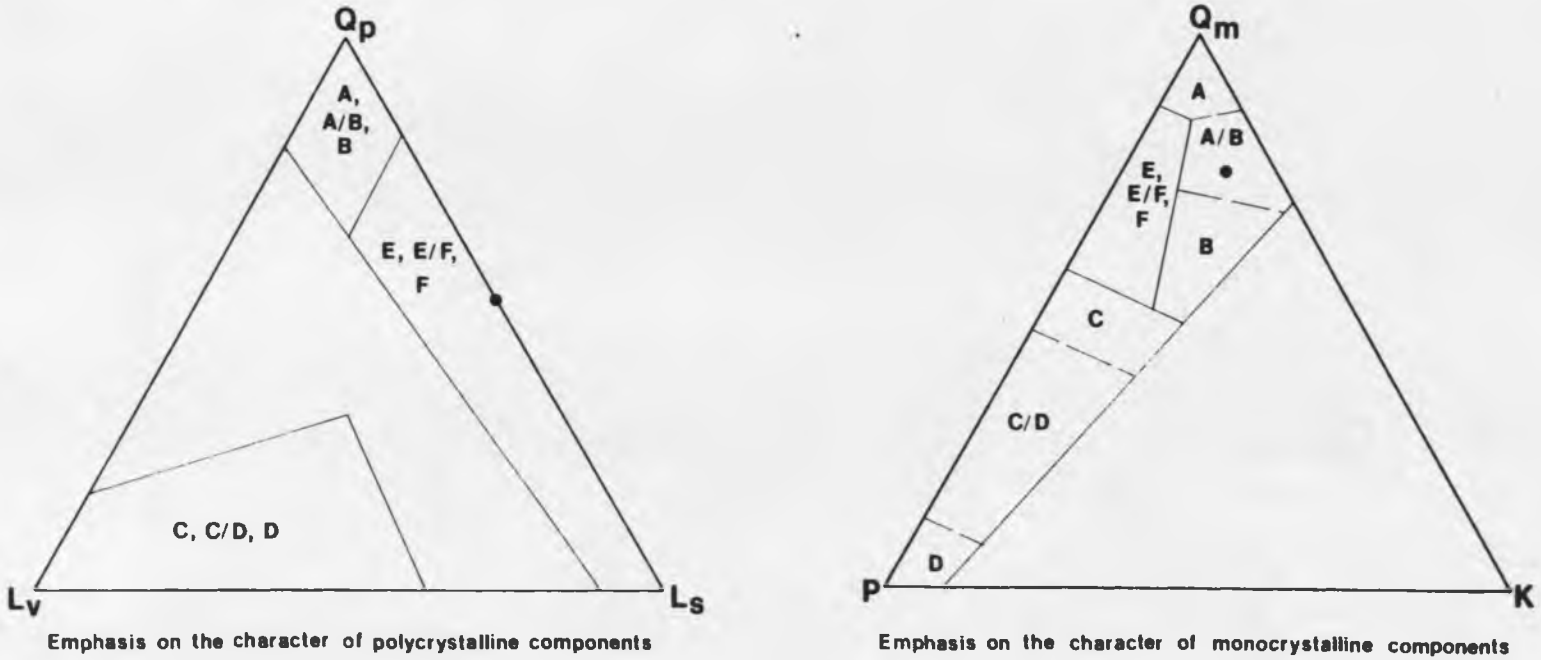

Figure 24. Tectonic Provenance Plots (Qp-Lv-Ls, Qm-P-K) of Bell Canyon and Cherry Canyon Sandstone Samples. The Qp-Lv-Ls plot indicates a recycled orogen provenance; however, this plot is probably least reliable because of the difficulty in accurately identifying rock fragments. As previously, the Qm-P-K plot suggests a provenance transitional between craton interior and uplifted basement.

turity and mineralogy, a more strictly-defined tectonic provenance can be defined. In this case, all plots suggest a continental block provenance, transitional between broad stable cratonic positive areas and locally uplifted basement blocks. This tectonic interpretation is in accord with suggested paleogeographic source areas.

Diagenetic Fabrics

The following sections describe various diagenetic features encountered in the Bell and Cherry Canyon Formations. Figures 25A through 25D, 26A through 26F, 27A through 27D, and 28A through 28F display these features. Further explanation is provided in the proceeding pages.

Quartz and Feldspar Overgrowths

Quartz overgrowths are present in most samples examined, although generally not exceeding a few percent (Figures 25A and 25B). They are difficult to detect in thin section mounts primarily because original grain surfaces lack observable coatings which would accentuate overgrowth presence. SEM examination reveals well-defined euhedral prismatic overgrowths projecting from detrital grain surfaces and generally not exceeding 15-20 micrometers in length (Figures 26A and 26C). Viewing with cathodoluminescence equipment failed to aid in detection be-

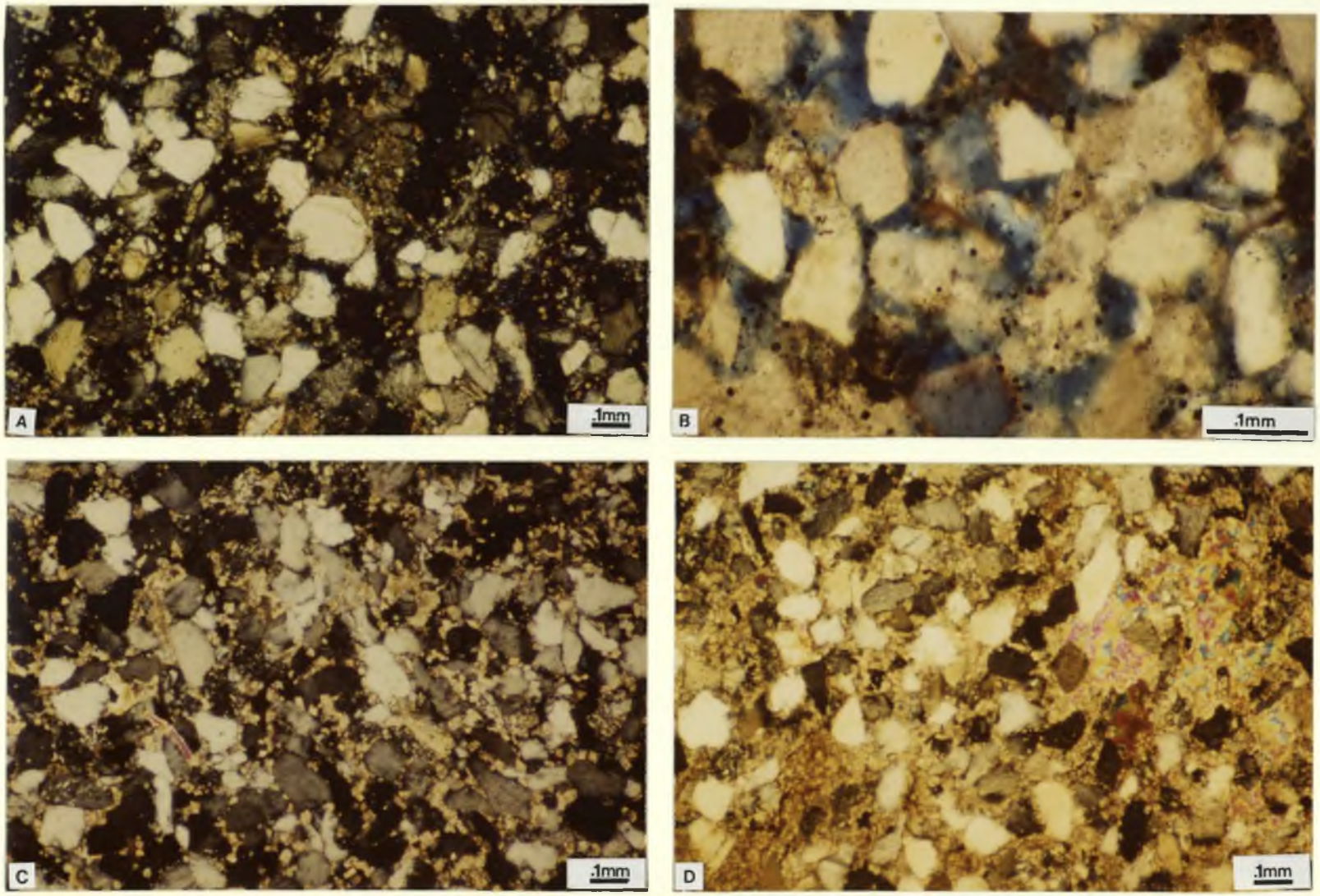

Figure 25. Thin Section Photomicrographs of Quartz Overgrowths and Carbonate Cements

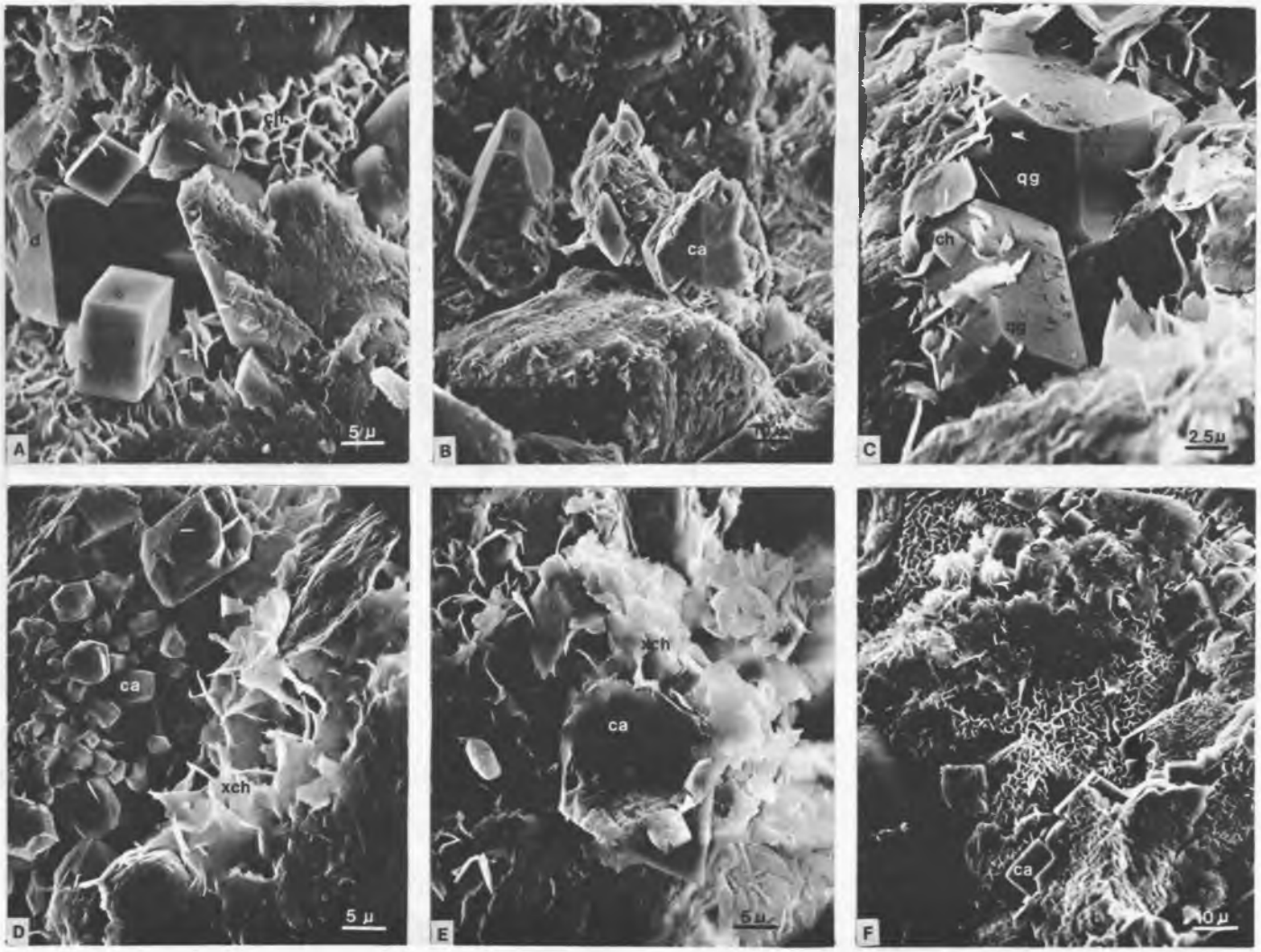

Figure 26. SEM Photomicrographs of Quartz and Feldspar Overgrowths and Calcite Cements

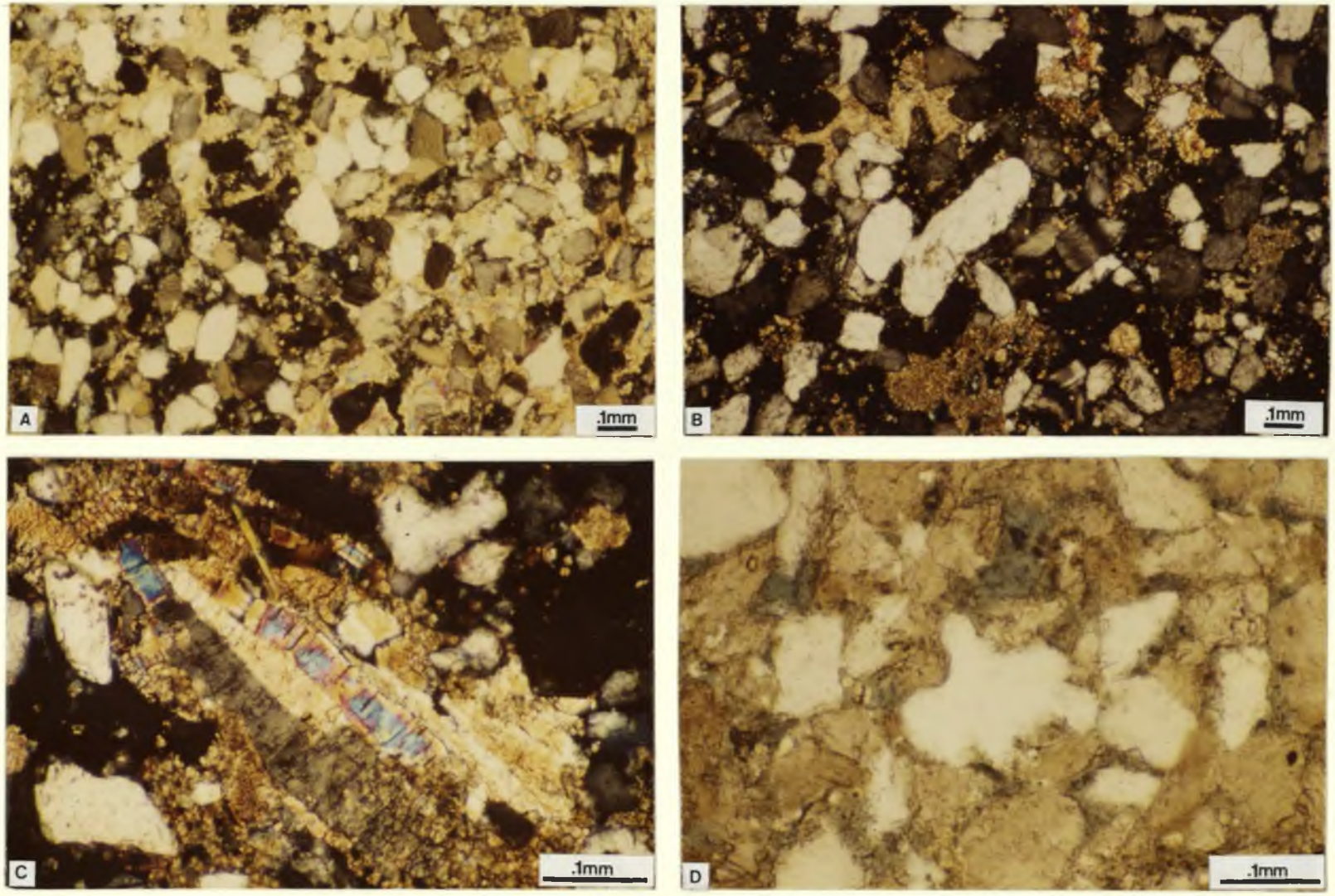

Figure 27. Thin Section Photomicrographs of Calcite, Dolomite and Anhydrite Cements, and Detrital Grain Embayment

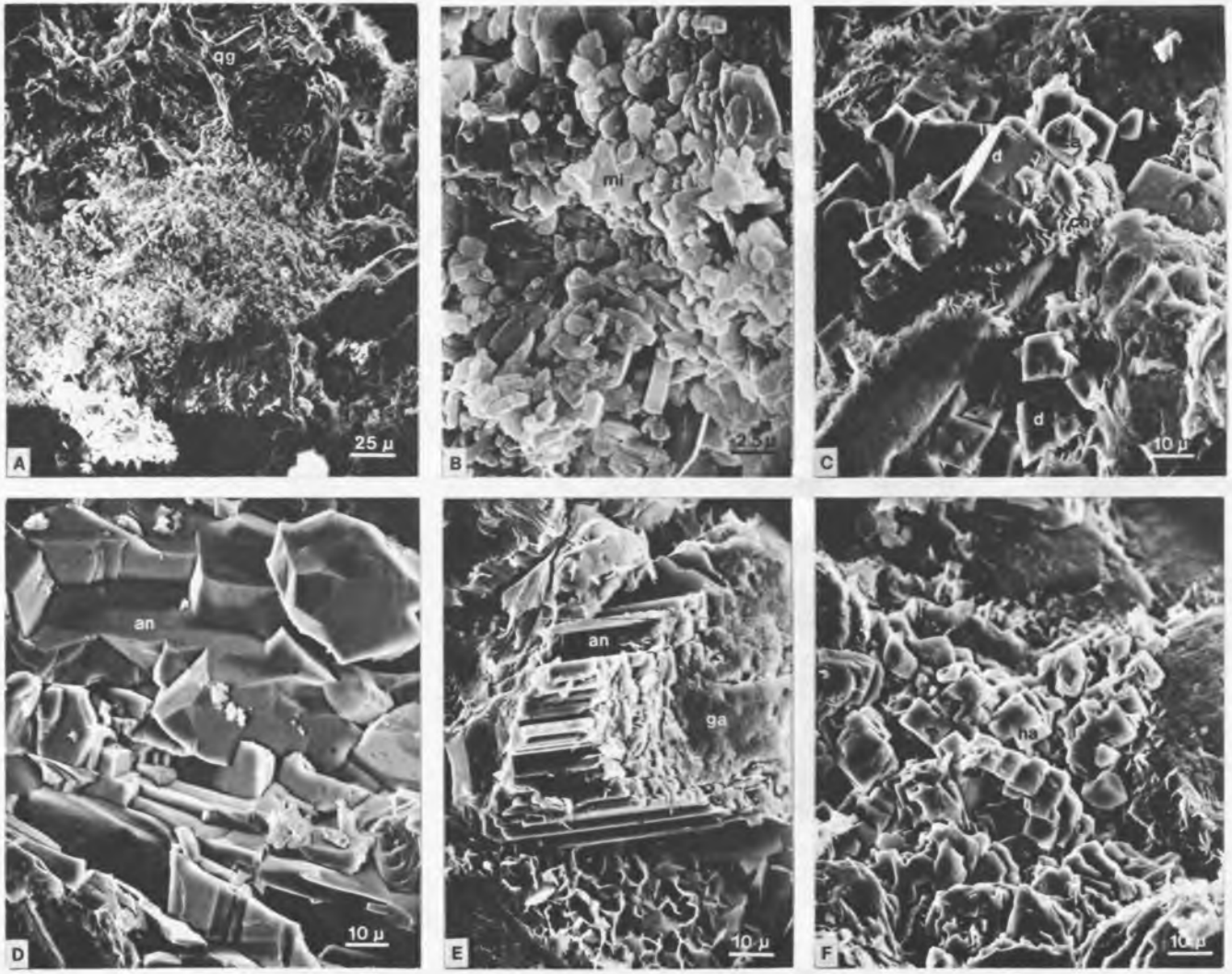

Figure 28. SEM Photomicrographs of Calcite, Dolomite, Anhydrite and Halite Cements

cause the fine grain size of the samples prevented good resolution of overgrowths.

In most instances authigenic quartz postdates the formation of diagenetic clay coatings. This is evident from the intervention of authigenic clay at points of overgrowth attachment, the relatively clay-free overgrowth surfaces and the overall paucity of authigenic quartz. It appears that secondary quartz growth has been prevented from developing by the presence of thick clay rims, being primarily restricted to detrital grain surfaces characterized by thin and interrupted clay coatings. This inhibition of overgrowth nucleation and subsequent development on detrital grain surfaces as a result of authigenic clay coatings has been discussed by Pittman and Lumsden (1967) and Heald and Larese (1974). A few samples display intergrowth of authigenic clay with overgrowth material thereby implying similar timing for these diagenetic events.

Feldspar overgrowths are less numerous, only rarely detected in thin sections or by SEM analysis. Alteration in original detrital feldspar grains prior to overgrowth formation facilitates the recognition of these features in thin section. SEM examination reveals clay-free euhedral overgrowths which are very similar in appearance to those developed on detrital quartz grains (Figures 26B). However, the sharp prismatic terminations characteristic of quartz are absent.

Development of feldspar overgrowths is probably contemporaneous with quartz overgrowth formation although in no situation did contact occur between the two materials to establish their relationship.

Cements

A wide variety of cementing agents have been identified in the Bell Canyon and Cherry Canyon Formations, including quartz and feldspar overgrowths, authigenic clay coatings, and carbonate and sulfate cements. The overgrowths, mentioned previously, are volumetrically insignificant with respect to the other cements. Authigenic clay coatings, although ubiquitous throughout the sections, constitute relatively weak bonds between the grains and do not contribute to pore space occlusion. The carbonate and sulfate cements represented by sparry calcite, dolomite and anhydrite comprise the most significant cementing agents. They account for most of the pore space reduction (besides compaction) that occurs within the sandstones, an important consideration in evaluating reservoir rock potential.

Calcium Carbonate. Calcium carbonate constitutes the greatest percentage of carbonate cement, occurring in nearly every Bell Canyon and Cherry Canyon interval examined, in amounts ranging from less than 1 to 20 percent (Figure 25C). Three distinct types of calcium carbonate are recognized by SEM-EDEX, the most significant being a

finely-crystalline (1 to 25 micrometers) sparry calcite occurring as isolated patches of aggregated crystals or more commonly as uniformly disseminated individual crystals incompletely filling pore spaces (Figures 25E and 26F). Individual crystals are characterized by thin, smooth surfaces, rhombic morphology and detectable magnesium, iron and manganese content (from EDEX analysis). Because of the high magnesium content and rhombic habit of these crystals, it is often difficult to distinguish them from associated dolomite necessitating the use of accompanying stained thin sections and x-ray diffraction analysis.

Very finely-crystalline (less than 10 micrometers) calcite polyhedra are recognized in a few samples (usually restricted to Bell Canyon units) occurring as isolated crystals or small aggregates of randomly oriented crystals attached to detrital grain surfaces (Figure 26D). They are distinguished from the aforementioned sparry calcite by crystal form and chemical composition, lacking detectable magnesium and manganese yet still indicating a slight iron content.

Micrite comprises the third variety of calcium carbonate, being characterized by very finely-crystalline (less than 5 micrometers), elongate to equant, randomly oriented calcite polyhedra (Figures 28A and 28B). It occurs primarily as a secondary replacement of detrital plagioclases and carbonate clasts. Although not encoun-

tered in SEM analysis in this capacity, micrite has also been recognized as a secondary cementing agent occurring in random patches in a few Cherry Canyon thin sections and is usually associated with more coarsely-crystalline sparry calcite cement.

It should also be noted that patches of poikilotopic sparry calcite cement (less than 0.5 mm) have been encountered in some thin sections, but because these areas were not viewed during SEM analyses little can be said concerning crystal morphology or chemical composition.

The formation of authigenic calcite cements appears to have occurred after the growth of initial chlorite rims on detrital grain surfaces. Rhombic calcite was probably the initial cement to form, commencing before the completion of clay growth. The presence of diagenetic clay between calcite rhombs and detrital grain surfaces, and the complex intergrowth of a number of these calcite crystals with authigenic clay flakes supports this conclusion. The polyhedral microcrystalline calcite and micrite display similar relationships with intervening authigenic clay, yet exhibit clay-free surfaces thereby implying a later formation. Lacking are observable contacts between rhombic and polyhedral calcite to substantiate this claim.

Dolomite. Finely-crystalline dolomite (5 to 25 micrometers) accounts for the remaining carbonate cement. Its occurrence in the upper Bell Canyon is insignificant

since it is concentrated primarily in lower Bell Canyon and Cherry Canyon sections. The clearly-defined smooth-faced euhedral dolomite rhombs observed in these lower sections are commonly well-dispersed throughout the formation and result in incomplete occlusion of pore space. In a few sandstone intervals, however, complete cementation has occurred, representing a situation rarely encountered in upper Bell Canyon sediments. Simultaneous development of dolomite and anhydrite suggests an interrelationship between the two authigenic minerals (Figure 25D). SEM-EDEX and x-ray analyses reveal the presence of iron in some of the dolomite, although not in amounts that would require a "ferroan" classification.

The relative time of dolomite formation appears to postdate clay and overgrowth development, yet occurs prior to completion of clay authigenesis as suggested by intergrowth of the two minerals. This is similar to the diagenetic sequence displayed by the sparry calcite cement.

Anhydrite. Anhydrite is restricted to lower Bell Canyon and Cherry Canyon intervals where it occurs as random patches of coarsely-crystalline (0.2 to 1.0 mm) poikilotopic cement (Figures 28D and 28E). In thin section it is easily recognized by its high birefringence (Figure 25D), while SEM examination reveals clay-free aggregates of uniformly oriented rectangular blocklike crystals. Because of its clay-free nature and overlapping contact with

carbonate cements, anhydrite appears to be a later stage diagenetic feature. Rarely dolomite rhombs are found contained within and replacing anhydrite crystals suggesting a late-stage period of dolomite formation, although this constitutes a relatively insignificant percentage of total cement.

Halite. Cubic halite crystals, displaying rounding and pitting as a result of solution, are evident in a few samples (Figure 28F). They represent late-stage crystallization from interstitial saline waters and brine drilling fluids upon reaching the surface. This is supported by the presence of patches of halite crystals exuding from smooth core surfaces and the lack of overprinting by other diagenetic fabrics.

Authigenic Clay

Extensive analyses were performed on the less than 4 micrometers fraction of 46 selected samples in an attempt to better define the composition, morphology and distribution of authigenic clays present in the Bell Canyon and Cherry Canyon Formations. SEM-EDEX examination combined with x-ray diffraction techniques proved to be the most effective means of analysis, with thin sections contributing little because of the extremely poor resolution of authigenic clays at high magnification. Definite relationships between morphology and composition as well as appar-

ent lithological and depth-controlled diagenetic trends can be discerned in samples examined.

Chlorite. The majority of authigenic clay material present is comprised of low temperature and pressure sedimentary chlorite referred to as Ib_d and Ib (β=97°) polytypes (Hayes, 1970). Presence of a broad and diffuse ($20\bar{3}$) reflection, or as in the case of the degraded Ib_d polytype, the absence of such a reflection, confirms this classification. These polytypes reflect the degree of structural ordering within the chlorite lattice, with poorly-ordered Ib_d types occurring at relatively shallow depths and better-ordered Ib types present at greater depths (usually exceeding 5500 feet in this region).

The chlorites occur as authigenic clay coatings on detrital grains, ranging from dense, complete coats to thin, interrupted patches of clay plates oriented perpendicular to grain surfaces (Figures 29A through 29E). The length of individual crystals averages 5 to 10 micrometers distinguishing them from the intermixed finer-grained authigenic illites. Convergence of clay growth in intergranular areas results in the bridging of pore spaces and the subsequent impedence of interstitial fluid flow. Semi-quantitative x-ray analysis (Griffin, 1971), (Table 6) reveals an average chlorite content among the less than 4 micrometers fraction of approximately 70 percent with extremes of 25 percent and 95 percent being recorded. Two

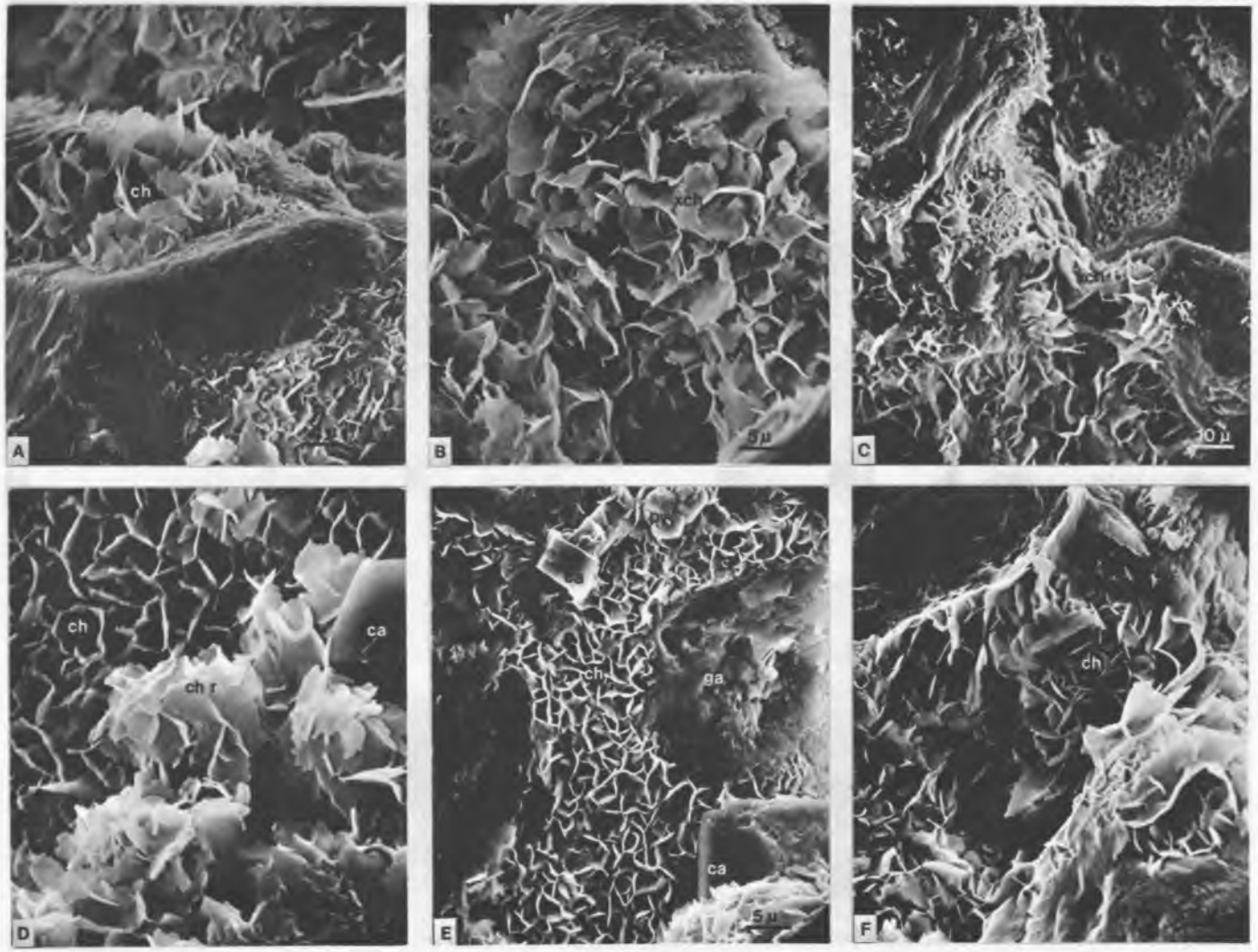

Figure 29. SEM Photomicrographs of Authigenic Chlorite Varieties

Table 6. Semi-Quantitative Determination of Clay Composition* from X-Ray Diffraction Analysis of Selected Bell Canyon and Cherry Canyon Samples**

Sample***	Relative amplitude of (001) reflections Cl / I / I-Cl	Percent chlorite Cl	Percent illite I	Percent mixed I-Cl
Pg-80-141	5.4 / 3.7	59.3%	40.6%	
Pg-80-96	11.0 / 6.7	62.1	37.9	
Pg-80-F	5.3 / 3.7	58.9	41.1	
Pg-80-127	8.9 / 4.7	65.5	34.5	
Pg-80-17	5.2 / 3.6	59.1	40.9	
Pg-80-150	13.4 / 3.7	78.4	21.6	
Pg-80-133	17.0 / 4.7	78.3	21.7	
Pg-80-77	18.1 / 4.2 / 1.3	76.7	17.8	5.5
Pg-80-A	8.3 / 3.9	68.0	32.0	
Pg-80-85	15.1 / 5.0	75.1	24.9	
Pg-80-124	18.1 / 3.4	84.2	15.8	
Pg-80-M	12.0 / 2.6	82.2	17.8	
Pg-80-C	18.2 / 4.0	82.0	18.0	
Pg-80-131	26.3 / 2.4	91.6	8.4	
Pg-80-30	20.7 / 1.4	93.7	6.3	
Pg-80-41	18.6 / 2.2 / 4.4	73.8	8.7	17.5
Pg-80-42	11.0 / 1.8 / 0.7	81.5	13.3	5.2
Pg-80-138	30.0 / 1.6	94.9	5.1	
Pg-80-G	11.3 / 1.7	86.9	13.1	
Pg-80-K	28.2 / 1.9	93.7	6.3	
Pg-80-89	26.1 / 2.9	90.0	10.0	
Pg-80-115	12.0 / 3.0 / 1.5	72.7	18.2	9.1
Pg-80-118	12.9 / 2.0 / 1.3	79.7	12.4	7.9
Pg-80-I	3.1 / 3.1	50.0	50.0	
Pg-80-J	19.9 / 3.1	86.5	13.5	
Pg-80-164	1.4 / 4.3	24.5	75.5	
Pg-80-45	2.2 / 1.0	68.7	31.3	
Pg-80-49	5.8 / 1.1	84.0	16.0	
Pg-80-D	10.3 / 2.3	81.7	18.3	
Pg-80-65	4.0 / 1.4	74.1	25.9	
Pg-80-111	13.4 / 5.3	71.6	28.4	
Pg-80-166	4.6 / 6.6	41.1	58.9	
Pg-80-59	27.2 / 2.2	92.5	7.5	
Pg-80-70	27.9 / 2.8	90.9	9.1	
Pg-80-N	20.4 / 3.7	84.6	15.4	
Pg-80-144	21.0 / 2.4	89.7	10.3	
Pg-80-97	5.6 / 4.1	57.7	42.3	

Table 6. -- Continued

Sample***	Relative amplitude of (001) reflections Cl / I / I-Cl	Percent chlorite Cl	Percent illite I	Percent mixed I-Cl
Pg-80-101	19.9 / 3.3 / 2.4	77.7	12.9	9.4
Pg-80-105	12.3 / 3.3	78.8	21.2	
Pg-80-189	2.6 / 2.7	49.0	51.0	
Pg-80-110	5.7 / 1.6 / 1.5	64.8	18.2	
Pg-80-L	10.3 / 4.5	69.6	30.4	
Pg-80-E	2.8 / 3.6	43.7	56.3	
Pg-80-192	1.5 / 1.6	48.4	51.6	
Pg-80-165	3.0 / 6.6	31.3	68.7	
Pg-80-161	2.0 / 4.8	29.4	70.6	

Chlorite

Mean = 71.5%
= 17.8

Illite

Mean = 26.6%
= 18.6

*Only the less than 4 micrometer fraction was considered.
**Technique according to Griffin, 1971.
***Samples arranged in order of increasing depth.

compositionally distinct chlorites can be recognized on the basis of the relative amplitude of initial basal, (001) to (004), reflections (Brown, 1955; Brindley and Gillery, 1956). Iron-rich chlorites display relatively weak first and third order basal reflections while magnesium-rich varieties exhibit equally intense reflections for all orders. Transitional members also occur. Quantitative analysis according to methods outlined by Schoen (1962) (Table 7) confirms qualitative compositional identifications with iron-rich varieties containing four or more iron atoms and magnesium-rich varieties containing 10 to 12 magnesium atoms per octahedral layer (octahedral layers are generally characterized by 12 magnesium atoms occupying all available positions prior to random substitution by iron atoms).

Variation in chlorite morphology is observed with depth. In addition, a corresponding change in chemical composition is also noted. The morphological varieties will be distinguished in the following paragraphs with apparent diagenetic clay zonation to be considered in a later section.

The first group of chlorites are represented by leafy, slightly crenulated, irregularly-edged plates arranged in a honeycomb-like cellular pattern (Figures 29A, 29B and 29C). The crenulation and ragged edges are probably a result of dehydration of expandable layers which

Table 7. Determination of Relative Iron and Magnesium Content of Chlorites from Selected Bell Canyon and Cherry Canyon Samples by Semi-Quantitative X-ray Diffraction Analysis

Sample	Intensity (001)	Intensity (002)	Intensity (003)	°2θ (001)	°2θ (002)	°2θ (003)	Structure Factor (F)[1] (001)	Structure Factor (F)[1] (002)	Structure Factor (F)[1] (003)	F(003)/ F(001)/	F_t (theoretical)[2] /(001)/	F_t (theoretical)[2] /(003)/	Mean[3] F_t/F	F_t (002)	Mg[4]	Fe[4]
Pg-80-17	17	23	6	6.14	12.47	18.76	0.96	1.61	1.02	1.06	87	91	90.0	145.0	8	4
Pg-80-30	68	100	28	6.15	12.42	18.69	1.92	3.31	2.18	1.13	84	94	43.5	142.0	8	4
Pg-80-41	62	82	22	6.21	12.52	18.74	1.84	3.01	1.93	1.05	87	91	47.2	142.0	8	4
Pg-80-42	36	68	20	6.11	12.32	18.59	1.39	2.72	1.83	1.31	77	101	55.3	150.0	8	4
Pg-80-45	7	7	2	6.11	12.38	18.70	0.61	0.87	0.57	0.93						
Pg-80-49	20	18	8	6.13	12.38	18.67	1.02	1.39	1.16	1.14	83	94	81.2	112.9	11	1
Pg-80-59	90	73	24	6.14	12.39	18.71	2.20	2.83	2.03	0.92						
Pg-80-65	13	10	4	6.23	12.49	18.70	0.85	1.04	0.84	0.98	91	88	106.0	110.2	11	1
Pg-80-70	93	86	28	6.15	12.39	18.74	2.24	3.07	2.18	0.97	91	88	40.5	124.0	10	2
Pg-70-77	60	53	14	6.23	12.46	18.80	1.81	2.42	1.51	0.83						
Pg-80-85	50	39	12	6.24	12.55	18.85	1.65	2.08	1.43	0.87						
Pg-80-89	87	98	27	6.18	12.48	18.67	2.17	3.28	2.13	0.98	91	88	41.6	136.4	9	3
Pg-80-96	35	26	7	6.20	12.53	18.72	1.38	1.70	1.09	0.79						
Pg-80-97	19	16	5	6.16	12.46	18.61	1.01	1.33	0.97	0.96	91	88	90.4	120.2	10	2
Pg-80-101	66	35	14	6.28	12.49	18.75	1.90	1.97	1.51	0.79						
Pg-80-105	41	28	15	6.23	12.46	18.76	1.50	1.76	1.59	1.06	87	91	57.6	101.4	12	0
Pg-80-110	19	11	4	6.24	12.43	18.79	1.02	1.10	0.82	0.80						
Pg-80-111	45	28	11	6.23	12.43	18.73	1.57	1.76	1.36	0.87						
Pg-80-115	40	39	12	6.18	12.47	18.71	1.47	2.07	1.42	0.97	91	88	61.9	128.1	9	3
Pg-80-118	43	48	14	6.30	12.51	18.78	1.54	2.29	1.54	1.00	89	89	57.8	132.3	9	3
Pg-80-124	60	91	25	6.22	12.49	18.71	1.81	3.16	2.06	0.55						
Pg-80-127	30	32	9	6.14	12.48	18.70	1.26	1.88	1.23	0.98	91	88	71.9	135.2	9	3
Pg-80-131	88	87	22	6.25	12.54	18.72	2.19	3.11	1.91	0.87						
Pg-80-133	56	40	12	6.24	12.50	18.76	1.75	2.10	1.43	0.82						
Pg-80-138	100	110	33	6.20	12.45	18.78	2.33	3.48	2.37	1.02	89	90	38.1	132.6	9	3
Pg-80-141	18	14	3	6.28	12.48	18.74	0.99	1.24	0.71	0.72						
Pg-80-144	70	55	22	6.25	12.45	18.80	1.96	2.46	1.93	0.98	91	88	46.0	113.2	11	1
Pg-80-150	45	32	9	6.28	12.46	18.84	1.57	1.86	1.24	0.79						
Pg-80-161	6	13	4	6.22	12.50	18.76	0.57	1.18	0.82	1.44	73	104	127.4	150.3	8	4
Pg-80-164	4	8	3	6.21	12.48	18.80	0.47	0.91	0.71	1.51	71	106	150.2	136.7	9	3
Pg-80-165	10	15	7	6.24	12.50	18.81	0.74	1.27	1.05	1.42	74	104	99.5	126.4	10	2
Pg-80-166	15	21	11	6.18	12.43	18.80	0.90	1.50	1.37	1.52	73	106	79.2	118.8	10	2
Pg-80-189	9	5	2	6.27	12.45	18.80	0.70	0.74	0.58	0.83						
Pg-80-192	5	5		6.10	12.50											
Pg-80-A	28	27	7	6.24	12.49	18.75	1.24	1.71	1.09	0.88	84	94	46.0	97.5	12	0
Pg-80-C	60	77	25	6.30	12.50	18.70	1.82	2.12	2.05	1.13	76	102	55.4	114.1	11	1
Pg-80-D	35	39	20	6.21	12.50	18.71	1.37	2.06	1.84	1.34	75	102	101.2	121.4	10	2
Pg-80-E	10	13	6	6.23	12.50	18.70	0.74	1.20	1.01	1.37	78	100	80.8	130.1	9	3
Pg-80-F	18	24	9	6.22	12.43	18.73	0.97	1.61	1.23	1.27	85	93	58.7	147.3	8	4
Pg-80-G	38	57	15	6.25	12.50	18.76	1.44	2.51	1.59	1.10	79	98	106.6	117.3	10	2
Pg-80-I	10	11	5	6.30	12.50	18.85	0.74	1.10	0.92	1.24	89	90	46.6	116.0	10	2
Pg-80-J	66	56	22	6.29	12.49	18.80	1.91	2.49	1.93	1.01						
Pg-80-K	93	73	22	6.28	12.49	18.73	2.26	2.84	1.91	0.84	89	89	64.2	104.6	11	1
Pg-80-L	35	24	12	6.20	12.48	18.65	1.38	1.63	1.39	1.00	85	93	56.9	134.8	9	3
Pg-80-M	40	51	16	6.22	12.48	18.76	1.48	2.37	1.65	1.12	85	93	43.9	121.2	10	2
Pg-80-N	68	69	27	6.20	12.50	18.74	1.92	2.76	2.14	1.11						

[1]Structure factor (F) = Intensity x $\frac{(1 + \cos^2 2\theta)}{\sin 2\theta}$

[2]Theoretical structure factor (F_t) obtained from table 1 in Schoen (1962)

[3]Mean $F_t/F = (F_t(003) / F(003)) + (F_t(001)/F(001)) / 2$

[4]Mg and Fe atoms per octahedral layer determined from table 1 in Schoen (1962)

Note: On the average, an Mg/Fe ratio of 9/3 seems to separate iron-rich and magnesium-rich varieties of chlorite (as determined, semi-quantitatively, by comparison of the relative intensities of the (001) through (004) basal reflections according to Brown (1965) and Brindley and Gillery (1956)). Comparison of the two methods suggests that ratios from 12Mg/0Fe to 9Mg/3Fe are magnesium-rich and 9Mg/3Fe to 8Mg/4Fe are iron-rich.

have been randomly incorporated into the chlorite structure. The presence of these expandable layers is recognized on x-ray diffraction traces by asymmetry on the low angle sides of the low order stable chlorite peaks ((001), (002), (003)), and the subsequent slight shift of these peaks upon glycolation of the sample (an average shift of 14.2 Å to 14.5 Å is recognized for the (001) reflection). The inconsistency displayed by this shift implies a random interlayering and a variability in amount of expandable layers per individual chlorite structures, referred to as "swelling chlorites" by Lucas (1963). Heat treatment (550°C for 2 hours) also confirms this variability of composition. Regular chlorite experiences sharp increases in the amplitude of the first order basal (001) reflection as a result of this treatment, while contamination by mixed expandable layers subdues this effect. Although the resultant morphology of these mixed-layer chlorites is similar in many respects to smectite (Wilson and Pittman, 1977), other features diagnostic of smectite such as a (001) basal reflection between 12 and 15 Å which subsequently expands to 17 Å upon glycolation, are absent.

These chlorites are generally found in upper Bell Canyon sections and are characterized by more iron-rich compositions (8 Mg/4 Fe to 10 Mg/2 Fe for the 12 octahedral atoms per unit layer).

The second group of chlorites exhibits better structural ordering and less interlayering of expandable material. They generally display smoother-edged, more uniformly-shaped plates which are again arranged in a honeycomb pattern (Figures 29E and 29F). Individual chlorite crystals, ranging from 5 to 10 micrometers, are more easily distinguished within thick aggregates of clay growth than the shallower expandable chlorite flakes which are nearly unresolvable. Rarely chlorite crystals, arranged in rosette clusters, are observed intergrown with individual chlorite flakes (Figure 29D).

This group of chlorites are characteristically observed at depths greater than 5500 feet in upper to middle Cherry Canyon intervals and display magnesium contents from 12 Mg/0 Fe to 10 Mg/2 Fe atoms per octahedral layers. The lack of expandable layers can probably be attributed to dewatering as a result of increased overburden; however, a greater magnesium content may have had some influence on the extent to which interlayering could occur within the chlorite structure.

Illite. Illites have also been identified in all samples examined, averaging 25 percent of the less than 4 micrometers fraction. Higher percentages are generally restricted to the siltstone facies while lower extremes tend to be associated with the very fine-grained sandstones. The higher illite content associated with siltstones may

not represent actual illite percentages. It is possible that a significant amount of finely-crushed detrital mica displaying basal reflections coincident with those of illite may have contaminated the less than 4 micrometers fraction, thereby increasing computed authigenic illite percentages.

X-ray diffraction yields distinct low order basal illite peaks ((001) at 10 Å, (002) at 5 Å) plus stable (upon treatment) peaks intermediate between chlorite and illite (8.5 to 8.7 Å) which may suggest some random interlayering of the two minerals. The illites recognized are dioctahedral which is confirmed by the presence of a distinct 5 Å reflection. It is difficult to determine the specific illite polytype as defined by Levinson (1955) because of the lack of diagnostic (hkl) reflections ((hkl) reflections are obtained through the use of unoriented samples). Because IM (degraded) and 2M polymorphs occur in sedimentary rocks (Levinson, 1955) the possibility exists that either are present in the samples examined. The slight asymmetry of the (001) reflection at 10 Å toward the low angle side and the (003) reflection at 3.3 Å toward the high angle side, in addition to a decrease in the (001) reflection's amplitude upon glycolation (Thoraz, 1976), suggests the presence of a degraded or "open" illite structure (Bradley, 1954; Kubler, 1962; Lucas, 1963). More specifically this is a member intermediate between pure and

mixed-layer illite varieties which contains minor amounts of interlayered material. These open illites can be classified as the I_c variety (Lucas, 1963), containing interlayered stable chlorite, with asymmetry of the (001) reflection toward the same basal chlorite peak and characterized by relative stability upon glycolation and heat treatment. Another possibility is the I_{cG} variety (modification of Lucas, 1963) in which very minor amounts of expandable chlorite are interlayered within the illite structure creating negligible expansion after glycolation (net peak shift of 0.01 to 0.05 Å (Figure 29C)).

Illite crystal size averges 3 to 7 micrometers with finger-like projections extending fractions of a micrometer from the platy crystal body (Figures 30A and 30B). The thin, long, delicate wisplike projections often associated with authigenic illites (Wilson and Pittman, 1977) are absent in almost all samples examined, possibly as a result of their destruction during specimen preparation. The dominance of chloritic clays masks the presence of illite in most samples.

Chemical composition of the illites was determined. Ratio tests for the determination of magnesium-rich ((001)/(002) 2) and iron-rich ((001)/002) 3) illites (White, 1962), (Table 8) proved to be nearly useless because of the small quantities of illite present, interlay-

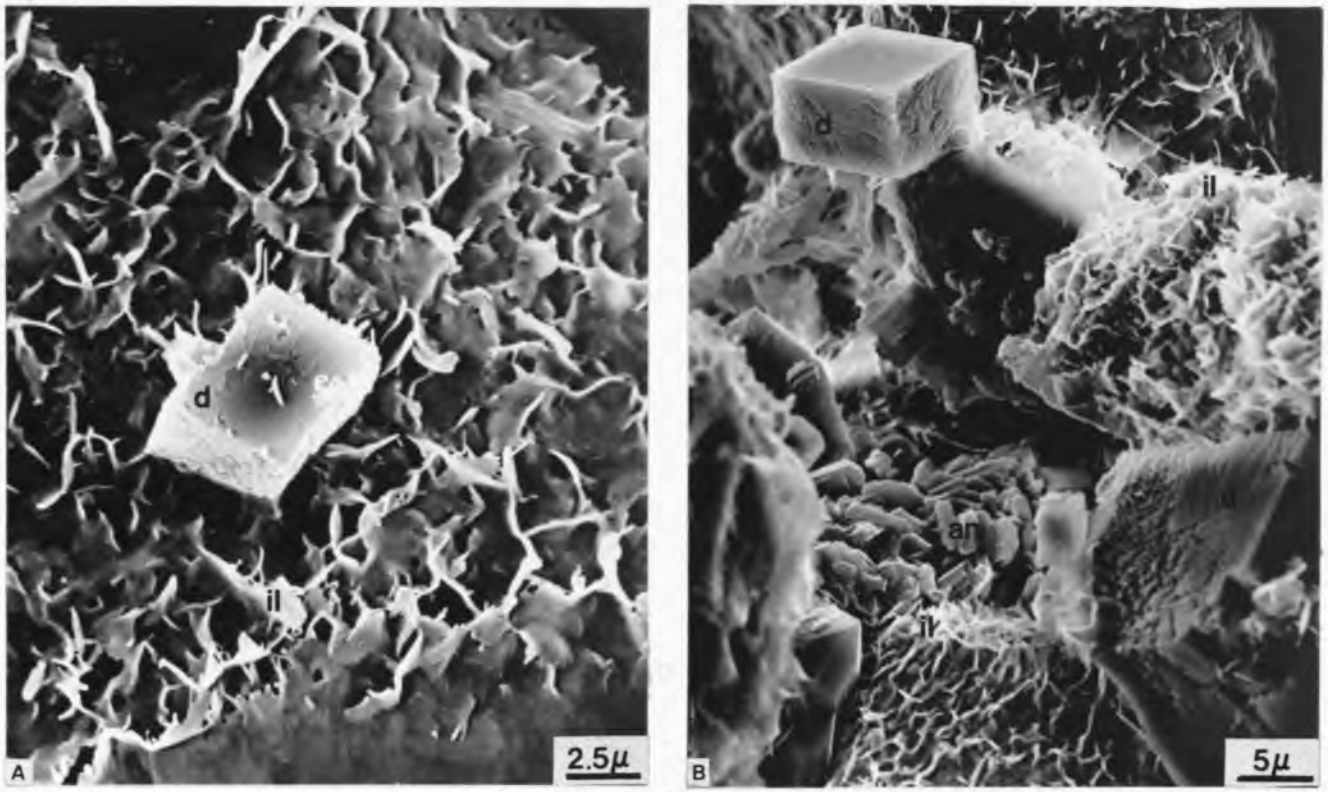

Figure 30. SEM Photomicrographs of Authigenic Illilte

A. Dolomite crystal (d) floating amidst authigenic illite (il). Note the very fine fibrous extensions along the edges of the illite crystals in the lower portion of the photo. Pg-80-E, 5975', 4000x.

B. Illite (il) is the dominant clay present, characterized by long, fibrous projections (upper right). Dolomite rhombs (d) also occur, projecting into interstitial areas, as do unoriented aggregates of rectangular anhydrite crystals (an), filling pore throats. Pg-80-E, 5975', 2000x.

Table 8. Determination of Relative Iron and Magnesium Content of Illites from Selected Bell Canyon and Cherry Canyon Samples by Semi-Quantitative X-Ray Diffraction Analysis*

Sample	(001)**	(002)**	(001)/(002)	Composition
Pg-80-17	16	6	2.7	Fe-Mg
Pg-80-30	6	1	6.0	Fe
Pg-80-41	10	8	1.3	Mg
Pg-80-42	8	6	1.3	Mg
Pg-80-45	4	3	1.3	Mg
Pg-80-49	5	4	1.3	Mg
Pg-80-59	10	6	1.7	Mg
Pg-80-65	6	5	1.2	Mg
Pg-80-70	12	10	1.2	Mg
Pg-80-77	18	9	2.0	Mg
Pg-80-85	21	13	1.6	Mg
Pg-80-89	13	11	1.2	Mg
Pg-80-96	29	9	3.2	Fe
Pg-80-97	17	6	2.8	Fe-Mg
Pg-80-101	14	11	1.3	Mg
Pg-80-105	14	7	2.0	Mg
Pg-80-110	7	5	1.4	Mg
Pg-80-111	23	14	1.6	Mg
Pg-80-115	13	7	1.9	Mg
Pg-80-118	9	7	1.3	Mg
Pg-80-124	15	10	1.5	Mg
Pg-80-127	19	10	1.9	Mg
Pg-80-131	10	12	0.8	Mg
Pg-80-133	20	10	2.0	Mg
Pg-80-138	7	13	0.5	Mg
Pg-80-141	15	7	2.1	Fe-Mg
Pg-80-144	10	9	1.1	Mg
Pg-80-150	16	9	1.8	Mg
Pg-80-161	20	6	3.3	Fe
Pg-80-164	18	5	3.6	Fe
Pg-80-165	27	7	3.9	Fe
Pg-80-166	28	11	2.5	Fe-Mg
Pg-80-189	11	0	-	-
Pg-80-192	7	0	-	-
Pg-80-A	16	6	2.7	Fe-Mg
Pg-80-C	17	11	1.5	Mg
Pg-80-D	10	6	1.7	Mg
Pg-80-E	16	7	2.3	Fe-Mg
Pg-80-F	15	6	2.5	Fe-Mg

*According to White, 1962
**Relative intensity of basal peaks

Table 8. -- Continued

Sample	(001)**	(002)**	(001)/(002)	Composition
Pg-80-G	7	5	1.4	Mg
Pg-80-I	12	4	3.0	Fe
Pg-80-J	13	9	1.4	Mg
Pg-80-K	8	13	0.6	Mg
Pg-80-L	19	11	1.7	Mg
Pg-80-M	11	9	1.2	Mg
Pg-80-N	15	10	1.5	Mg

(001)/(002) 2 - Magnesium-rich illites
(001)/(002) 3 - Iron-rich illites

ering within the illite structure and abundance of ratio values in the 2 to 3 range.

Figures 31, 32 and 33 display characteristic x-ray diffraction patterns for the less than 4 micrometers fraction of selected sandstone and siltstone samples. Note the changes in clay type, chlorite composition and mixed-layer varieties present in the samples examined.

Discussion. The few authors (Dahl, 1965; Watson, 1974; Williamson, 1978) who have investigated clays within the Delaware Mountain Group have identified a variety of clay species, primarily occurring in the northern half of the Delaware basin. In all studies, stable chlorite and an expandable mixed-layer chlorite have been recognized, although a variety of expandable materials have been suggested (Dahl, 1965 - montmorillonite; Watson, 1974 - corrensite-like vermiculite; Williamson, 1978 - smectite). Illite (and the associated expandable and chloritic mixed-layer varieties) has also been identified by Dahl (1965) and Williamson (1978). Watson (1974) has also proposed the presence of kaolinite in the subsurface. However, this is poorly supported in similar studies, although its presence has been noted through thin section examination of outcrop samples (Berg, 1979).

Authigenic clay formation, relative to the development of other diagenetic fabrics, took place over a considerable span of time. Clay growth occurred prior to and

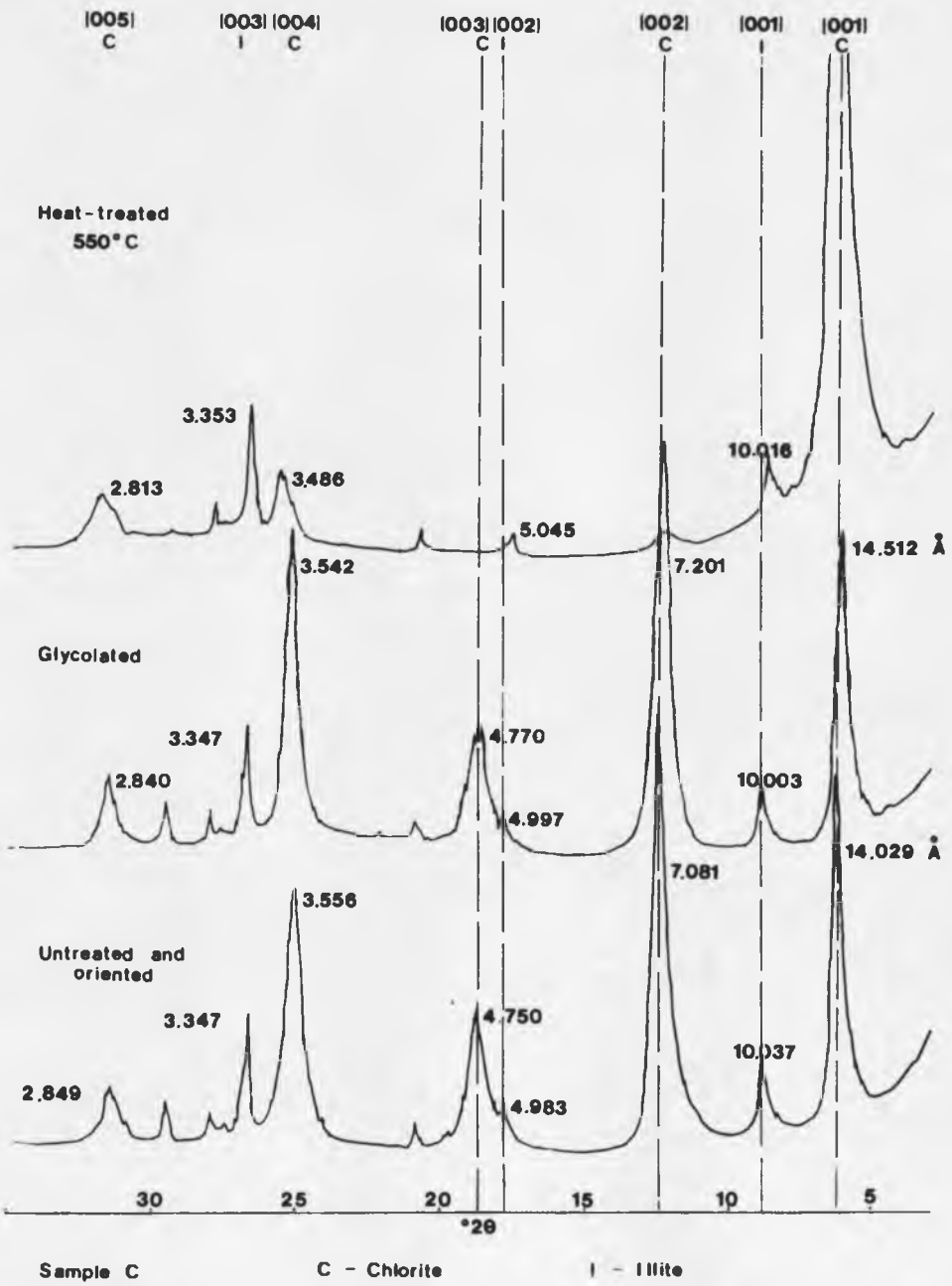

Figure 31. Clay Fraction Obtained from Bell Canyon Sandstone Displaying Authigenic Expandable Chlorite and Illite. Note that the dominant chlorite species displays a nearly imperceptible shift in lower basal peaks upon glycolation which suggests the presence of expandable layers. Illite is the subordinate clay species with evidence of an open illite structure reflected in the a symmetry of the basal peaks.

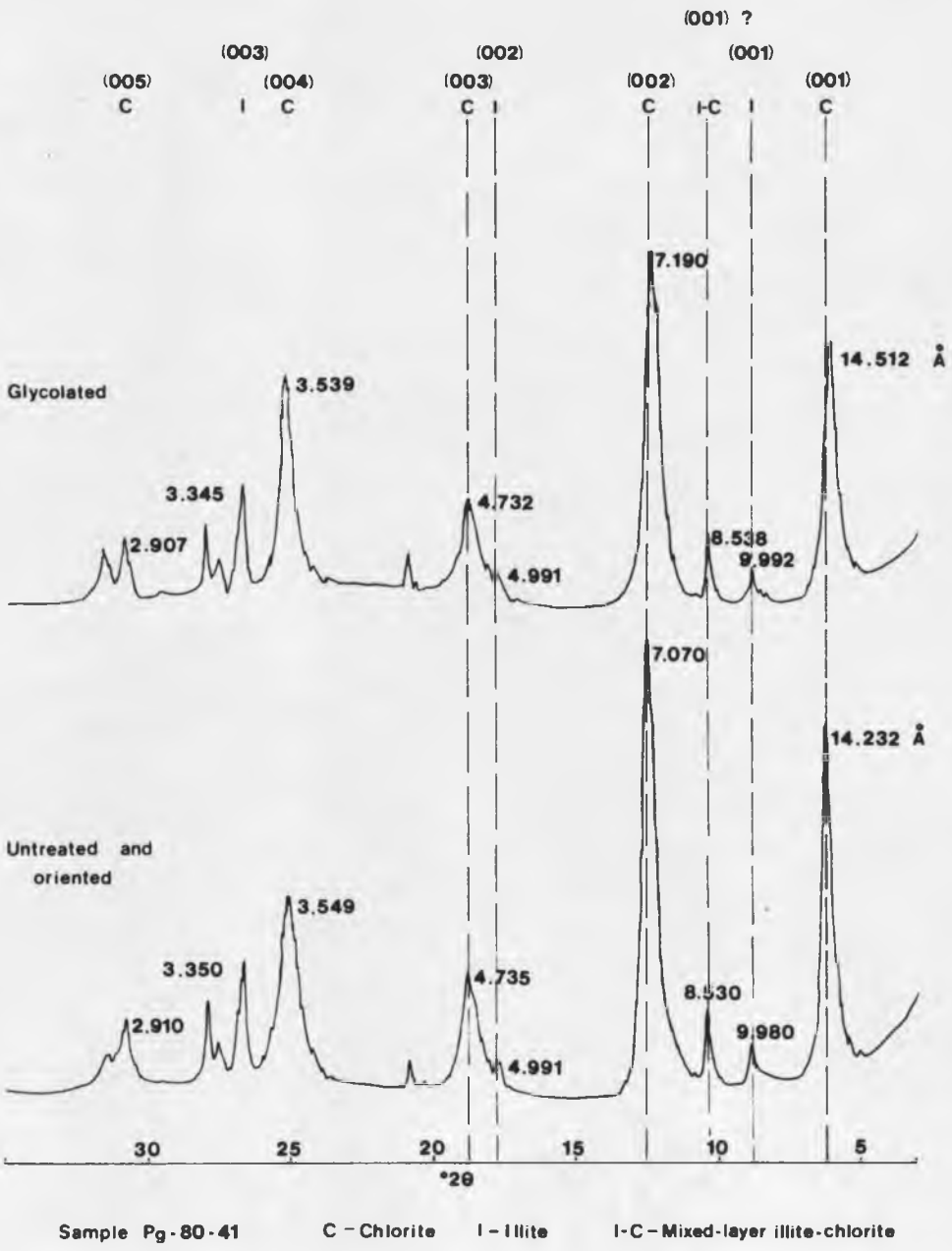

Figure 32. Clay Fraction Obtained from Bell Canyon Sandstone Displaying Authigenic Slightly Expandable Chlorite, Illite and Mixed-Layer Illite-Chlorite. The illite and illite-chlorite peaks display stability upon treatment with chlorite shifting only slightly to the right.

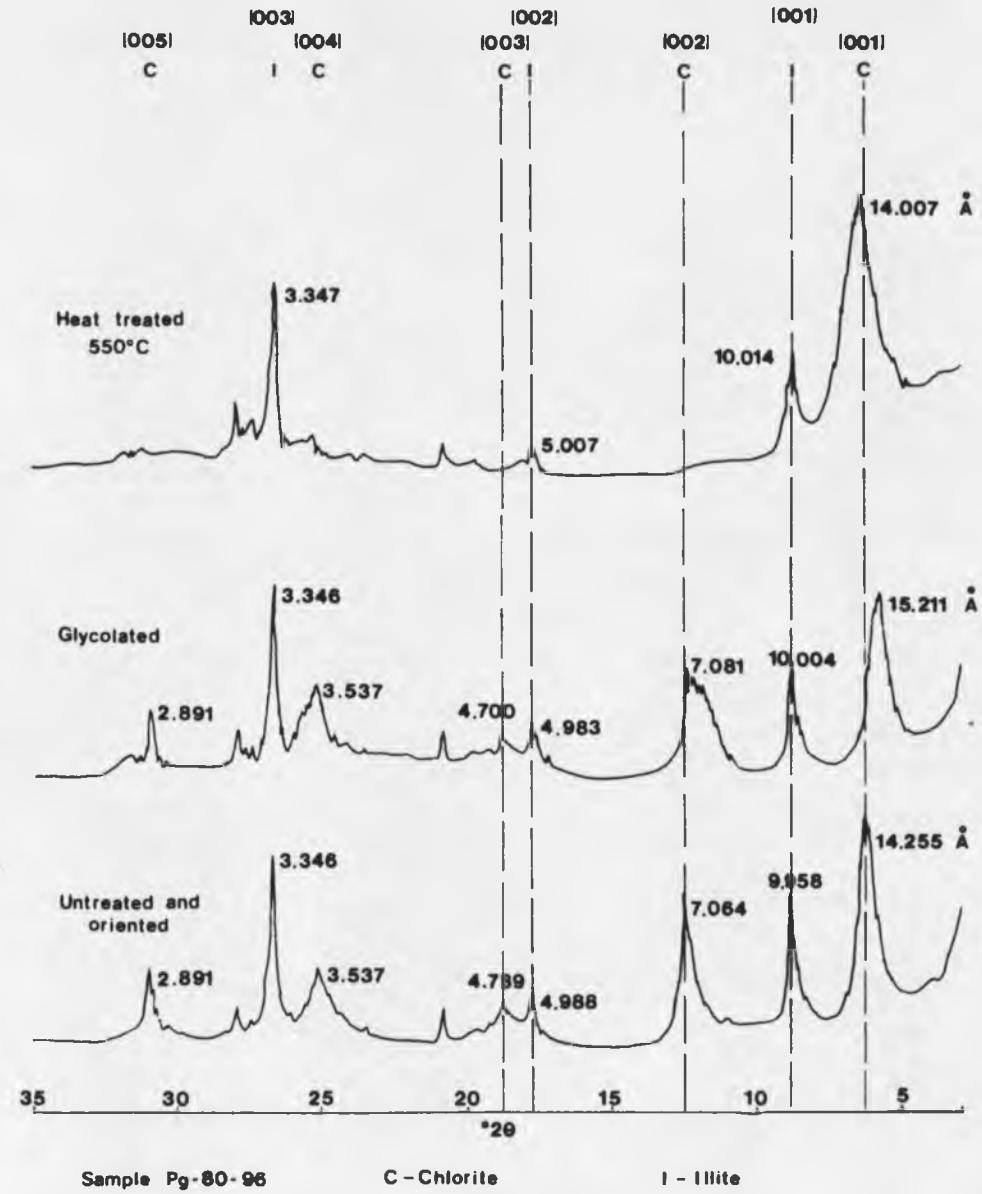

Figure 33. Clay Fraction Obtained from Bell Canyon Shaly Siltstone. Chlorite contains a significant amount of expandable layers. Strong illite peaks reflect an increased dominance of this clay species. Asymmetry of illite, and the slight shift and reduction of the (001) peak upon glycolation suggests the presence of an open illite structure.

contemporaneous with the development of carbonate cements and grain alteration fabrics. There may have been periods of significant clay growth following carbonate cementation as suggested by the ability of heavy cementation to impede further formation of clay coats on detrital grains.

Pyrite

Authigenic pyrite occurs as very fine, disseminated cubes or octahedra approximately 5 to 20 micrometers in diameter (Figure 25B). Pyrite has an affinity for the siltstone units because of the higher concentration of contained organic matter, although its occurrence is not limited to these units. Growth is restricted primarily to interstitial areas with minor replacement of framework grains and carbonate cement also evident.

Other Diagenetic Features

Additional diagenetic features were encountered during sample examination including framework grain corrosion and embayment, pressure solutioning and subsequent suturing of grain boundaries, detrital grain deformation and minor developemnt of secondary porosity.

Surface corrosion of detrital grains is evident in a few samples as a result of replacement by microcrystalline calcite and micrite. This carbonate material has replaced detrital carbonate clasts which were incorporated into massive sand bodies during transport into the basin.

Subsequent burial resulted in deformation, dissolution and/or replacement of these clasts, the timing of which is difficult to determine at the present state of diagenesis. Concurrent with these events was dissolution and replacement of detrital grains at points of contact with the clasts. It is evident that a greater amount of detrital carbonate material was formerly included in the units by the presence of a number of embayed (due to solution corrosion) plutonic quartz grains not presently in contact with carbonate clasts. Dissolution of the carbonate clasts resulted in the development of a minor amount of secondary porosity which was subsequently occluded by carbonate cement. Much of this cement was probably derived during clast dissolution.

Another type of grain alteration is displayed by the feldspars, previously described in an earlier section. It is of interest to note that feldspar alteration has been so complete in some instances that all that remains is the thick authigenic clay coat.

Grain to grain contacts between framework components are predominantly of the concavo-convex or straight type. In samples derived from depths greater than 5200 feet, closer packing, random occurrences of sutured boundaries and occasional deformation of lithic clasts are evident. Overall one might anticipate closer packing and more evidence of overburden effects in these samples because of

the absence of grain supportive primary and secondary cements. Perhaps the early development of thick clay coats has alleviated these effects in the absence of cementing agents.

CHAPTER 6

DIAGENESIS OF THE BELL CANYON AND CHERRY CANYON FORMATIONS

Diagenetic Sequence of Fabric and Feature Development

The relative timing of diagenetic events (Figure 34) can be determined from the overlapping relationships of the secondary fabrics involved (Figures 35A through 35F). However, the same events cannot easily be placed within the strict constraints of absolute time because of the inability to isolate individual authigenic materials and perform the necessary time-determinative analyses. Fortunately in most situations knowledge of relative timing is sufficient to unravel the unit's diagenetic history and determine its subsequent hydrocarbon potential.

Deposition of Bell Canyon and Cherry Canyon sediments resulted in the accumulation of irregular sandstone channels and laterally uniform siltstone units displaying high initial porosities and permeabilities. This can be attributed to the well-sorting of the framework components in addition to the lack of detrital clay-size material included within the units. Because of the significant content of micaceous material, the siltstones demonstrated a

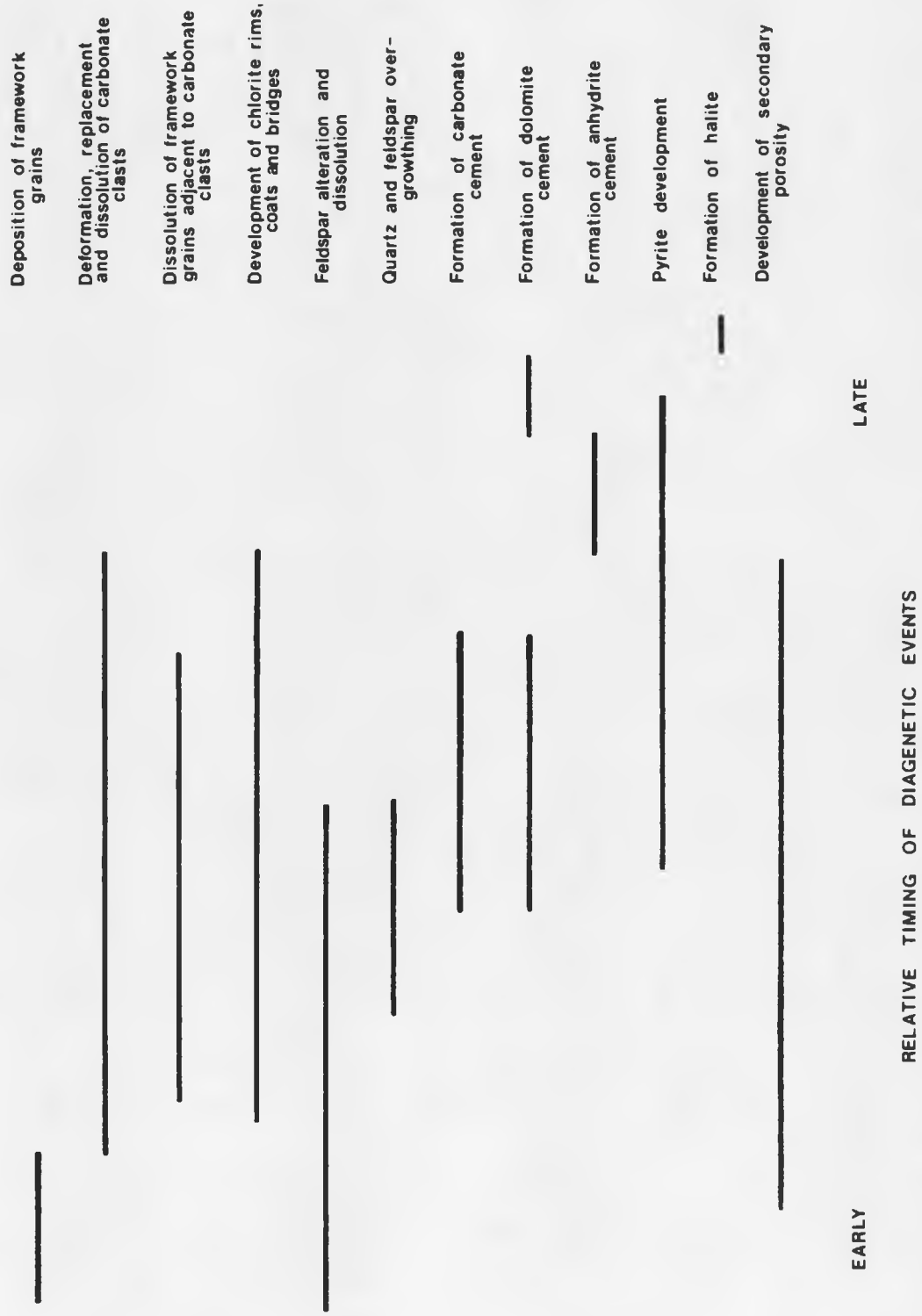

Figure 34. Relative Ordering of Diagenetic Fabric and Feature Development

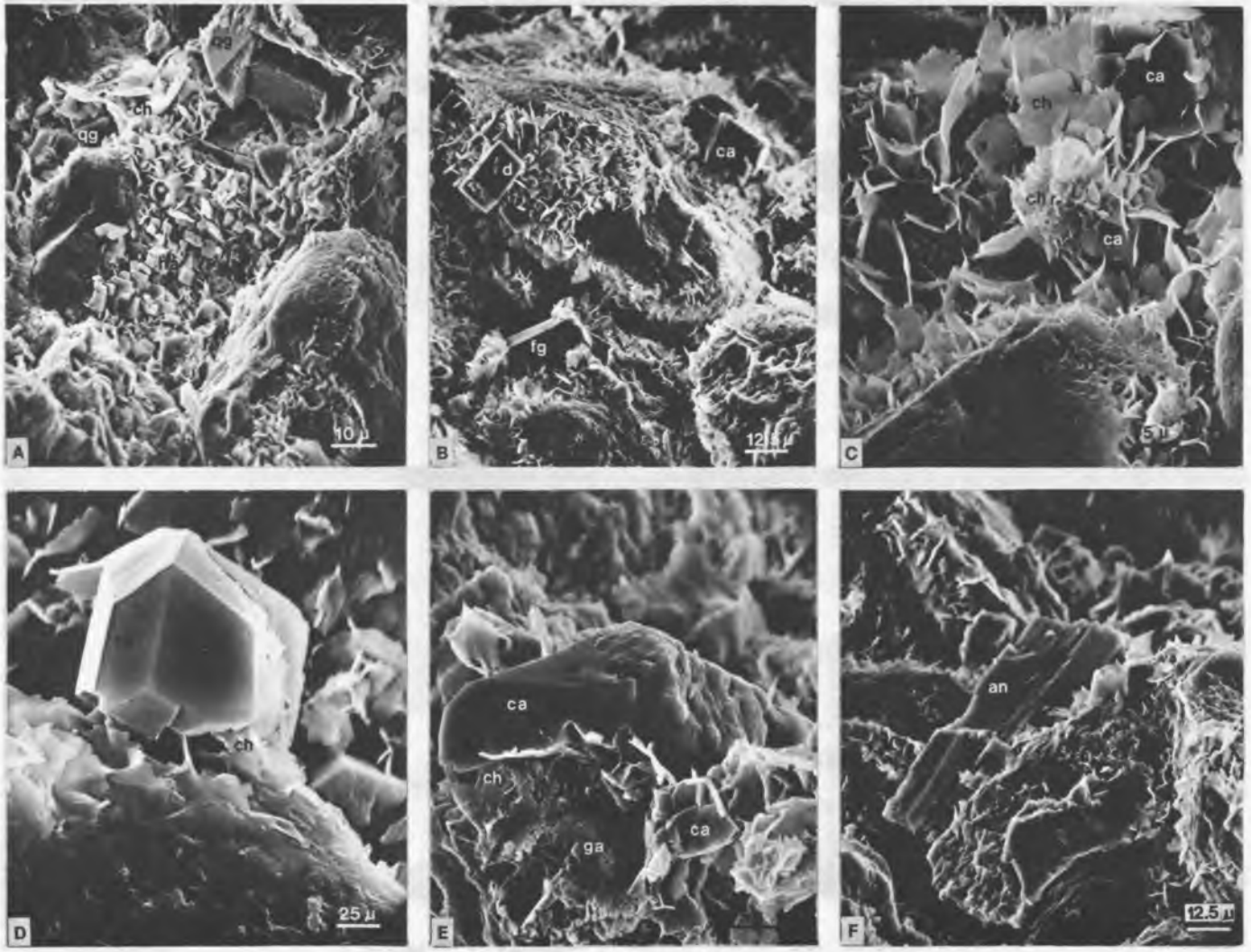

Figure 35. SEM Photomicrographs of Detrital Grain and Diagenetic Fabric Relationships

more reduced vertical permeability resulting in an overall permeability decrease. Compaction due to overburden occurred with continuous sedimentation resulting in deformation of the less stable framework members, which included the metasedimentary rock fragments, chert and carbonate clasts. Considerable deformation is observed in the carbonate clasts which have undergone replacement by micrite during this early diagenetic phase and have concurrently devoured quartz and feldspar fragments at points of contact. Dissolution of the clasts supplied sufficient carbonate material for later periods of cementation. At this stage, initial clay formation, manifest as thick to irregular clay coatings on detrital grains, commenced representing a process which spanned a major portion of the units' diagenetic history. Clay growth proceeded until significant coating of grains had occurred preventing major development of quartz and feldspar overgrowths (Figure 35A). Feldspar degradation, although beginning with initial sediment transport prior to deposition, reached a maximum at this time. This diagenetic process is dramatically displayed by self-supporting clay rims where the enclosed detrital grain has been completely dissolved creating a very minor amount of secondary porosity. Carbonate deposition, both in the form of sparry calcite and dolomite (dependent on the interstitial water chemistry) closely proceeded initial clay formation with intergrowth of the two components commonly occur-

ring (Figure 35B through 35E). It is difficult to determine if carbonate deposition was an inhibiting factor in clay formation or vice versa since the two appear to be inversely proportional to each other. Anhydrite formation occurred relatively late as witnessed in the interstitial clay-free crystals (Figure 35F). It is possible that a very late-stage period of minor dolomite formation occurred as suggested by the infrequent dolomite replacement of anhydrite crystals (Figure 27C). The precipitation of dolomite signaled the final phase of in situ diagenetic processes.

In the context of absolute time, diagenesis began with initial sediment deposition during the middle to late Guadalupian. The major portion of the authigenic material (overgrowths, clays, carbonates and sulfates) was derived from overlying Ochoan evaporites in the form of expulsed interstitial fluids (see Williamson, 1978 for detailed thermodynamic derivation of authigenic materials) which infiltrated down into underlying Guadalupian units. Thus, a post-Ochoan date is required for most diagenetic fabrics. Maximum burial of the Guadalupian sediments was attained during the Triassic and early Jurassic when up to 4000 feet of continental deposits were laid over basinal units. However, tilting and uplift during the early Cenozoic removed almost all traces of these continental beds, leaving the Paleozoic deposits which have remained relatively undis-

turbed up to and including present time. The diagenetic fabrics and features witnessed today reflect equilibrium conditions at present burial temperatures and pressures (Williamson, 1978).

Regional Trends in Clay Diagenesis

General Statement

Delineation of regional diagenetic clay trends in the Coyanosa field and adjacent areas is crucial to the development of proper well-treatment programs ensuring maximum hydrocarbon production. In an attempt to define such vertical and lateral trends all wells incorporated in this study were examined with at least one sample representing each formation present per well. X-ray and SEM-EDEX analyses of these samples reveal distinct clay composition trends and improvement in structural ordering with increasing overburden. Authigenic clays also exhibit definite lithologic affinities as well as predictable associations with coexistent diagenetic fabrics. Lateral trends in diagenetic clay development were not apparent in this study.

Elemental Trends in Chlorite Composition

The authigenic chlorites and randomly mixed-layered expandable chlorites display variations in relative degree of magnesium and iron content with increasing depth of burial. Uppermost Bell Canyon units in the Coyanosa field are characterized by chlorites with compositions of 8 Mg/4

Fe to 10 Mg/2 Fe atoms per octahedral layer. A sampling gap occurs in the middle to lower Bell Canyon before upper Cherry Canyon units are encountered. The majority of these underlying chlorites tend to display a stronger magnesium component reflected in a distribution of 12 Mg/0 Fe to 10 Mg/2 Fe atoms per octahedral layer. The few basinal samples examined, although representing correlative Bell Canyon and Cherry Canyon intervals, occur at greater depths and suggest similar trends in composition.

It is difficult to attribute these trends in composition merely to depth of burial. The association of chlorites with other secondary minerals and the degree to which these minerals are enriched in iron and magnesium appear to be the more reasonable limiting factors. It is apparent that the chlorites displaying the greatest magnesium contents are confined to upper Cherry Canyon intervals which tend to be characterized by significant amounts of dolomite and magnesium-rich calcites. Thus, the interstitial fluids from which these authigenic minerals have been created appear to have undergone enrichment in magnesium content with increasing depth of burial. However, this may be only apparent because of the lack of continuous core material available for examination.

Trends in Clay Type

Distinct trends in authigenic clay type and their subsequent structural ordering can be observed in the Coyanosa field and adjacent areas. Trends appear to be depth-related; therefore, laterally consistent clay zones occurring at uniform depths should be observed throughout the basin. Three zones have been identified and will be described in the following paragraphs. Figure 36 summarizes characteristics of these zones.

Uppermost zones situated within the Bell Canyon Formation at depths between 4700 and 5500 feet display a predominance of chlorite containing randomly interstratified swelling layers (Figure 37). The degree of interstratification varies, although generally not exceeding 20 to 30 percent expandable layers (based on a maximum of 50 percent for expansion of the (001) reflection to 15.4 Å when glycolated, (Lucas, 1963)). This slightly expandable mixed-layer chlorite averages 85 percent of the clay fraction found in sandstone units and 68 percent present in siltstone units. Chlorites are ubiquitous throughout this section, forming extremely variable grain coatings, both in the manner in which they are distributed and their relative thicknesses. Also present is a minor amount of slightly degraded illite comprising an average of 14 and 32 percent of authigenic clay material obtained from sandstones and siltstones, respectively. Five samples indicate

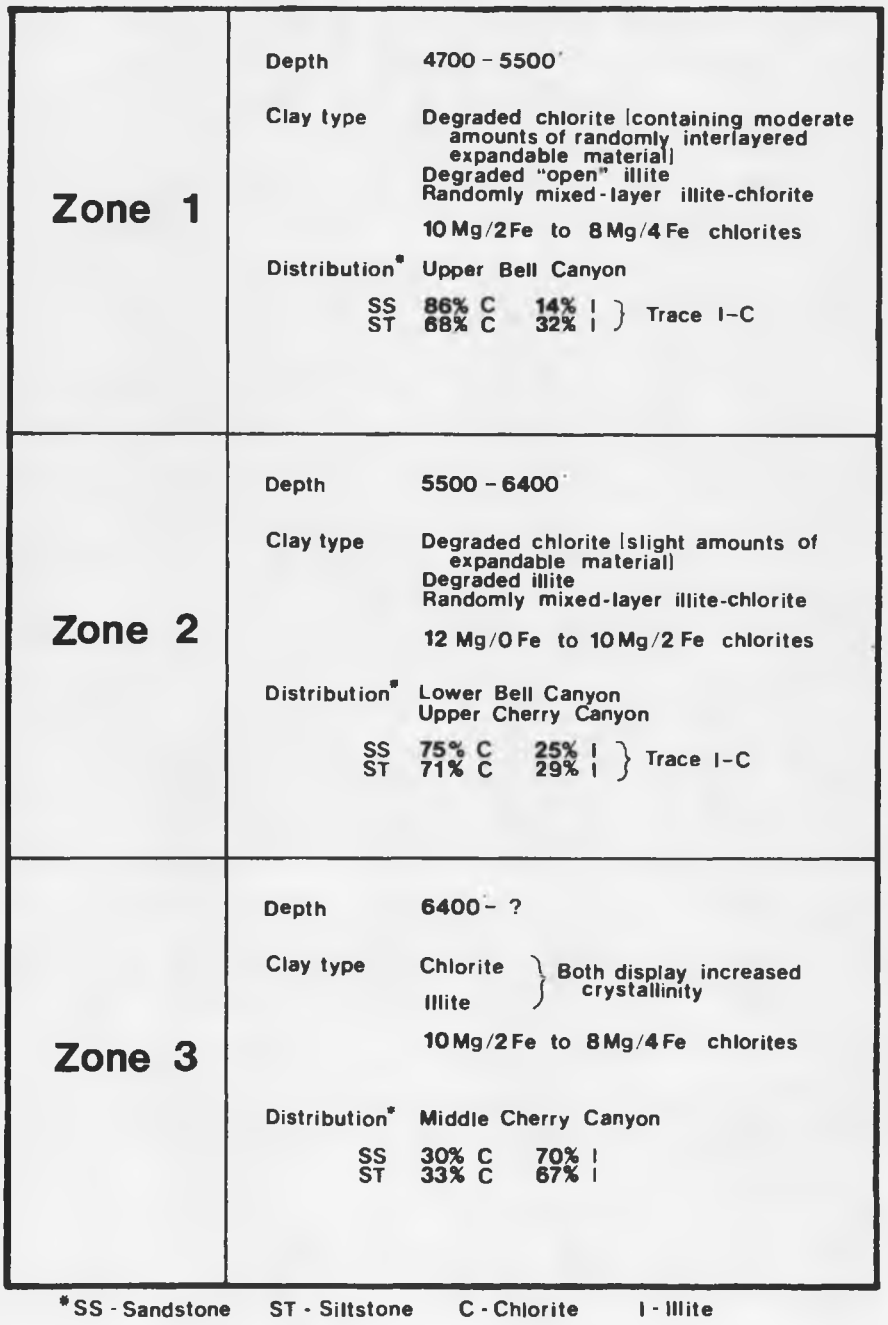

Figure 36. Characteristics of Diagenetic Clay Zones Identified in the Coyanosa Field Area

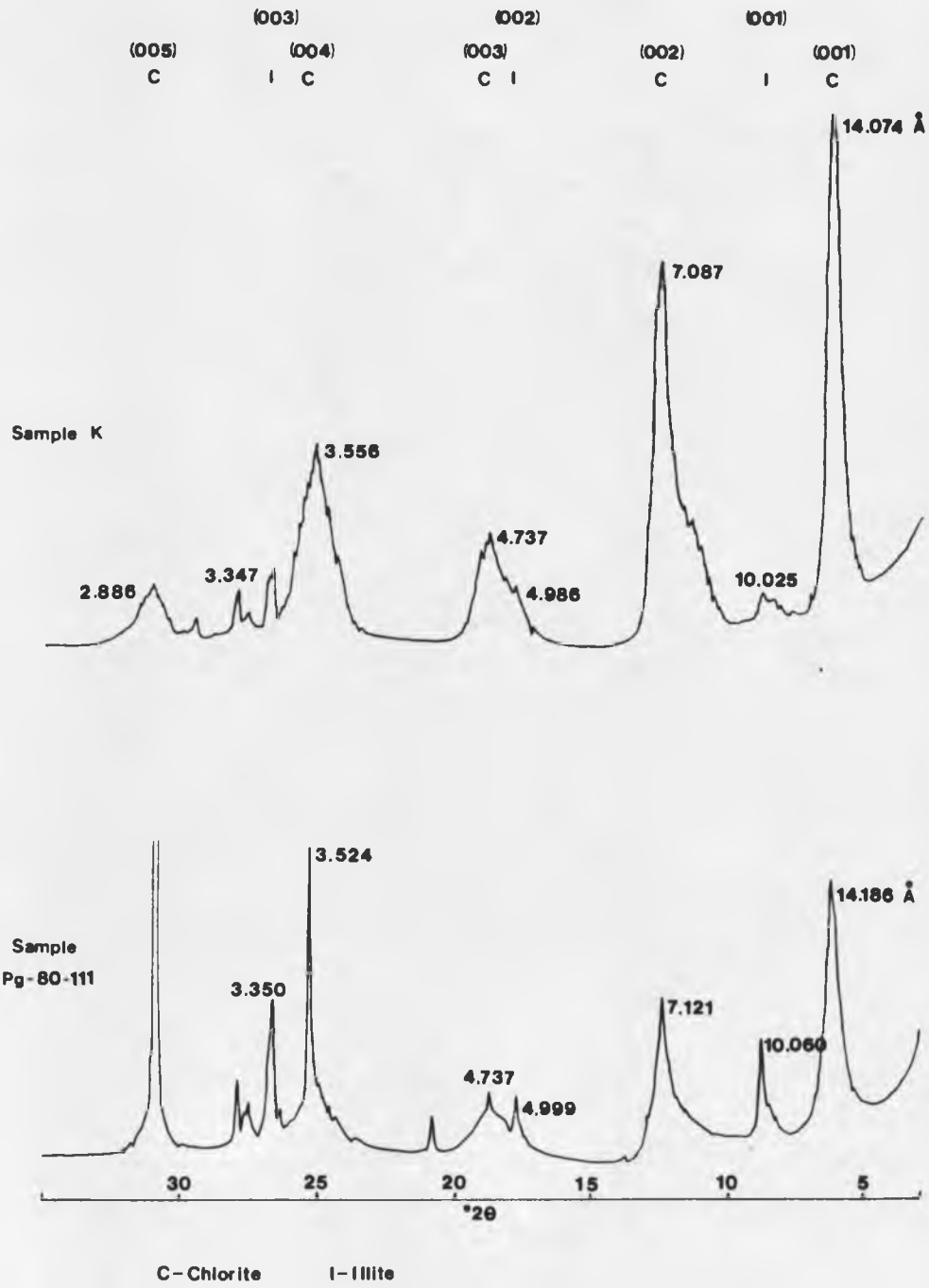

Figure 37. Clay Fractions Obtained from Bell Canyon and Cherry Canyon Sandstones Displaying Extremes in Structural Ordering of Authigenic Clays

the presence of a mixed-layer illite-chlorite, which generally does not exceed 8 percent of the total clay fraction.

The underlying Cherry Canyon Formation reflects a change in chlorite structure as increasing overburden results in "dewatering" of expandable layers. This second zone spans approximately 1000 feet, to depths of 6500 feet. There still exists a small percentage of expandable material (approximately 10 percent) within the chlorite structure as indicated by the slight to almost imperceptible shift in the (001) refection upon glycolation, in addition to the slightly crenulated appearance of the chlorite plates. Generally, though, the chlorites display an increased ordering within their structures toward a more stable chlorite end member. Illite comprises a greater percentage of the less than 4 micrometers fraction in the sandstone units than the previously described zone, amounting to 25 percent in some instances. Chlorites and slightly expandable chlorites comprise the remaining 75 percent. Increased symmetry and sharpness of the 10 Å (001) reflection, although slight, indicates improved crystallinity of the illite component (Dunoyer de Segonzac, 1969). This observation is an accord with expected increased structural ordering with depth and subsequent decrease in amount of degraded illite species.

Samples examined from lower Cherry Canyon intervals (zone three which extends from 6600 to 6900 feet)

exhibit little lithologic preferences by diagenetic clay species. Chlorite, appearing well-crystallized with no discernible expandable layers, is the subordinate clay component, comprising 30 percent of the total authigenic clay material (Figure 37). Illite, also displaying increased crystallinity on x-ray diffraction traces, provides the remaining 70 percent. Although no supporting SEM or core lab analyses are available for these samples, the relative weakness of authigenic clay reflections (as compared with all other samples) seems to suggest a paucity of authigenic clay growth at these depths.

The overall modification of authigenic clay species with depth has been considered by a number of authors (Perry and Hower, 1972; Foscolos and Powell, 1979; Seemann, 1979; Nagtegaal, 1979; Sarkisan, 1972; Dunoyer de Segonzac, 1969). Their results support a sequence of depth-related diagenetic zones characterized by predictable clay species (Figure 38). Shallow depths, usually defined as less than 8000 feet, favor the formation of kaolinite under acidic conditions or montmorillonite in alkaline environments. Increasing overburden (to 10,000 feet) results in the destruction of kaolinite and dehydration of expandable clays in favor of mixed-layer varieties and illites. Greater depths (exceeding 10,000 feet) are conducive to formation of stable clay varieties such as chlorite or illite, depending on the elemental composition (magnesium or po-

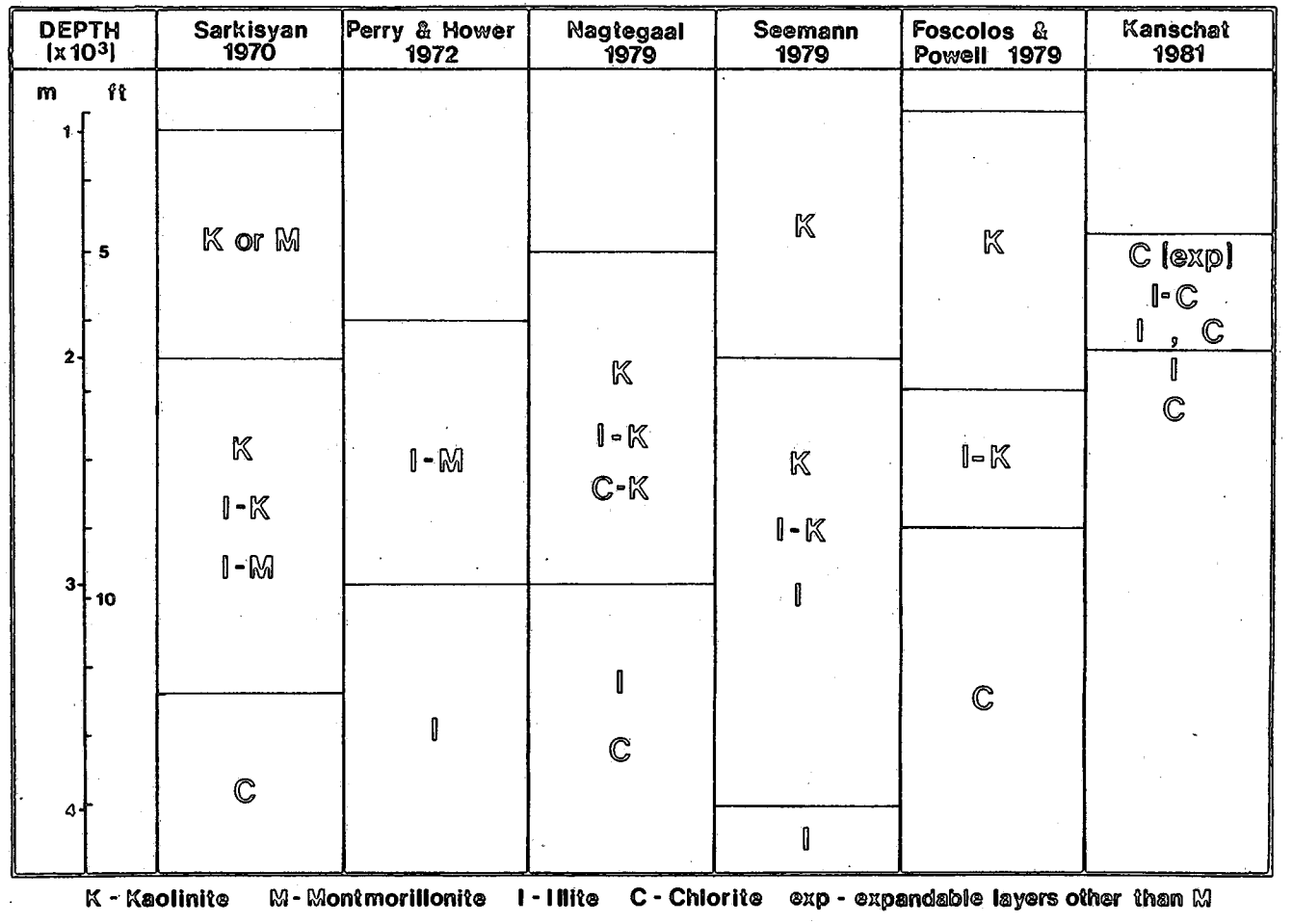

Figure 38. Comparison of Depth-Related Diagenetic Clay Zonation as Recognized by Various Authors. Addition of 3000 to 4000 feet of overburden to present study area would place the identified clay species at the depth necessary for proposed clay transformations.

tassium) of the interstitial fluids. Further burial produces improved structural ordering within the two clay species toward a low-grade metamorphic end member. This sequence appears to be consistent in all geographic areas examined.

The diagenetic clay sequence observed in the Coyanosa field area is quite similar to that predicted above. However, the depths at which clay mineral transformations are observed within the field are anomalously shallow in comparison. This problem can be rectified if it is assumed that the present clay mineral species reflect maximum burial depths which were attained during the late Mesozoic, prior to erosion of 3000 to 4000 feet of emergent marine deposits. (See Figure 39 for the relationships between tectonic events and clay diagenesis in the Coyanosa field.) But this, too, poses a problem in that one should anticipate degraded clay products at present depths of shallower burial. Perhaps this is what is presently observed with "open" illite and slightly expandable interstratified chlorite structures. Another possibility is that variables such as geothermal gradient, pore fluid chemistry and hydrostatic pressures have modified the depths at which clay mineral transformations have occurred within the Bell Canyon and Cherry Canyon Formations. However, time has precluded analyses of these variables in

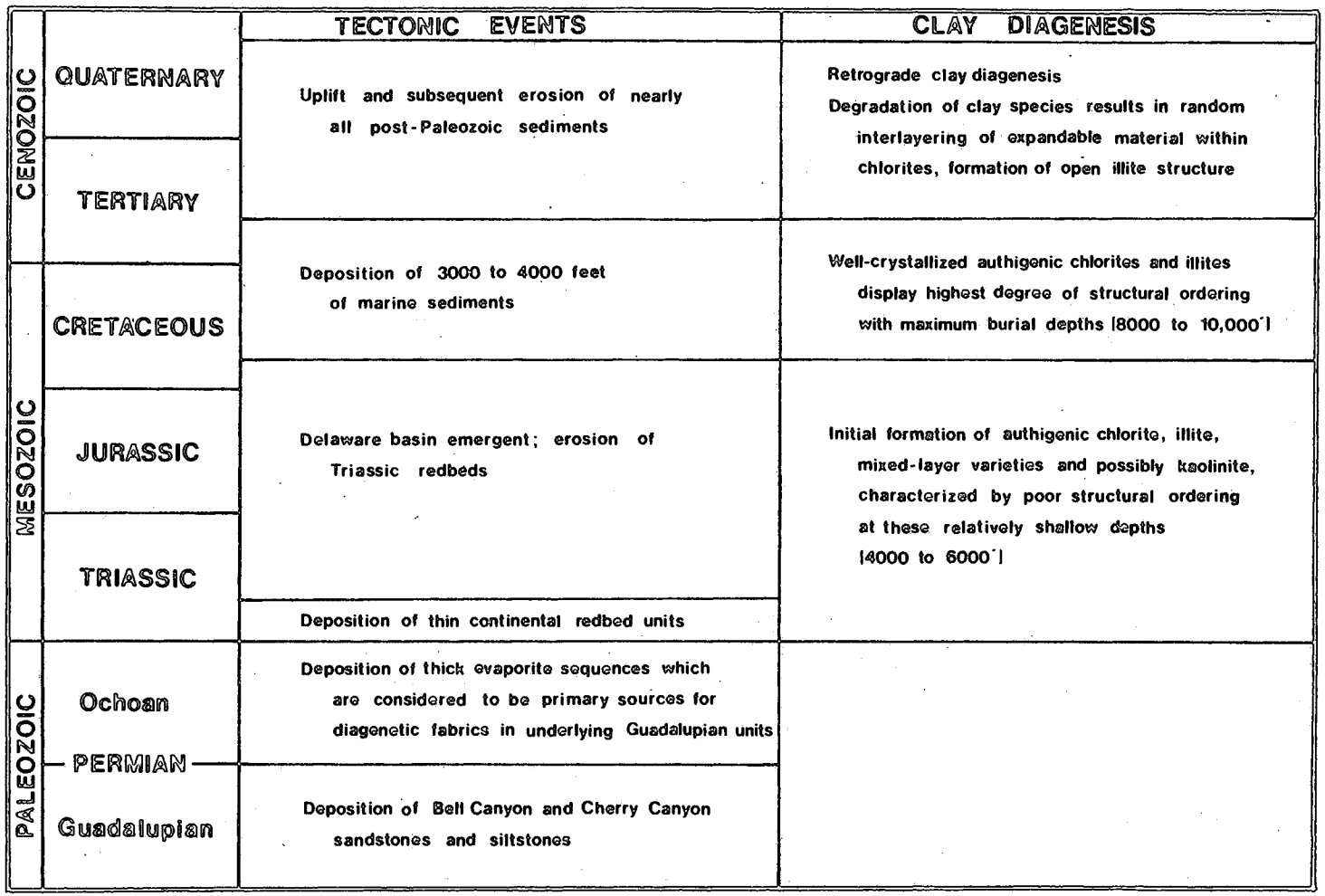

Figure 39. Relationship Between Diagenetic Clay Development and Tectonic Events Associated with the Bell Canyon and Cherry Canyon Formations within the Coyanosa Field Area

this study and thus their subsequent influence on authigenic clay development cannot be predicted.

Lithologic Affinities

As previously mentioned, chlorites and their associated expandable mixed-layer varieties demonstrate a preference for massive sandstone members within the Bell Canyon and Cherry Canyon Formations. Illites, on the other hand, display affinities for the siltstone and shaly siltstone units. This latter relationship is possibly a result of the readily available supply of potassium from degrading detrital micas preferentially deposited in these finer-grained members.

Diagenetic Fabric Associations

Inverse relationships between degree of authigenic clay formation and subsequent overgrowth and cement development are observed in the massive sandstone samples examined. Thick, uniform clay coatings preclude later development of secondary fabrics by enveloping available attachment surfaces on detrital grains. Irregularity or absence of these clay rims provides an opportunity for these secondary fabrics to develop.

The distribution of authigenic clay within individual massive sandstone bodies appears to be uniform with no apparent preference for interior sections or portions adjacent to underlying or overlying siltstone bodies. It has

been noted that edges of sandstone bodies display poorer porosity and permeability as a result of increased cementation along these contacts, although clay growth appears to be relatively uniform throughout the sandstone unit (Williamson, 1978). Thus, it is implied that cement precipitation is controlled more by available material in solution, perhaps derived from "dewatering" of adjacent shaly siltstone units, than by the inhibiting effect of authigenic clay growth. With respect to interior sections of sandstone bodies, more cement attachment surfaces are available than potential cement held in solution by interstitial fluids.

Concluding Remarks

Studies by Williamson (1978) and Watson (1974) acknowledge the presence of expandable mixed-layer chlorites in uppermost Bell Canyon sections in the north-central portions of the Delaware basin at depths approximating 5000 and 3000 feet, respectively. Although their studies are limited to examination of a few samples, the results obtained fit into the diagenetic clay sequence presented in this paper. The suggested presence of kaolinite by Watson (1974) at relatively shallow depths of less than 3000 feet, although difficult to confirm, lends additional support to a depth-related diagenetic zonation. However, it should be emphasized that kaolinite is very similar to chlorite in

x-ray character and thus the presence of kaolinite may also be attributed to misinterpretation of x-ray data.

On a regional scope, assuming consistent lithologies and secondary mineral development for the Bell Canyon and Cherry Canyon Formations within the Delaware basin, similar diagenetic clay zonation with respect to clay type should be encountered elsewhere in the basin. However, these zones will not necessarily coincide with identical stratigraphic intervals throughout the basin. For any given stratigraphic interval, less intense clay diagenesis will be observed in the northern and western portions of the basin because of shallower burial. This is a result of relative uplift of these areas which occurred during the Cenozoic. The clays encountered will differ from those found in similar stratigraphic intervals in the eastern and southern portions of the basin and treatment of the wells will have to vary to accommodate the differences in clay type.

CHAPTER 7

IMPACT OF DIAGENESIS ON RESERVOIR CHARACTERISTICS

Introduction

In order to accurately estimate reservoir potential it is necessary to evaluate reservoir textural parameters with respect to inferred diagenetic trends. Only the massive sandstone units were considered in this aspect of the study because of their demonstration of reservoir potential. A strong correlation exists between permeability and authigenic clay formation, as well as porosity and degree of secondary cementation. Authigenic clay growth results in extreme permeability reduction, inhibition of cement development and high irreducible water saturations (thin layers of adsorbed water held to detrital grains and discontinuous pendular water around grain contacts held by capillary pressure). The extreme variability in clay composition and distribution, and the difficulty in recognition because of extremely fine size complicates prediction of favorable productive trends within the formations. Conversely, porosity/cement relationships exhibit a predictable uniformity within the massive sandstone units. Lithologic homogeneity, well-sorting and an overall paucity of cement-

ing material contribute to the development of good porosity within these units. Slight increases in cementation and compaction have reduced the porosity in some instances, but the resultant effect has had minimal impact on reservoir development.

Porosity

The porosity characterizing the Bell Canyon and Cherry Canyon Formations is predominantly primary in origin. Fluid density currents allowed for separation of grain size classes resulting in deposition of extremely clean, well-sorted, very fine-grained sandstone units. Secondary intergranular porosity developed as a consequence of dissolution of carbonate clasts which had been incorporated into the sandstone units. In addition, a very minor amount of secondary intragranular or moldic porosity resulted from feldspar dissolution. However, the amount of secondary porosity developed was probably offset by deposition of carbonate and silica cements derived from the associated dissolution processes. It is difficult to determine the original amount of detrital carbonate material present but lack of large irregular pore spaces, rare occurrences of embayed and corroded grains, scattered remains of micrite-replaced carbonate clasts and paucity of secondary carbonate cement imply relatively small initial volumes.

As mentioned in an earlier section, porosity ranges from 15 to 25 percent for the massive sandstones and 2 to 23 percent for associated siltstone intervals (as measured by commercial laboratories according to Boyle's law). Although it is difficult to discern from routine petrographic analysis, the intergranular porosity displayed is only apparent. An intergranular microporous system actually exists as a result of partitioning of pore space by authigenic clay growth. This does not affect the net amount of porosity but it severely restricts permeability of the units.

Occlusion of porosity is primarily accomplished by precipitation of calcite, dolomite and anhydrite cements, usually amounting to less than 10 percent of total rock volume (Figure 40). There appears to be no discernible pattern to cementation within the sandstone bodies. Occasionally uppermost beds display greater degrees of cementation as do a number of interior bed which are adjacent to thin interbedded shaly units. The occurrence of these more heavily-cemented beds, though, is too inconsistent to establish trends within the study area. It is possible that in some situations fine-grained shaly units are able to supply increased amounts of interstitial fluids to adjacent sandstone units upon dewatering under the influence of compaction.

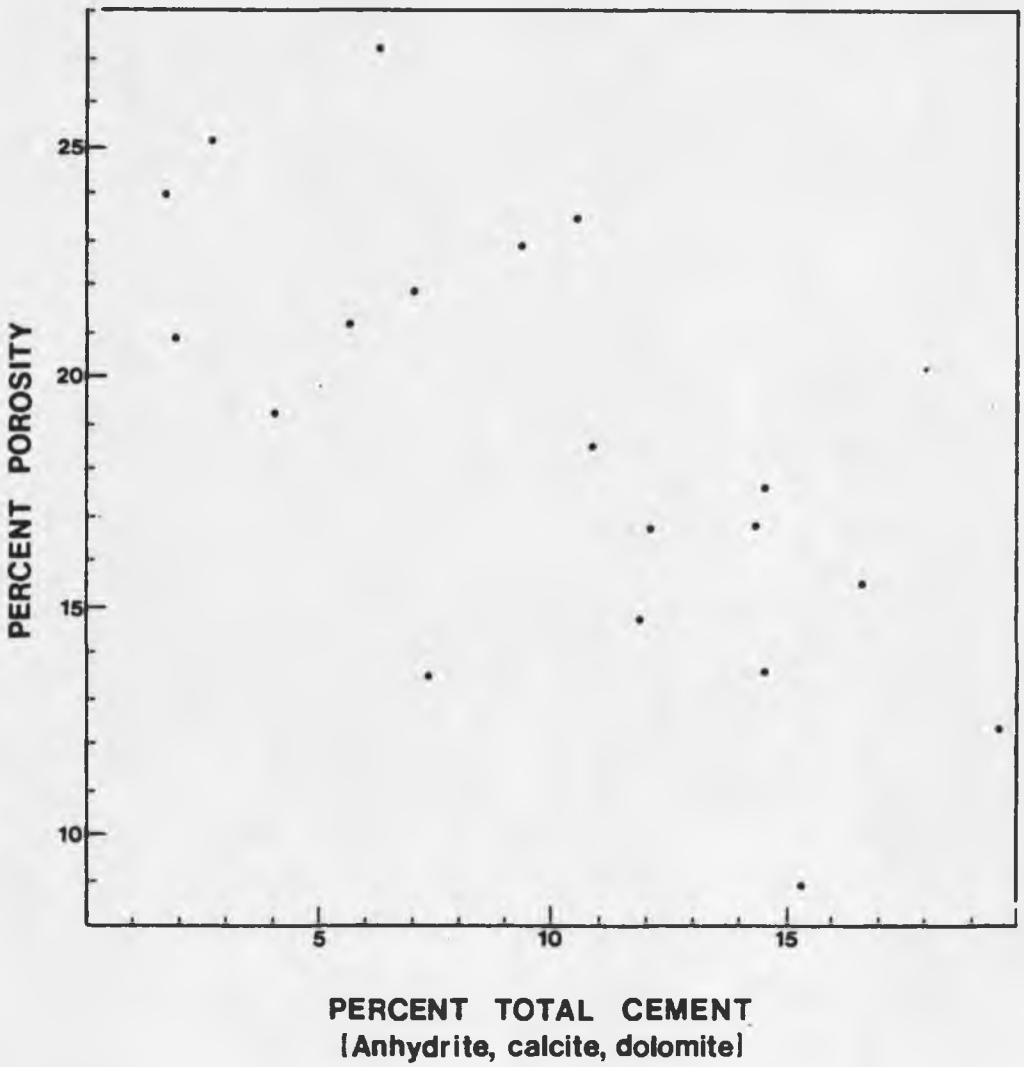

Figure 40. Relationship Between Porosity and Degree of Cementation in Selected Bell Canyon and Cherry Canyon Sandstone Samples. Porosity is laboratory-derived; cement percentages have been obtained by thin section point counting methods and include calcite, dolomite and anhydrite cements.

Cementation is better, overall, in the Cherry Canyon Formation. This can be attributed to increased amounts of available carbonate material which originates in the numerous interbedded limestones and dolomites. Dewatering of clays may also contribute to increases in interstitial fluids occurring within the formation. Anhydrite and pyrite deposition is also favored in these intervals.

Development of quartz and feldspar overgrowths accounts for very minor occlusion of porosity. Compaction also results in porosity reduction as displayed in Figure 41. Presence of increased grain deformation, tighter packing and predominance of sutured, concavo-convex contacts confirms this relationship.

It should be emphasized that although variations in porosity have been identified within the massive sandstones, they have been relatively insignificant in affecting overall reservoir potential. Even in sections displaying relatively heavy cementation, a considerable amount of effective porosity still exists. The indirect influence of authigenic clay growth on porosity development also needs to be stressed. The early diagenetic development of clay rims by occupying available attachment surfaces and reducing flow of interstitial fluids controls the subsequent formation of overgrowth and cementing materials. In addition, clay growth has alleviated compaction in the absence of supportive secondary cements. Thus, porosity is best de-

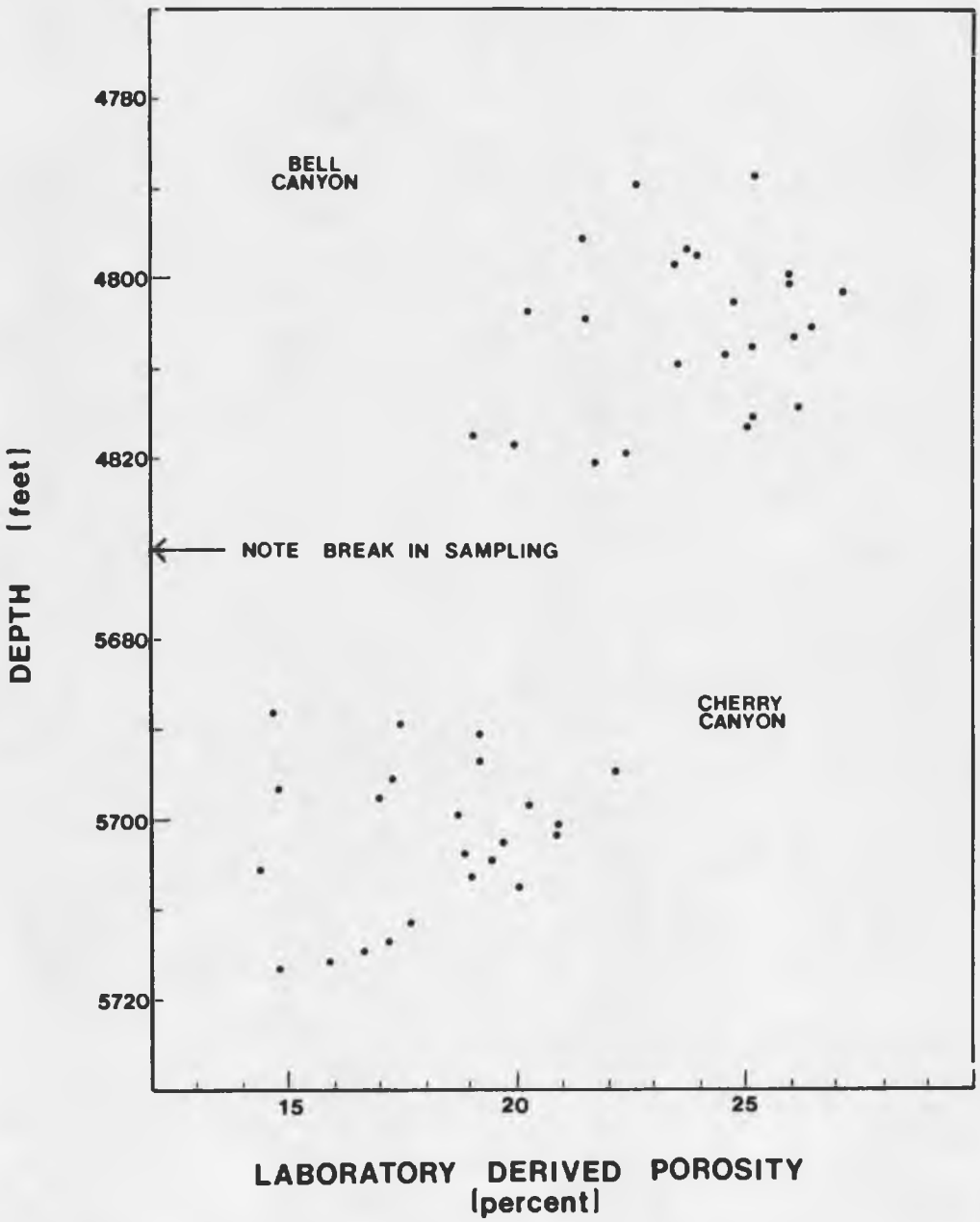

Figure 41. Decrease in Porosity as a Result of Depth-Related Compaction. Well examined is the Mobil, Coyanosa Plant "A" SWD #1.

veloped in the presence of thick authigenic clay growth. However, the accompanying reduction in permeability tends to negate any benefits.

Permeability

Permeability bears only a slight relationship to porosity values (Figure 42). For the most part, permeability displays wide variation for any given range of porosities.

Siltstone units display relatively greater horizontal permeabilities as a consequence of their laminated structure and corresponding preferred orientation of detrital grains. Conversely, vertical permeabilities are poor, making the siltstones effective permeability barriers to fluids contained in enclosed sandstone bodies. Sandstones display no tendencies toward horizontal or vertical movement of fluid as a result of their homogeneous nature. Permeabilities range from less than 0.1 to 120 millidarcies with no discernible trends in development.

The primary control on permeability is the formation of authigenic clays. Their occurrence as pore linings and bridges greatly increases the surface area in contact with interstitial fluids. Subsequently, drag is increased on the fluids resulting in sharp permeability declines.

Although locally permeability trends are difficult to predict because of the irregularity in distribution be-

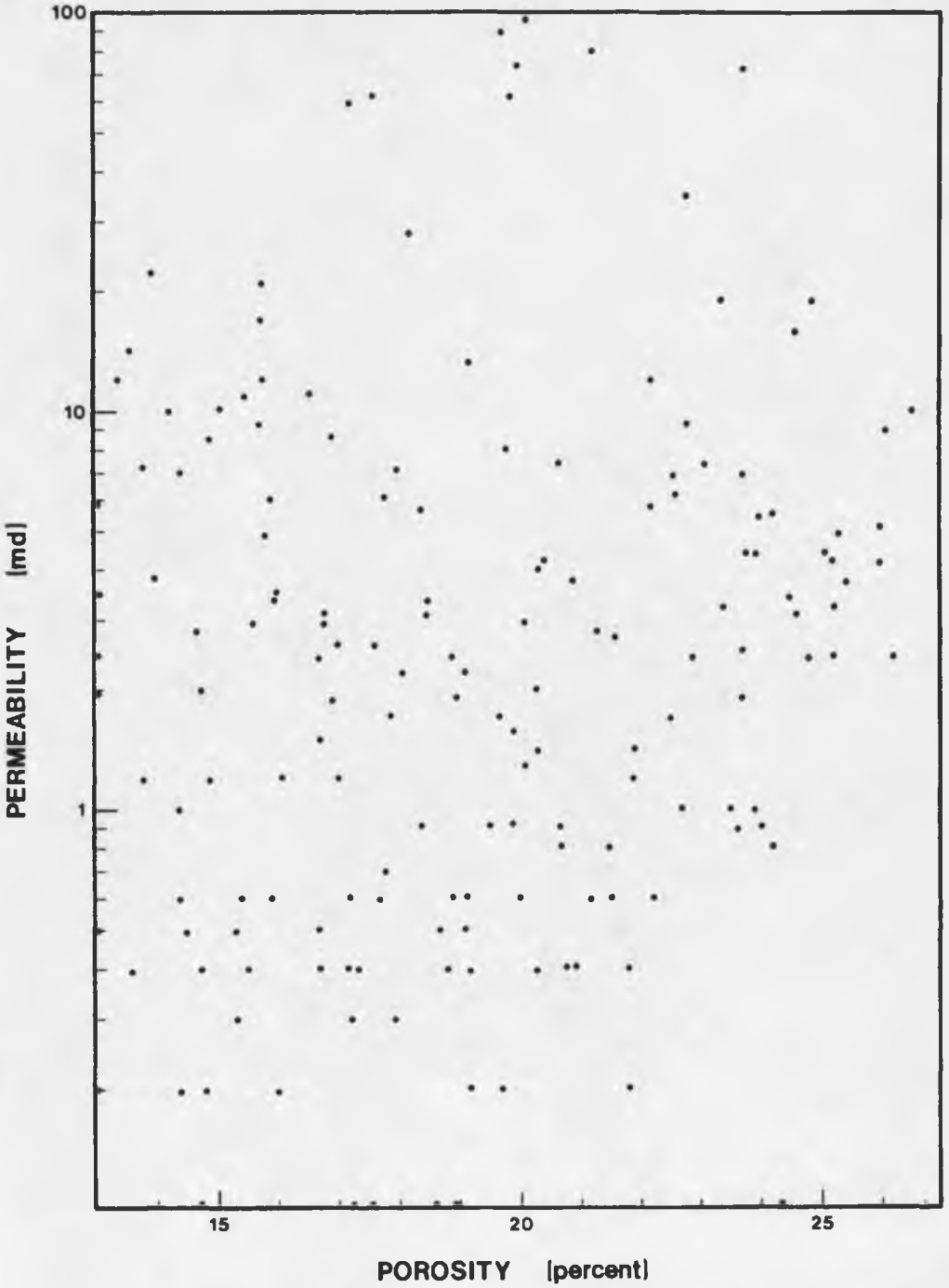

Figure 42. Relationship Between Porosity and Permeability for the Wells Examined in the Coyanosa Field Area.

cause of the authigenic clay developed, regional patterns can be distinguished. A plot of permeability values versus clay zone occurrence (Figure 43) for nine Coyanosa field area wells suggests that permeability is influenced to some extent by the suite of clay minerals present at that depth. The upper zone (4700 to 5500 feet), which is characterized by randomly interstratified mixed-layer expandable chlorites, illite and mixed-layer illite-chlorite, displays overall greater average permeabilities. Zone two clays (5500 to 6400 feet), consisting of chlorite, slightly expandable chlorite and increased amounts of illite, exhibit lower average permeabilities in all but one well. Perhaps the greater surface area exposed to fluids due to increased amounts of authigenic illite has resulted in decreased permeabilities within the lower zone. However, the relationships observed may prove to be only apparent because other variables such as compaction effects, degree of cementation, variations in amount and distribution of clays and the dehydrated state of the clays during measurement may also influence permeability measurements.

Another property which depends primarily on the amount, distribution and composition of the authigenic clays and in turn influences the effective permeability is water saturation (Figure 44). Authigenic clays tend to hold considerable irreducible water saturations because of their high surface area to volume ratios and increased

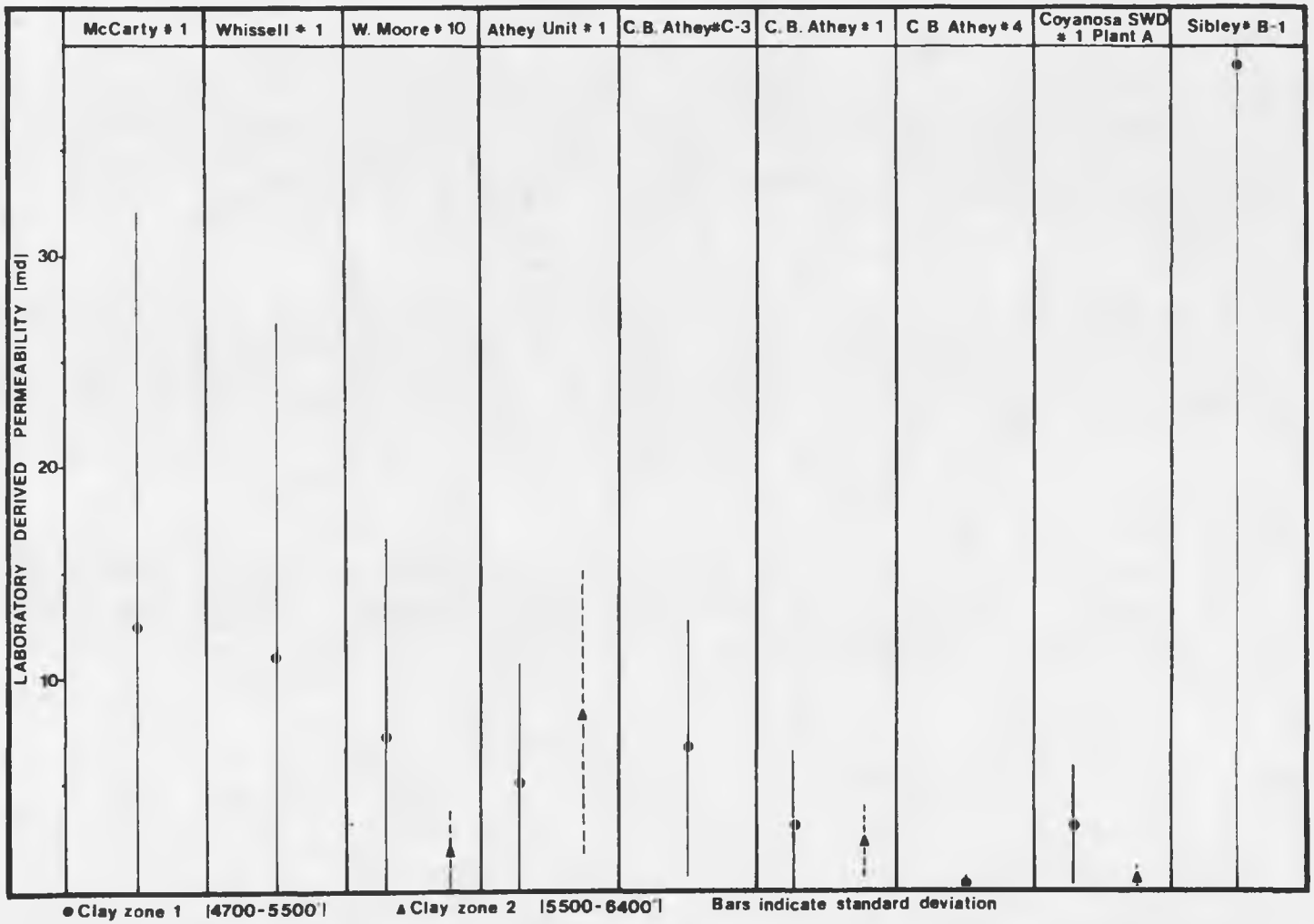

Figure 43. Plot of Averaged Laboratory-Derived Permeabilities versus Clay Zone Occurrences for Wells Examined in the Coyanosa Field Area. Comparison with Figure 45 reveals an inverse relationship between permeability and water saturation.

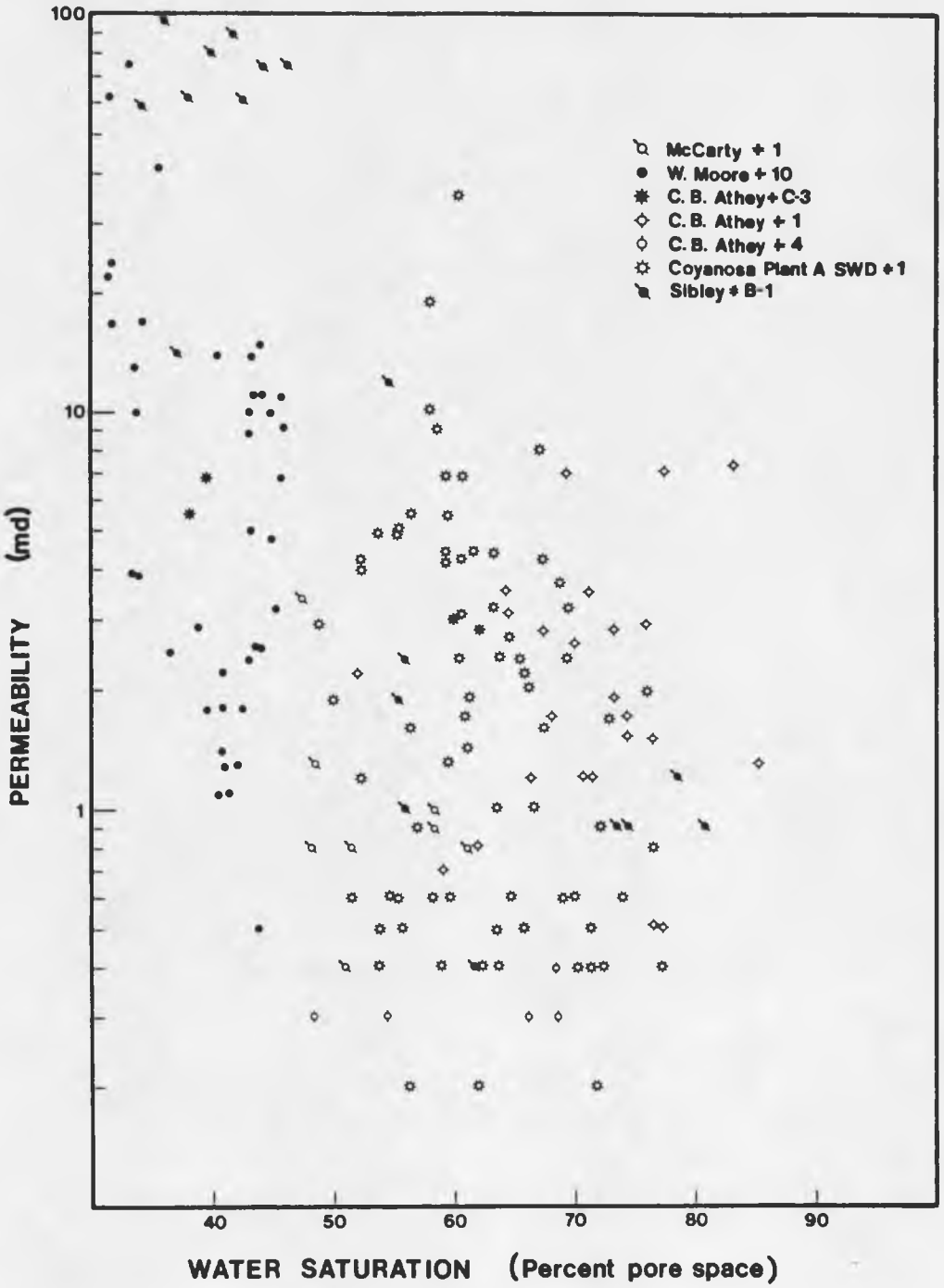

Figure 44. Relationship between Permeability and Water Saturation for Selected Wells Used in the Present Study

ionic activities at clay surface/interstitial water contacts. In addition, expandable layers within mixed-layer and degraded clay species incorporate water into the clay structure thereby increasing the amount of unextractable water. Water saturations, as derived by commercial laboratories, were also plotted against authigenic clay zone occurrence (Figure 45). Clay zone two, which had previously displayed lower average permeabilities, is associated with relatively higher average water saturations. Conversely, clay zone one, which was characterized by higher permeabilities, reflects lower average water saturations. Because of the migration of pore-blocking fines, the extremely high surface areas in contact with interstitial fluids and the relative increase in amount with respect to other authigenic clay types, the illites of zone two may account for a greater reduction in permeability and higher water saturation then zone one. Zone one contains predominantly moderately to slightly expandable chloritic clays which are capable of interlayer entrapment of water by the expandable layers. However, the expandable layers are not as significant in total water-trapping volume as those properties associated with illites. The fact that swelling clays are less sensitive to the saline interstitial waters (as opposed to fresh waters) and thus less apt to incorporate vast amounts of water into their structures may account for the relatively reduced water saturations

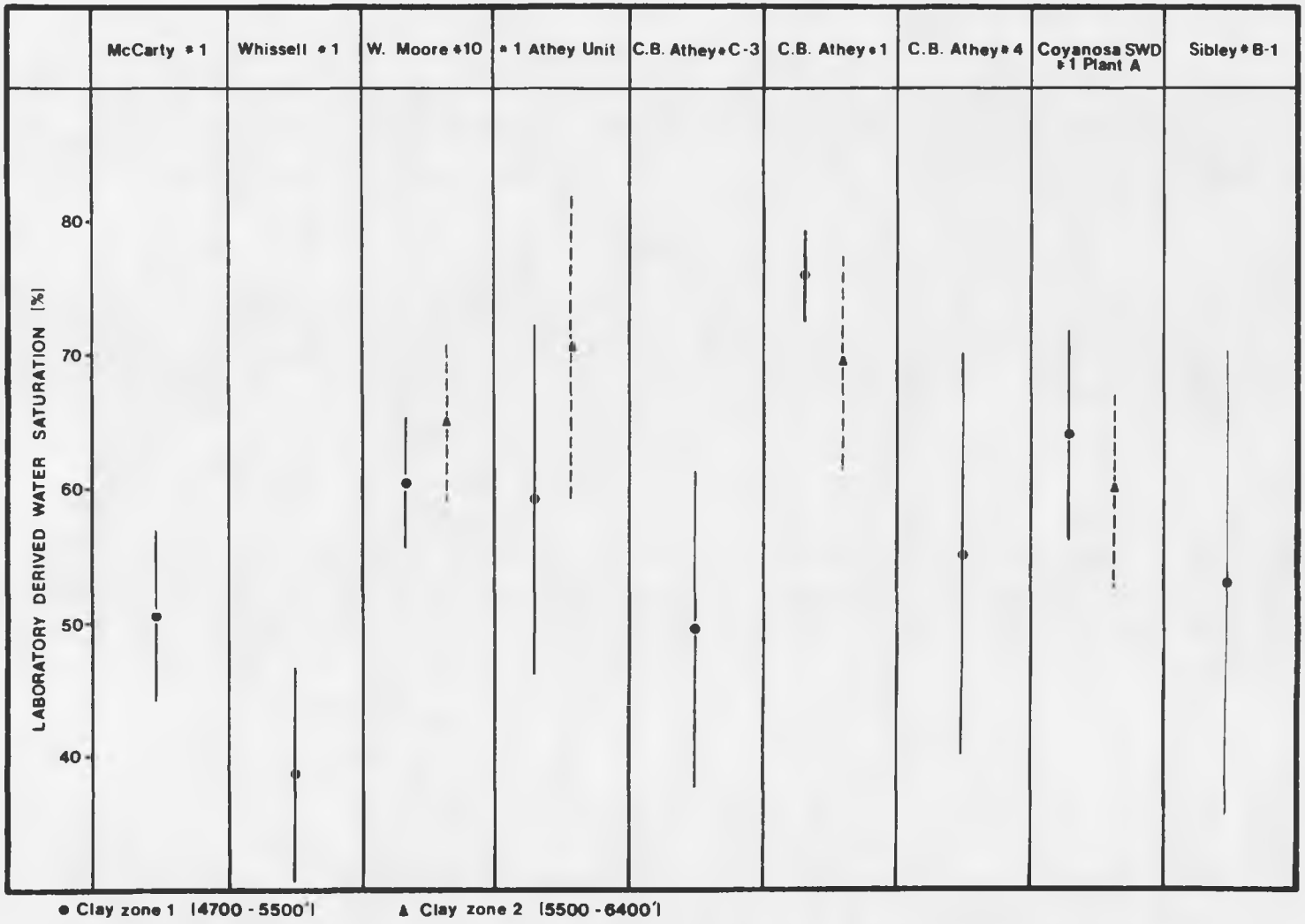

Figure 45. Plot of Average Laboratory-Derived Water Saturations versus Clay Zone Occurences for Wells Examined in the Coyanosa Field Area. Bars indicated the standard deviations of the values.

in zone one. It is interesting to note that Bell Canyon permeability studies by Jenkins (1961) reveal that significant permeability reductions do not occur even when the formation is saturated with fresh water. These results are supported by Williamson (1978). This lack of sensitivity by the swelling clays may be a consequence of there being only minor amounts of expandable material interlayered in the chlorite structure plus their departure from true smectite structure. It is this latter smectite structure on which most water sensitivity studies have been concentrated and assumptions extracted.

It should be stressed that the permeability measurements utilized in these analyses are higher than the actual permeabilities because they have not been corrected for air slippage, lack of overburden, or absence of irreducible water saturation (the sample has been completely voided of interstitial fluids for these measurements). See LeRoy and Le Roy (1977) for detailed correction of laboratory measured permeabilities to obtain in situ values. Without corrections, permeability values obtained from fine-grained clastics may be 10 to 10,000 times greater than actual values. In this case, since overriding conditions were fairly homogeneous and the primary objective was to obtain relative trends in permeability values, actual magnitude determination was not crucial to interpretations.

Recognition of Authigenic Clay Growth on Subsurface Logs

Subsurface logs routinely run in the Coyanosa field area include sonic, gamma-ray-neutron, formation density and/or induction-electrical logs. The first three delineate porosity and lithologic trends while the latter is primarily useful in determining fluid saturations by observing relative resistivities within the formation.

Detailed analysis of subsurface logs was not performed for the wells involved in this study because of the lack of available logs and the restricted interpretive ability of the author. Regardless, a few qualitative statements concerning authigenic clay detection on subsurface logs can be made:

1) Resistivity logs are especially sensitive to authigenic clay growth. The extremely high surface areas offered by authigenic clays are covered by thin films of bond water characterized by elevated ionic concentration which display high conductivities. These zones will subsequently appear water-saturated although interstitial areas may contain no water, or hydrocarbons. (Almon, 1979).
2) Porosities obtained from sonic logs are 5 to 15 percent higher than actual porosities (measured according to Boyle's law). The presence of bound water on clay surfaces tends

to decrease the velocity range predicted for sandstones. Thus, velocity-derived porosities will exceed actual values.

3) Neutron logs, because they are sensitive indicators of all water contained in a formation, will display an apparent porosity which is greater than actual effective porosity. This is a consequence of the assumption that contained water occurs only interstitially and thus bound water on clay surfaces is inaccurately interpreted to be a pore-filling fluid.

Clay Treatment Programs

Reaction of authigenic clays to poorly planned well-treatment programs can magnify permeability problems already present within the formation. In the case of the Coyanosa field area attention must be given to three types of clays - chlorite, illite and randomly-interstratified expandable layers.

Chlorites are volumetrically the most important clay contained within the Bell Canyon and Cherry Canyon Formations, although probably not exceeding 5 to 7 percent of total rock constituents. As with the other authigenic clays, permeability is restricted within the formations by intricate networks of microporosity established as a result

of thick clay coats, pore-bridging and pore filling (Figures 46A through 46F).

Additional permeability loss results from the introduction of hydrochloric acid into the formation during well completion. This is usually standard procedure in formations containing carbonate cements. The iron that is present in the chlorites reacts readily with the acid. The original chlorite structure is dissolved and subsequently reprecipitated as a gelatinous ferric hydroxide ($Fe(OH)_3$) in the presence of oxygenated waters. This ferric hydroxide tends to precipitate as large crystals which exceed pore diameters and effectively impede fluid flow. This problem can be avoided if iron chelating agents and an appropriate oxygen scavenger are added to the hydrochloric acid prior to treatment. Simulation of treatment techniques was attempted on the Bell Canyon Formation under laboratory conditions but results were poor (Figure 46F). This was probably a consequence of not reproducing in situ reservoir pressure and temperature conditions during the experiment.

Also present are illites which demonstrate an increase in relative amounts with depth. They are difficult to visually detect in the presence of other authigenic clays which often leads to their underestimation in the formations examined. Because of their high surface areas the illites can easily bind considerable amounts of water

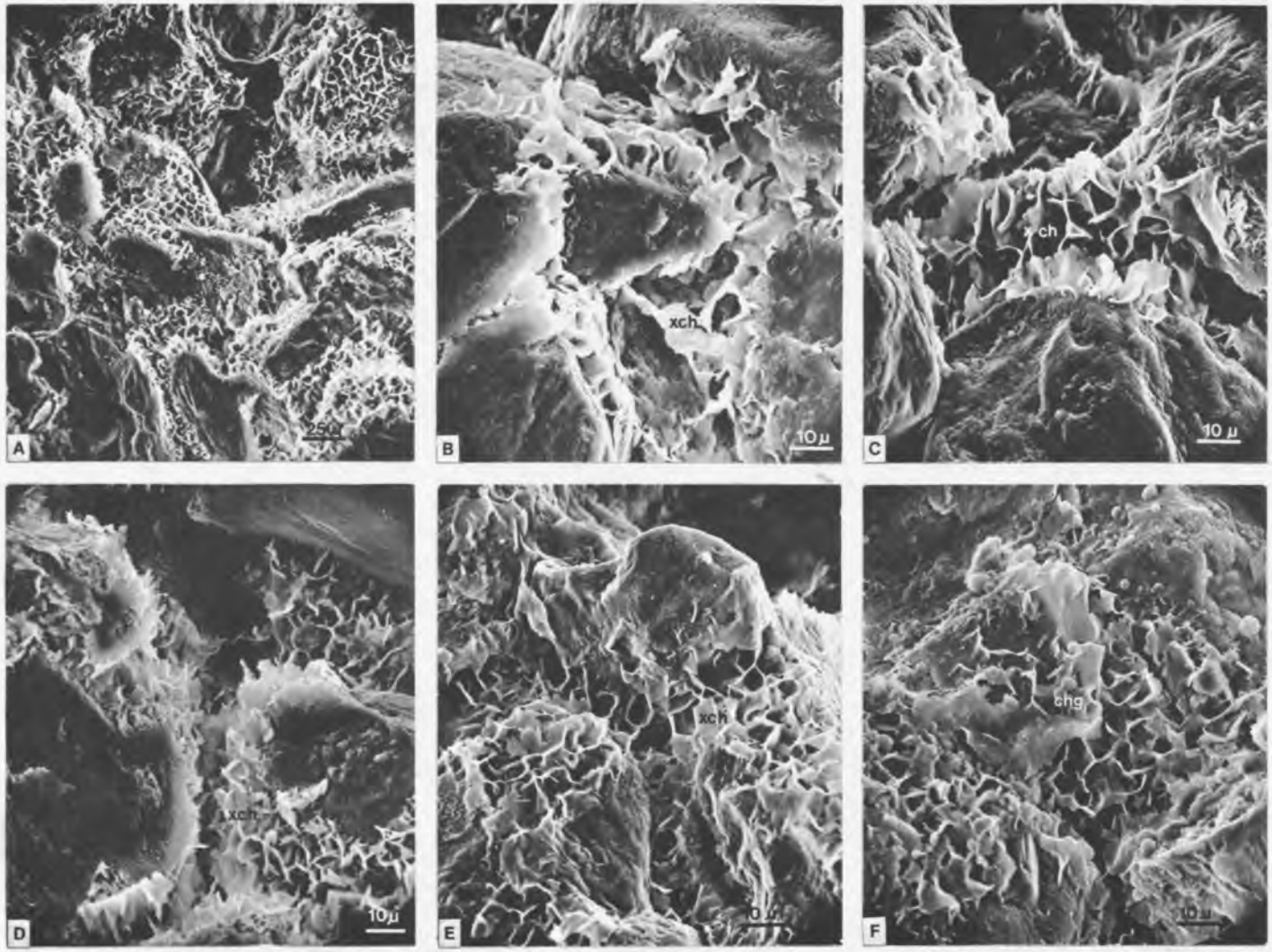

Figure 46. SEM Photomicrographs of Authigenic Clay Distribution within Bell Canyon Sandstones

to detrital grain surfaces creating significant irreducible water saturations. Also, the fibrous extensions along illite crystal edges are readily broken off and consequently swept into pore throats by interstitial fluids. In the presence of fresh water these fibers tend to clump together. Addition of a hydrochloric and hydrofluoric mixture to the formation can adequately dissolve the illites.

The expandable layers are present primarily within the chlorites with minor amounts detected in the degraded illite structure. Because of their random interlayering, expandable layers amount to less than 20 to 25 percent of mixed-layer structures. They do tend to imbibe water in random interlayer positions; however, they do not appear to have a particular sensitivity to fresh or saline waters as do true smectities. Because they do not display as intense swelling as smectites, they are less prone to break free from detrital grain surfaces upon swelling. Their dominant effect is to create a slightly higher surface area for the more stable clay members in which they are contained, thereby increasing irreducible water saturations. Because of their apparent insensitivity to the salinity of interstital fluids, they can be treated essentially the same as the dominant clay mineral with which they are associated.

Clay Treatment Presently Employed in the Coyanosa Field Area

Stimulation programs presently employed in the Coyanosa field area by Mobil operators recognize that the Delaware sands are water-sensitive and contain appreciable amounts of chlorite. Therefore the formations are not exposed to acid or water-base fracture treatments (Montgomery, 1981, written communication). Where acid is absolutely necessary it has been recommended that iron-chelating agents and oxygen scavengers be used in conjunction (Randerson, 1980, written communication). These suggested treatments are in accord with identified authigenic clays.

The following recommendations should be considered in improving well production. Although the procedures mentioned above are acceptable with regard to clays present in the two formations, further improvements are possible. Presently sand-fracturing with an oil-base medium is the only treatment utilized on the Delaware sands. This stabilizes the clays present but it does not significantly improve in situ permeability values. Increased use of acidization, both hydrochloric and hydrofluoric, with proper chelating agents and oxygen scavengers could remove chlorite, illite and mixed-layer varieties. However, employment of these techniques requires that rigorous controls be followed to ensure that proper results are obtained. In particular, extreme care must be taken to completely remove spent acids.

CHAPTER 8

CONCLUSIONS

The following statements briefly summarize conclusions obtained from the investigation of the Bell Canyon and Cherry Canyon Formations in the Coyanosa field area, Pecos County, Texas.

1) Very fine-grained, well-sorted, massive sandstone units, displaying horizontal and large-scale cross-bedding, in addition to scour surfaces, were deposited from stratified saline fluid density currents as long linear submarine channel systems. These were incised into underlying silty units and oriented perpendicular to basin margins. The fluid density currents, originating in evaporitic back-reef areas, allowed for excellent separation of grain size classes resulting in textural homogeneity within the units.

2) Coarse to medium-grained, moderately-sorted, very thinly-laminated, shaly siltstones, compositionally similar to massive sandstones, were deposited from suspension during periods of low sand influx into the basin forming laterally continuous, evenly bedded units which mantled sandstone units. In many instances, intense bioturbation has disrupted bedding.

3) Examination of framework grains indicates a subarkose classification for both the massive sandstone and thinly-laminated siltstone units. The presence of monocrystalline, slightly undulose quartz, potassium feldspar, plagioclase, metamorphic rock fragments and detrital micas suggest a plutonic source, primarily in the Pedernal uplift of southeastern New Mexico. Additional sediment contribution was from the Wichita and Arbuckle uplifts in Oklahoma, slight uplift in south-central Texas and the surrounding carbonate reef bank. Tectonic interpretation indicates a continental block provenance, transitional between stable cratonic platforms and uplifted block-faulted areas.

4) A clearly defined diagenetic sequence is observed in the sandstones and siltstones examined. Authigenic clays, comprised of chlorite (Ib and Ib_d polytypes), degraded illite, slightly expandable mixed-layer chlorite and minor mixed-layer illite-chlorite, form thick and continuous to thin and interrupted detrital grain coatings, and pore throat bridges and linings. Subsequent quartz and feldspar overgrowth development, inhibited to a degree by clay coatings, and feldspar dissolution were proceeded by scattered deposition of calcium carbonate and dolomite cements. Continuation of clay development occurred concurrently with these processes. Late-stage anhydrite deposition followed cessation of all previous diagenetic events.

Additional diagenetic features observed include detrital grain deformation, dissolution, embayment and suturing.

With respect to absolute time, development of diagenetic fabrics followed deposition of overlying Ochoan evaporites, the suggested source for many of the authigenic materials.

5) A depth-related diagenetic clay zonation can be identified within the Coyanosa field area. Increasing depths resulted in improved structural ordering, decrease in randomly interlayered expandable material and enrichment in magnesium with respect to iron within the authigenic chlorites and illites. In addition, an overall increase in relative amounts of illite is also noted. On the basis of observed clay transformations, three vertical zones (4700 to 5500 feet, 5500 to 6400 feet, greater than 6400 feet), characterized by distinct authigenic clay suites have been delineated in the field area. Comparison of this diagenetic clay sequence with similar studies suggests that formation of initial clay species occurred at maximum burial depths (8000 to 10,000 feet) attained during Late Triassic and Early Jurassic. Signs of degradation are detected in the clay species under present pressures and temperatures.

6) Lateral diagenetic clay trends cannot be distinguished in the Coyanosa field area. This is primarily a conse-

quence of the mineralogical and textural uniformity displayed within the massive sandstone units.

7) The impact of authigenic clay growth on reservoir parameters is marked. Authigenic clay growth accounts for extreme variability and reduction in permeabilities and increased water saturations within the two formations. Illite clays tend to have the greatest detrimental effect on these parameters. Net porosity is not affected; however, primary intergranular porosity is replaced by intricate microporous networks, established as a result of authigenic clay growth.

8) Well-stimulation programs can be adversely affected if specific clay types are not properly treated. Therefore, within the Coyanosa field area it is necessary to recognize the fresh-water sensitivity of illites and expandable layers (although it has been suggested that the expandable material present is not affected by salinity changes), the migration of broken illite appendages and the acid-sensitivity of iron-containing chlorites. It is also important to stress that in all cases successful clay removal can be attained, exceeding benefits obtained from clay stabilization techniques.

APPENDIX I

DETAILED CORE AND CORE CHIP SECTIONS WITH ACCOMPANYING X-RAY DIFFRACTION TRACES AND DIAGENETIC FEATURES

Slabbed core sections and core chip samples obtained from the 14 wells utilized in this study are displayed in detail in the following section. Lithology, sample position and depth, in feet, are indicated for all cored intervals. Sedimentary structures are shown only for slabbed core sections since core chip samples were too small to allow detection of such structures. In addition, x-ray diffraction traces have been included to the right of each section. Although quantitative analyis is not possible with the reduced traces, semi-quantitative determination of chemical composition and relative clay amounts can be made. To the left of each column is a summary of the diagenetic features present in that interval. Legends are provided on the following pages to assist in interpretation of lithologies and diagenetic features.

Diagenetic Features

Q Og	Quartz overgrowth	Bio	Bioclastic material, allochem ghosts
F Og	Feldspar overgrowth	Mc	Micrite clasts
Ca	Sparry calcite	Dt Cl	Detrital clay, matrix material
Dol	Dolomite	Dt Mi	Detrital micas
An	Anhydrite	Pr Su	Pressure solution, grain suturing
Ch	Chlorite coatings	Alt F	Altered and degraded feldspars
Py	Authigenic pyrite	Gr Cr	Grain corrosion (primarily at micrite) clast/grain boundaries)

____ Presence of diagenetic feature supported by core, thin section or SEM examination.

... Presence of diagenetic feature interpolated between known occurrences. Homogeneity assumed within individual lithologic units.

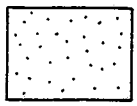
Light grey, very fine-grained to fine-grained very friable to moderately friable massive sandstone

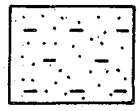
Light grey, coarse-grained, slightly shaly, thinly-laminated siltstone

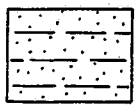
Medium to dark grey, medium to coarse-grained very shaly, thinly-laminated siltstone


Dark grey shale

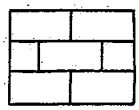
Medium to dark grey limestone

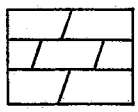
Medium to dark grey, finely-crystalline dolomite

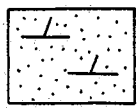
Light grey, very fine-grained to fine-grained dolomitic sandstone

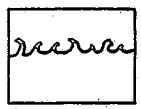
Disturbed and convoluted shaly beds, primarily occurring in massive sandstone units

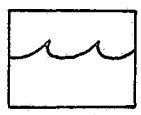
Ripple-drift cross-lamination


Large-scale trough cross-bedding, often occurring at high angles and proceeding scour and channeling of underlying sandstone units

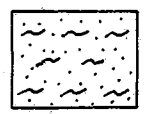
Bioturbated, slightly shaly sandstone and siltstone represented by horizontal and vertical burrowing, and back-filled grazing trails

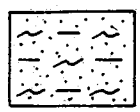
Bioturbated, very shaly sandstone and siltstone

MOBIL

COYANOSA PLANT 'A' SWDW #1

Section 48 Block OW
Pecos County

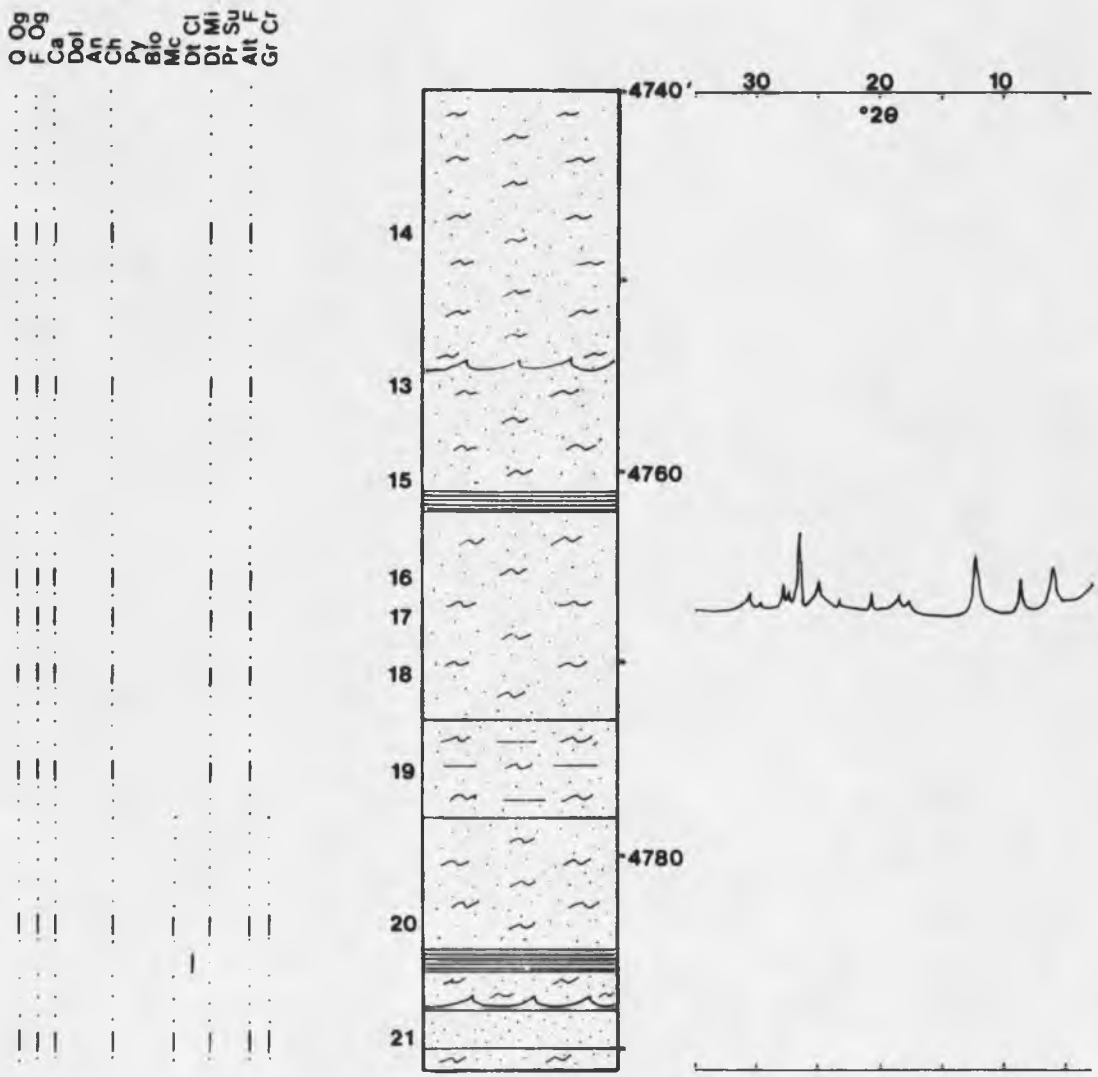

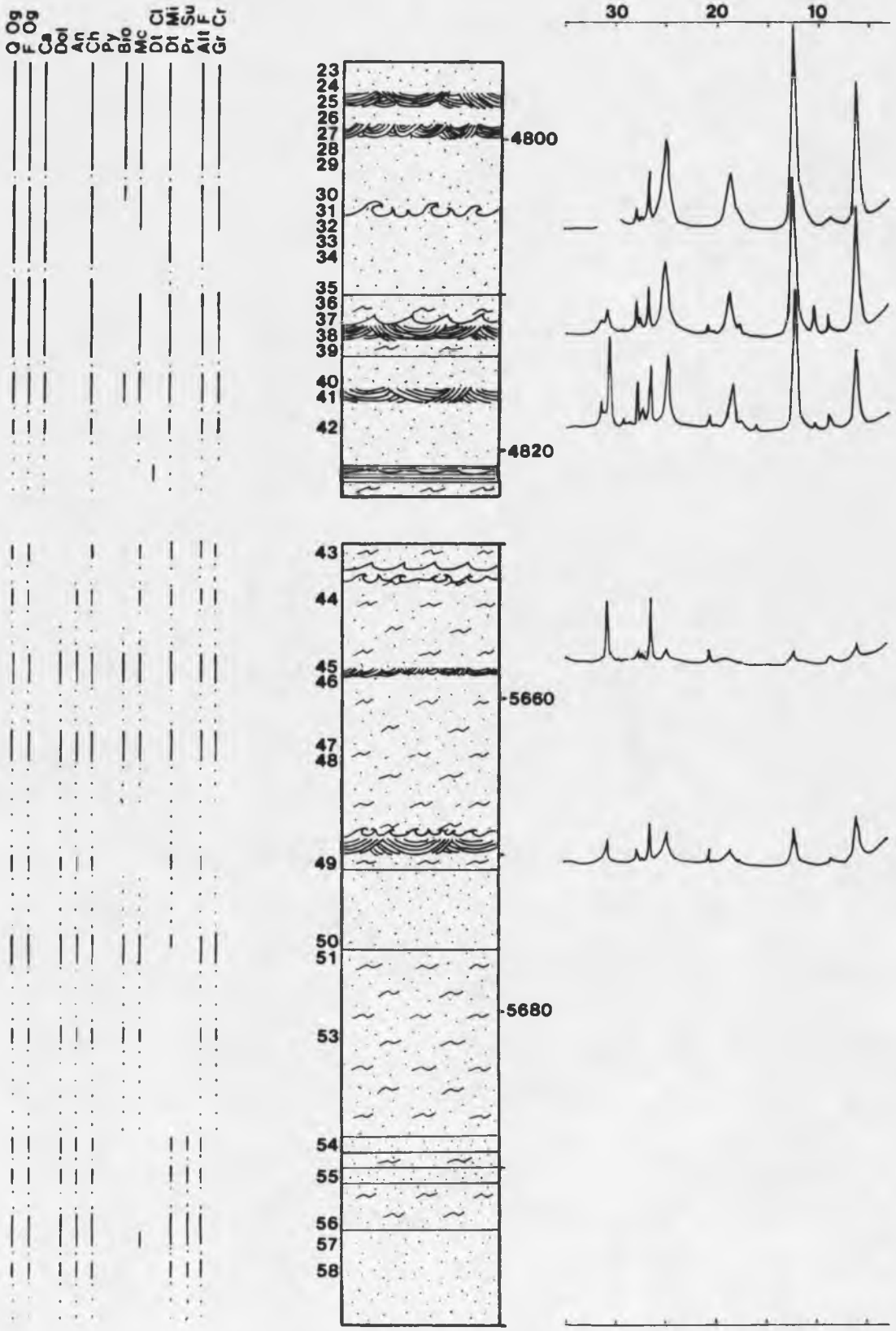
30
20
10
4800
4820
5660
5680

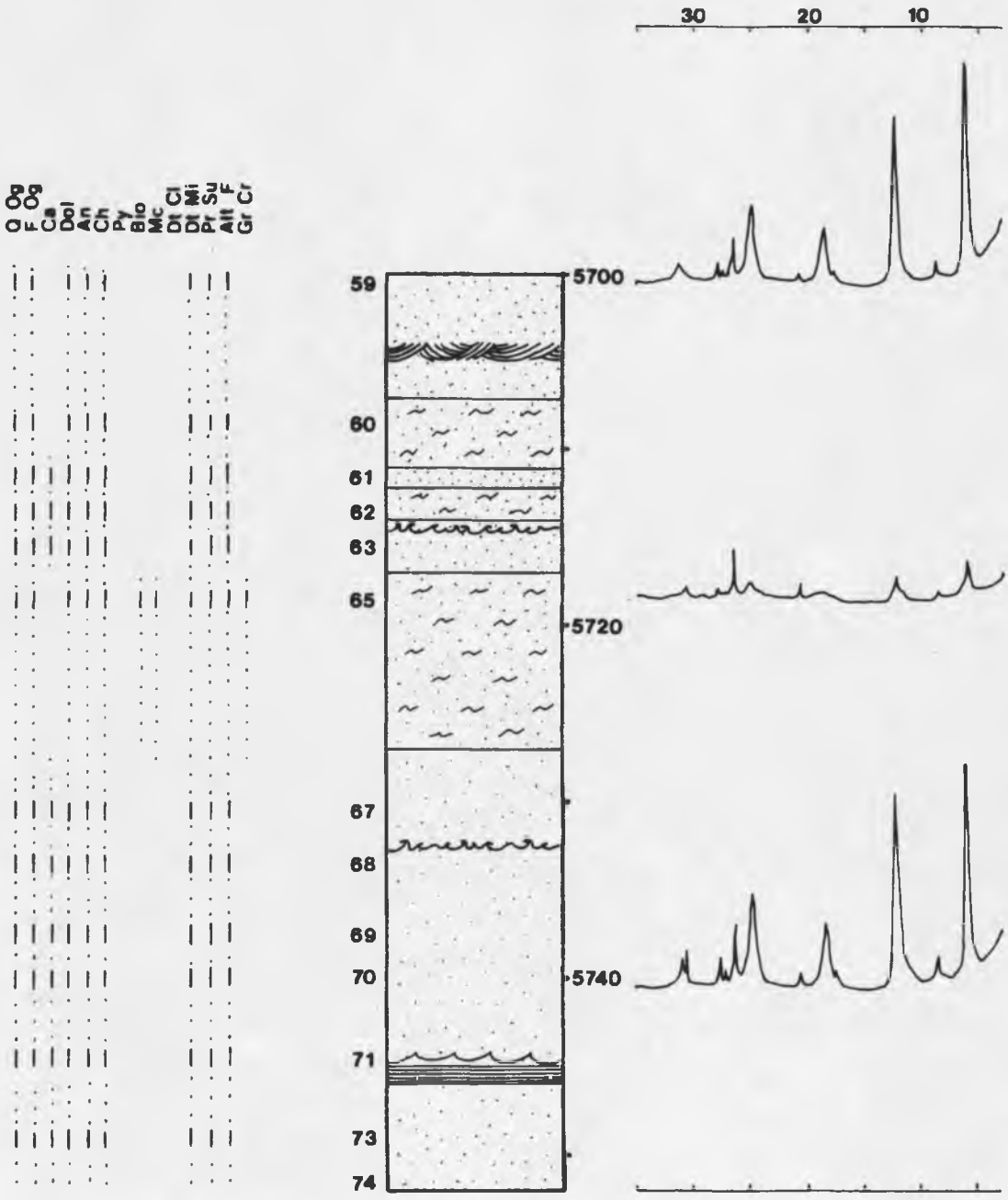
30
20
10
59
60
61
62
63
65
67
68
69
70
71
73
74
5700
5720
5740

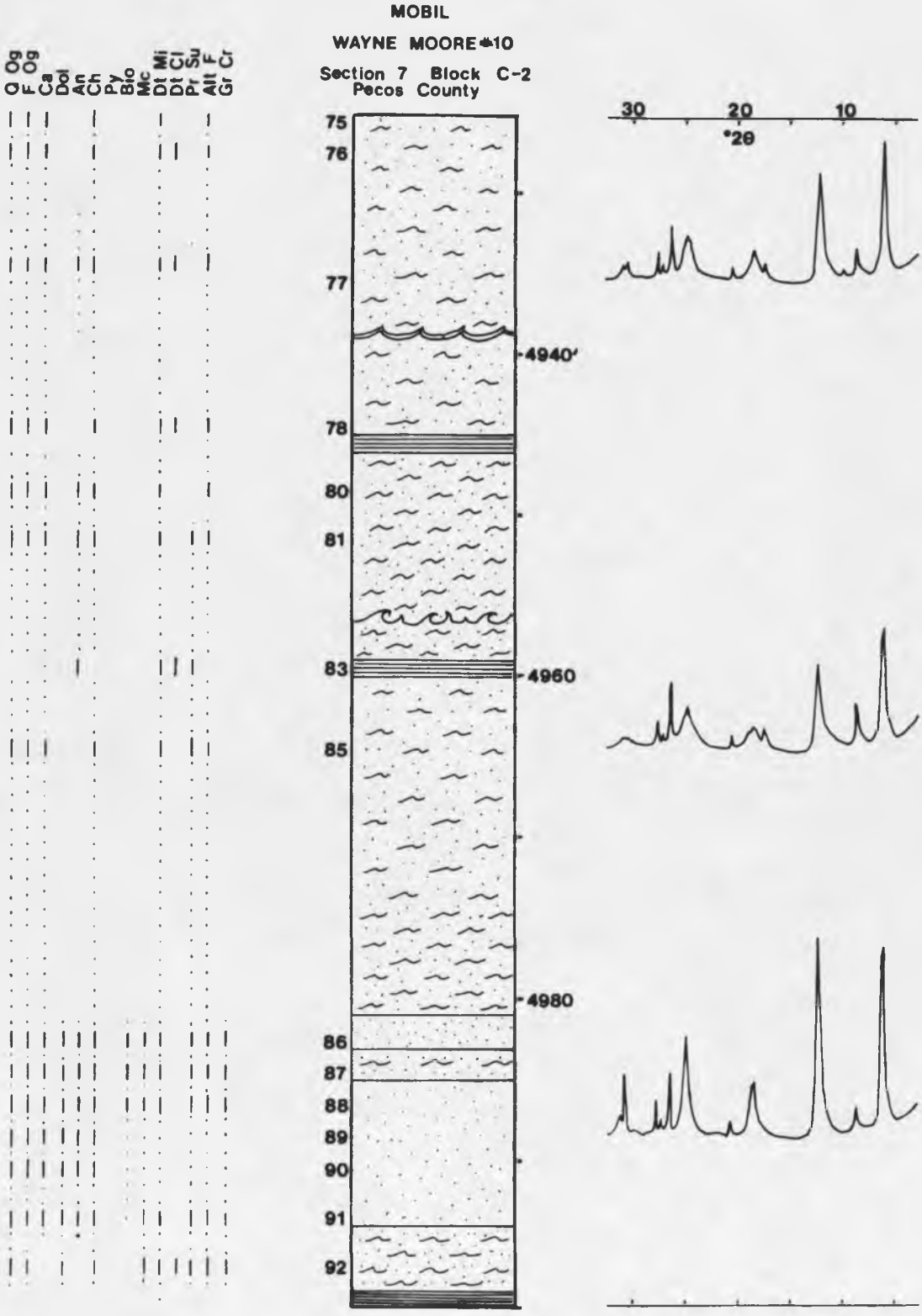
Og
Og
Gl
Dol
Ac
Ac
Py
Bio
Mc
Mi
Ch
Dr
Pr
Gu
Alt
F
Cr
Gr
MOBIL
WAYNE MOORE #10
Section 7 Block C-2
Pecos County
75
76
77
78
80
81
83
85
86
87
88
89
90
91
92
4940'
4960
4980
30
20
10
°2θ

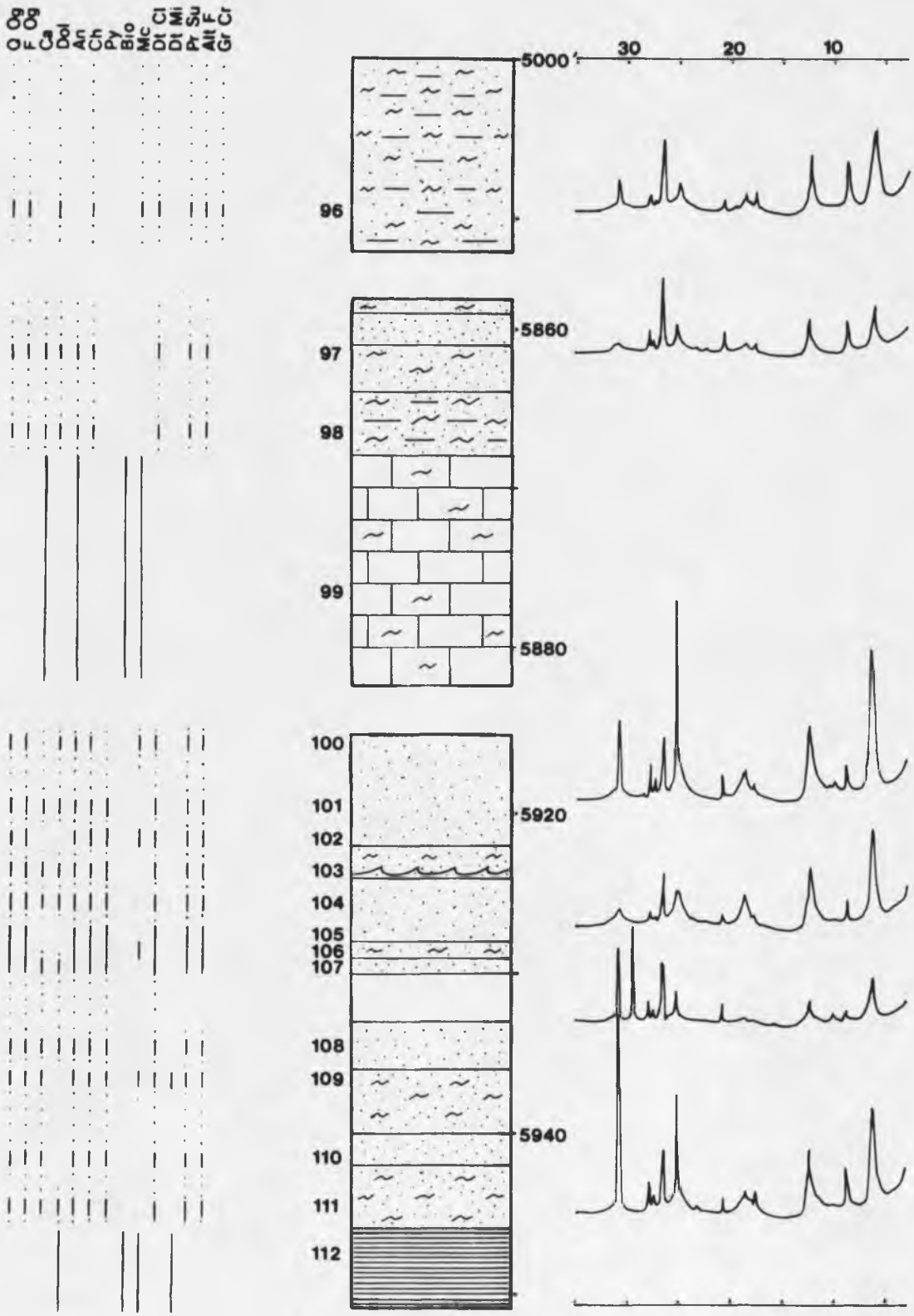
30
20
10
5000'
96
5860
97
98
99
5880
100
101
5920
102
103
104
105
106
107
108
109
5940
110
111
112

CACTUS DRILLING

McCARTY #1

Section 14 Block 49
Pecos County

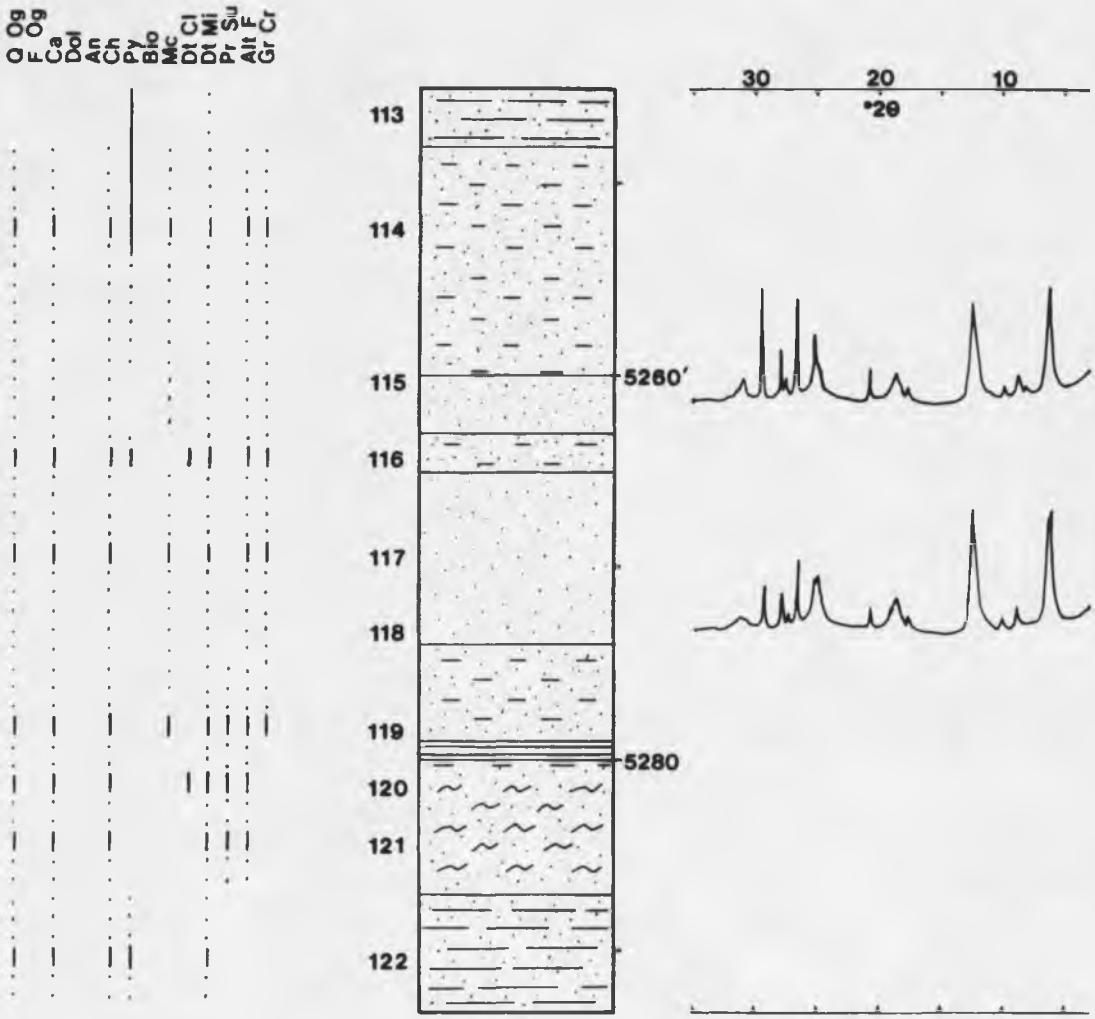

MOBIL

CHARLES B. ATHEY #C-3

Section 44 Block OW
Pecos County

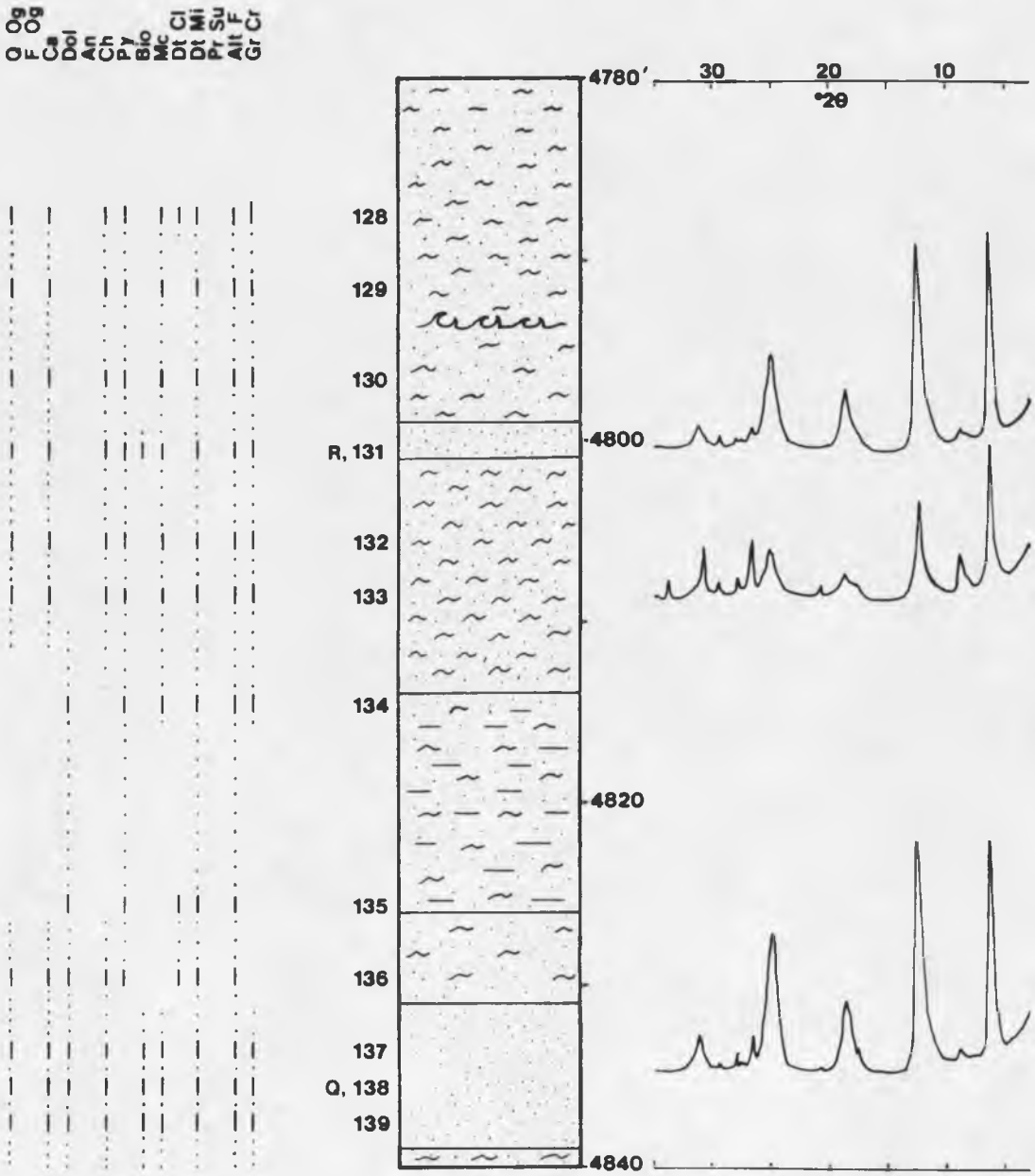

MOBIL

CHARLES B. ATHEY # 4

Section 52 Block OW
Pecos County

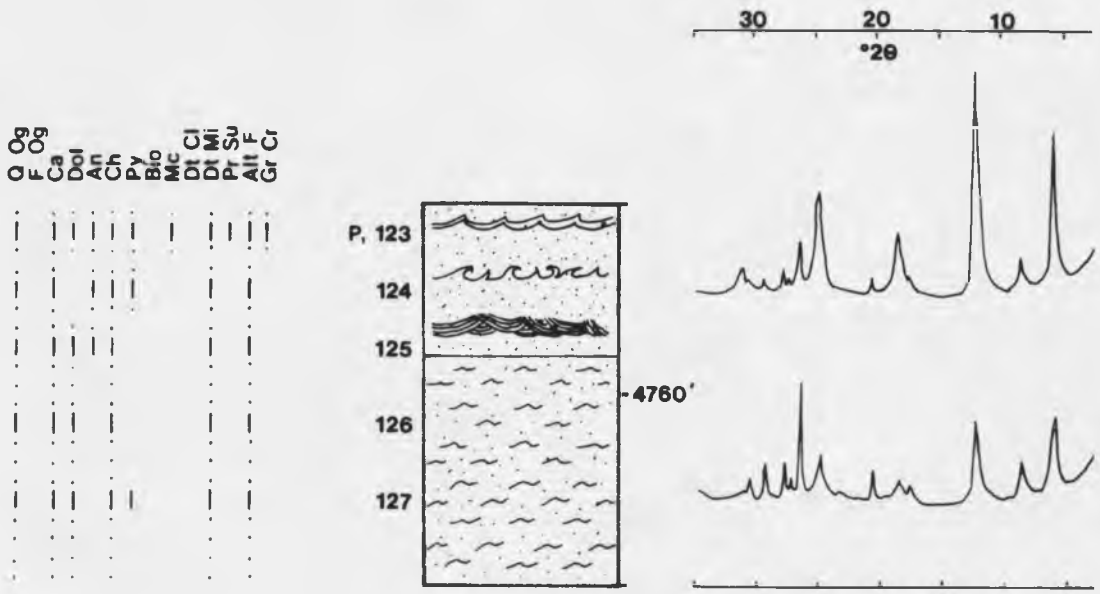

MOBIL

#1 ATHEY UNIT

Section 44 Block OW
Pecos County

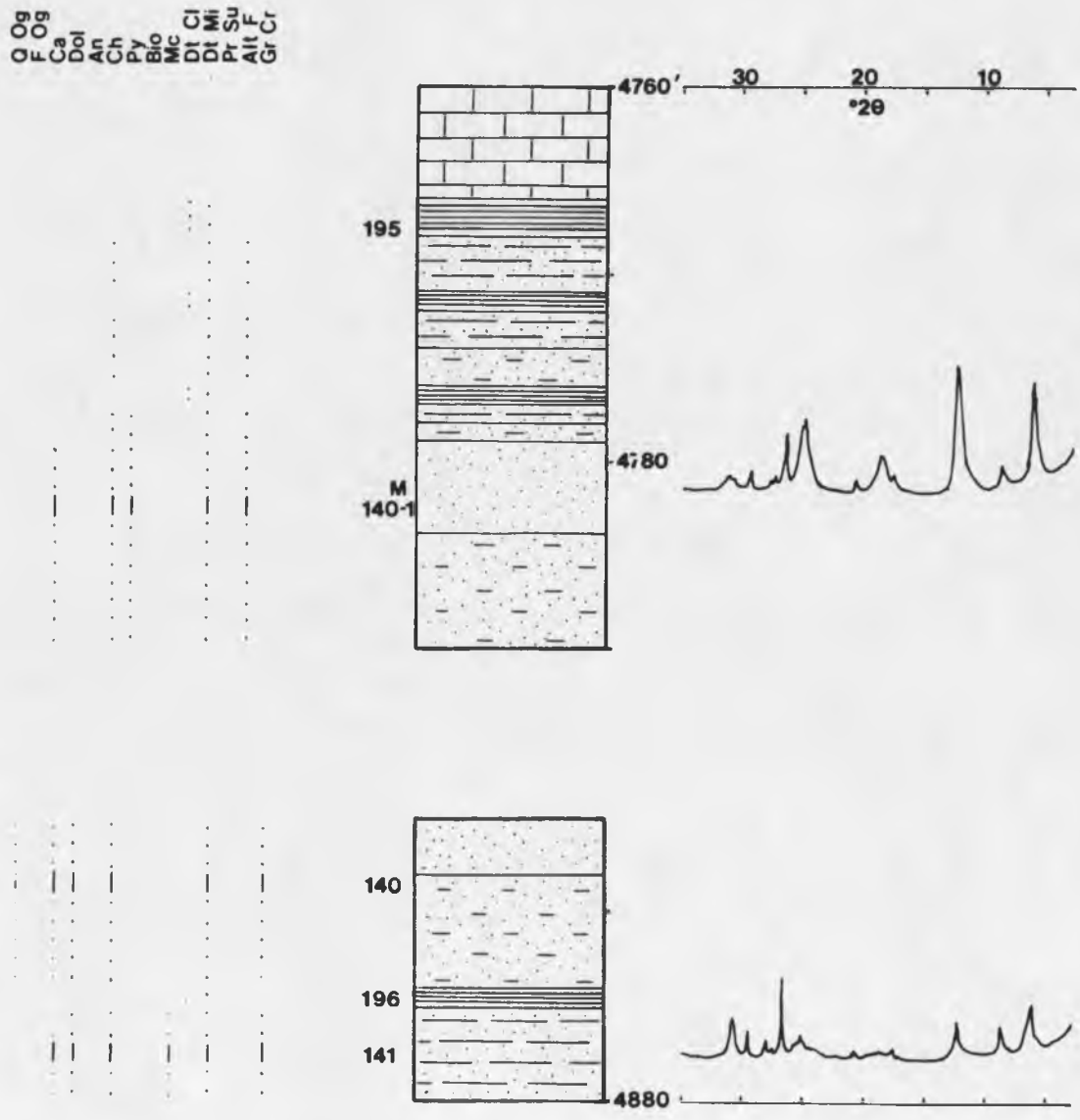

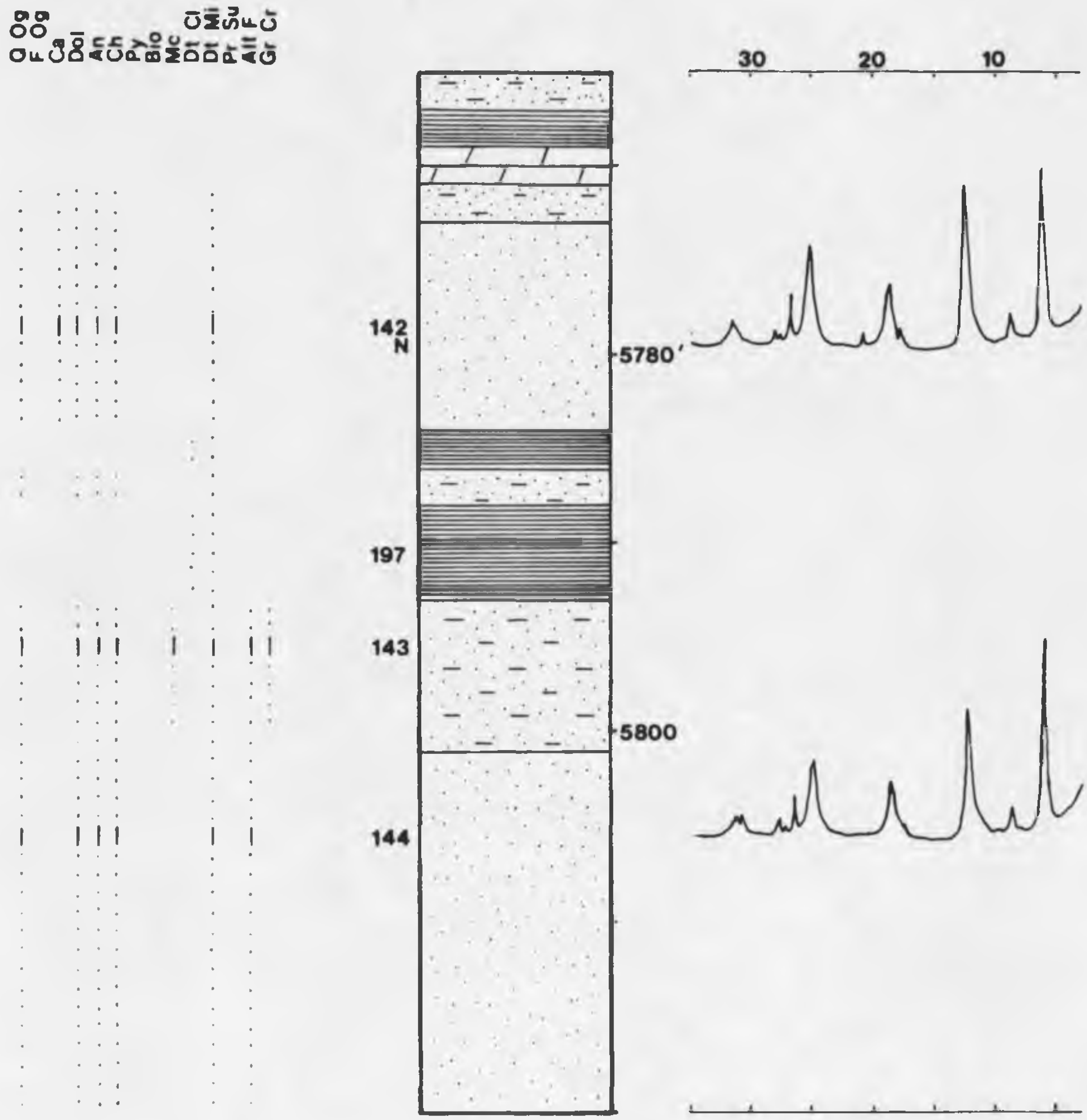
Q Qg
F Qg
Ca
Dol
An
Ch
Py
Bio
Mc
Dt Cl
Dt Mi
Pt Su
All F
Gr Cr
30
20
10
142
N
5780'
197
143
5800
144

MOBIL

STATE IVEY #1

Section 12 Block 43
Pecos County

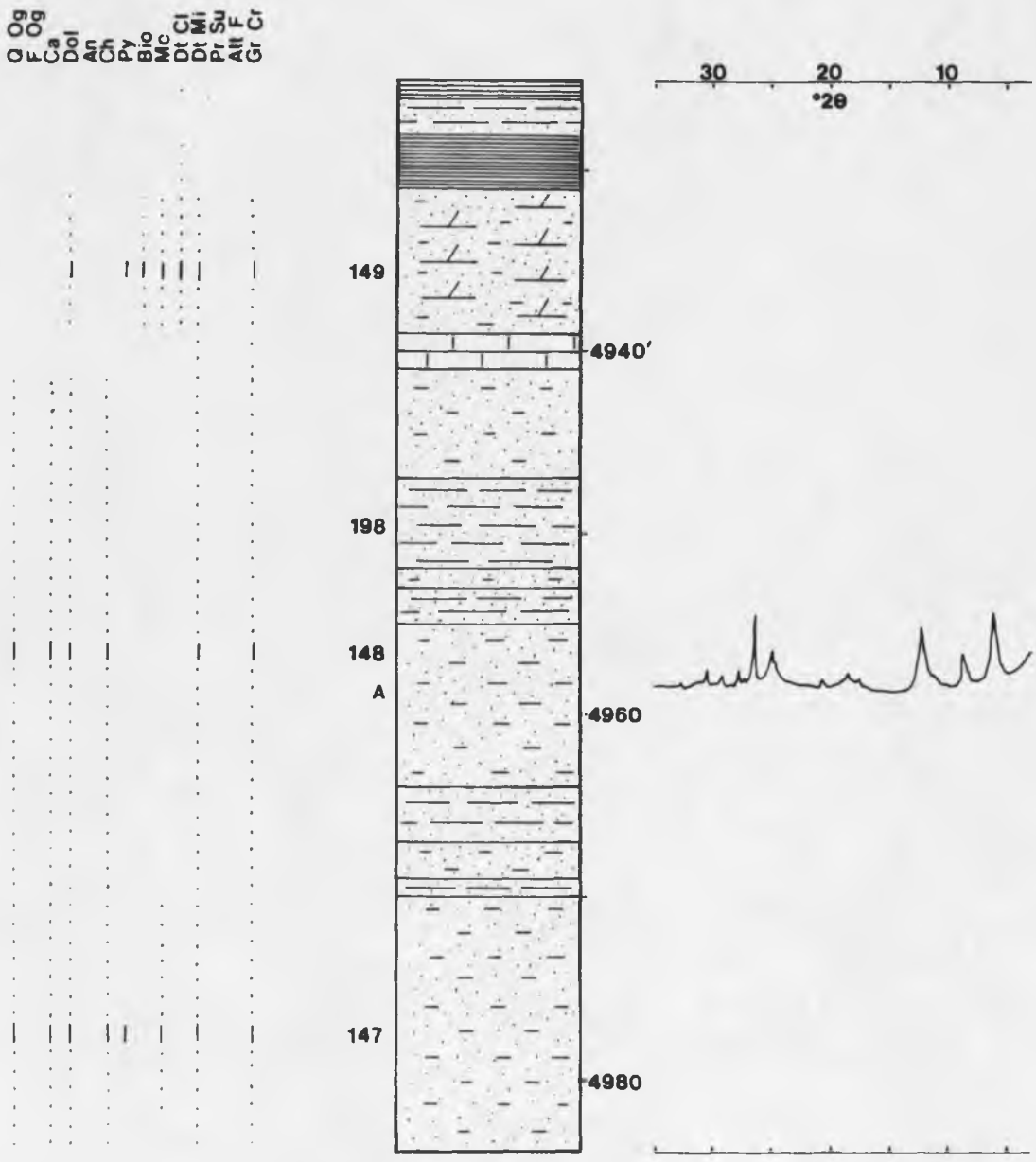

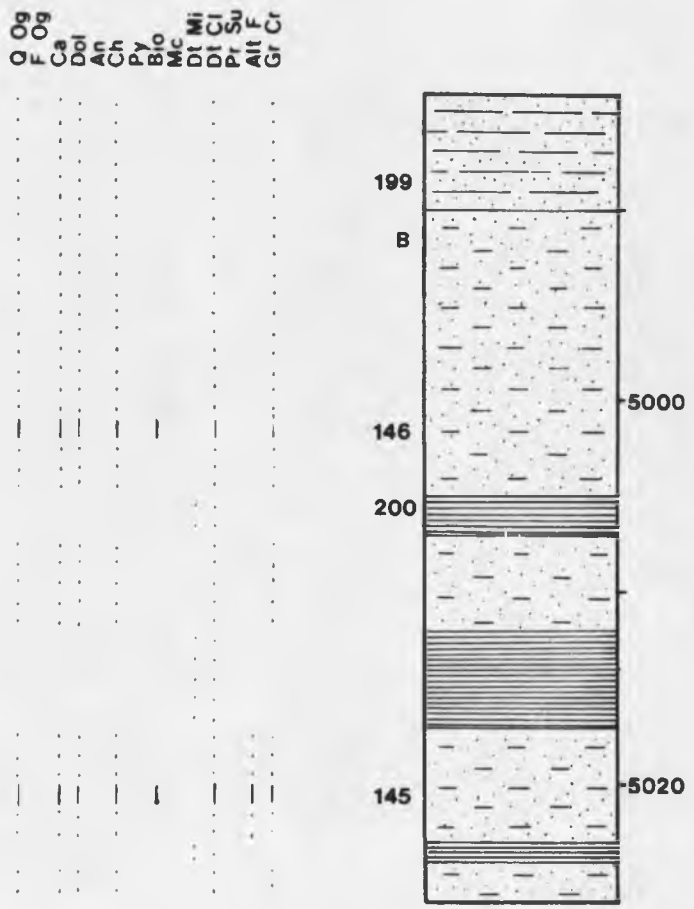
Og
Og
Q F Ca Dol Ap Ch Py Bio Mc Mi
Dr Cl
Pr Su
Alt F Cr
Gr
199
B
146
200
145
5000
5020

MOBIL

J. O. NEAL #2

Section 47 Block OW
Pecos County

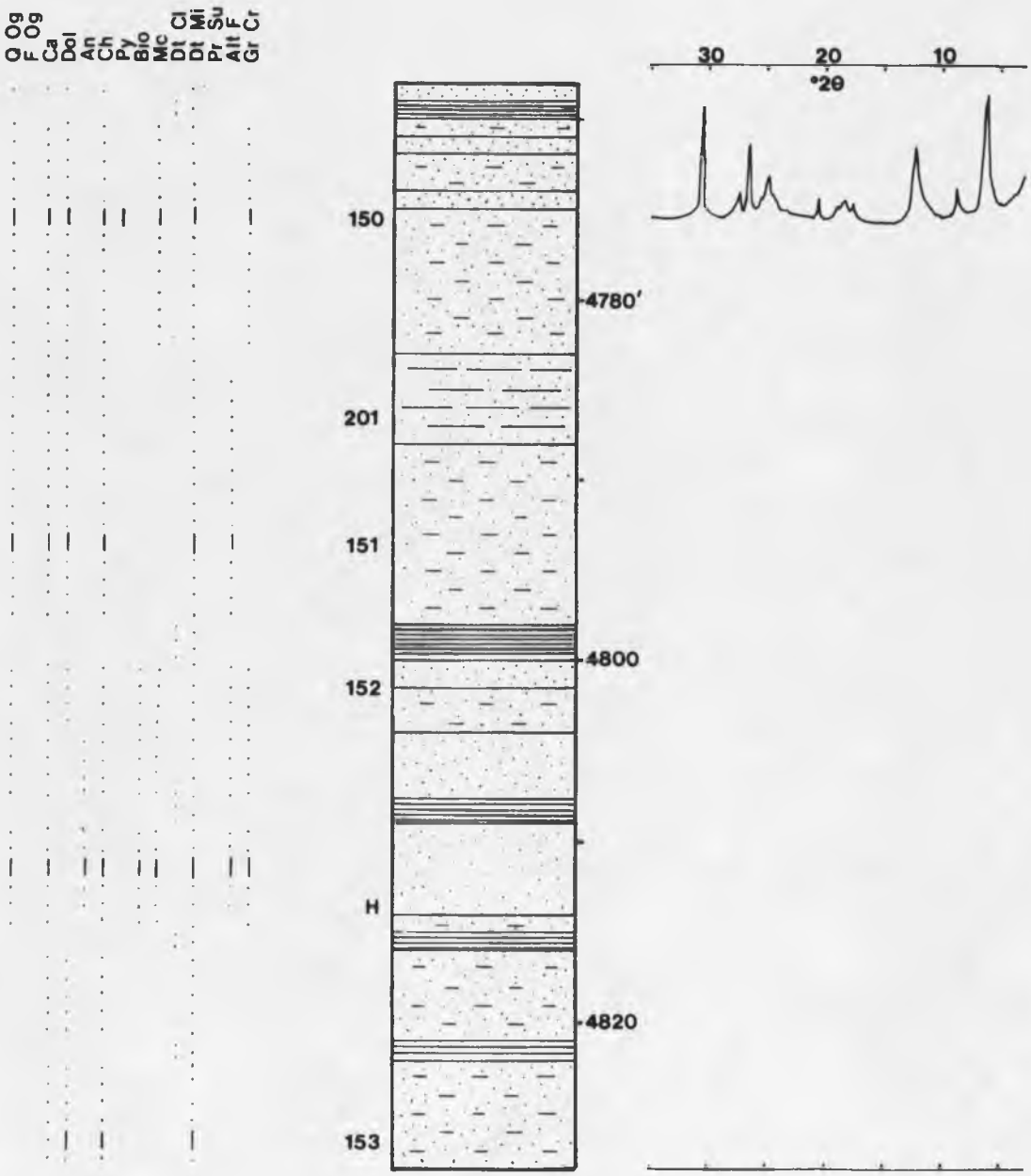

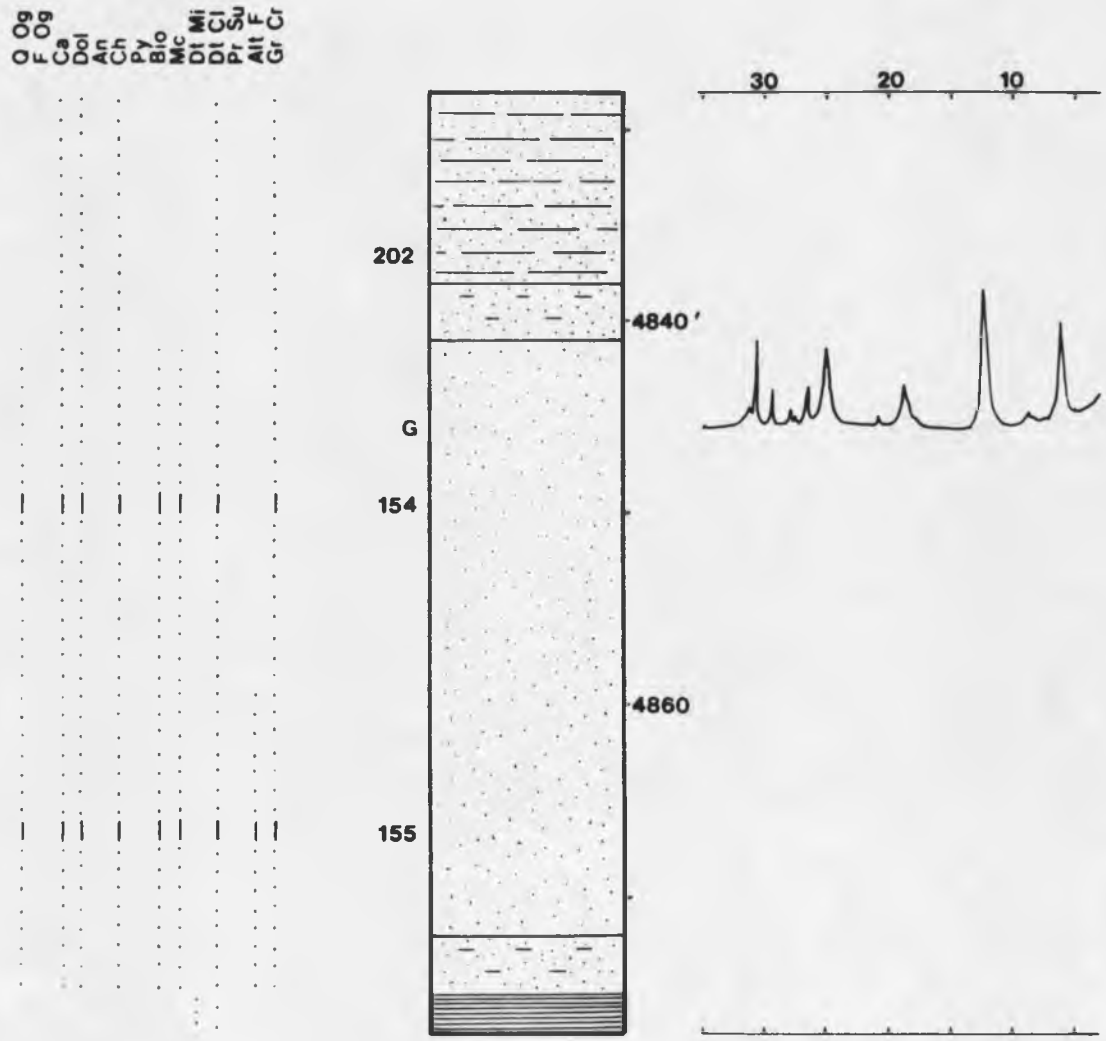
Q Og
F Og
Ca
Dol
An
Ch
Py
Bio
Mc
Di Mi
Di Cl
Pr Su
Alt F
Gr Cr
30
20
10
202
4840'
G
154
4860
155

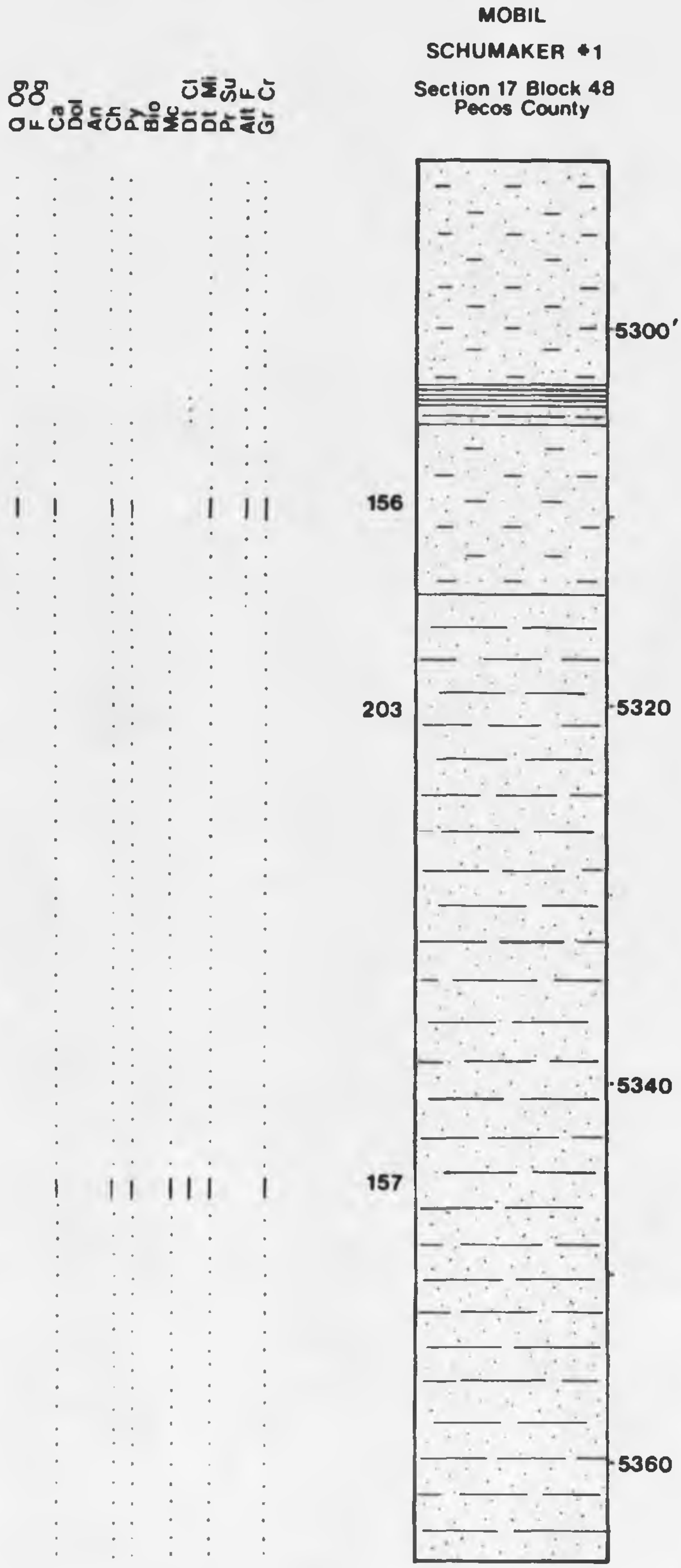
MOBIL
SCHUMAKER #1
Section 17 Block 48
Pecos County
Q Og
F Og
Ca
Dol
An
Ch
Py
Bio
Mc
Dt Cl
Dt Mi
Pr Su
Alt F
Gr Cr
156
203
157
5300′
5320
5340
5360

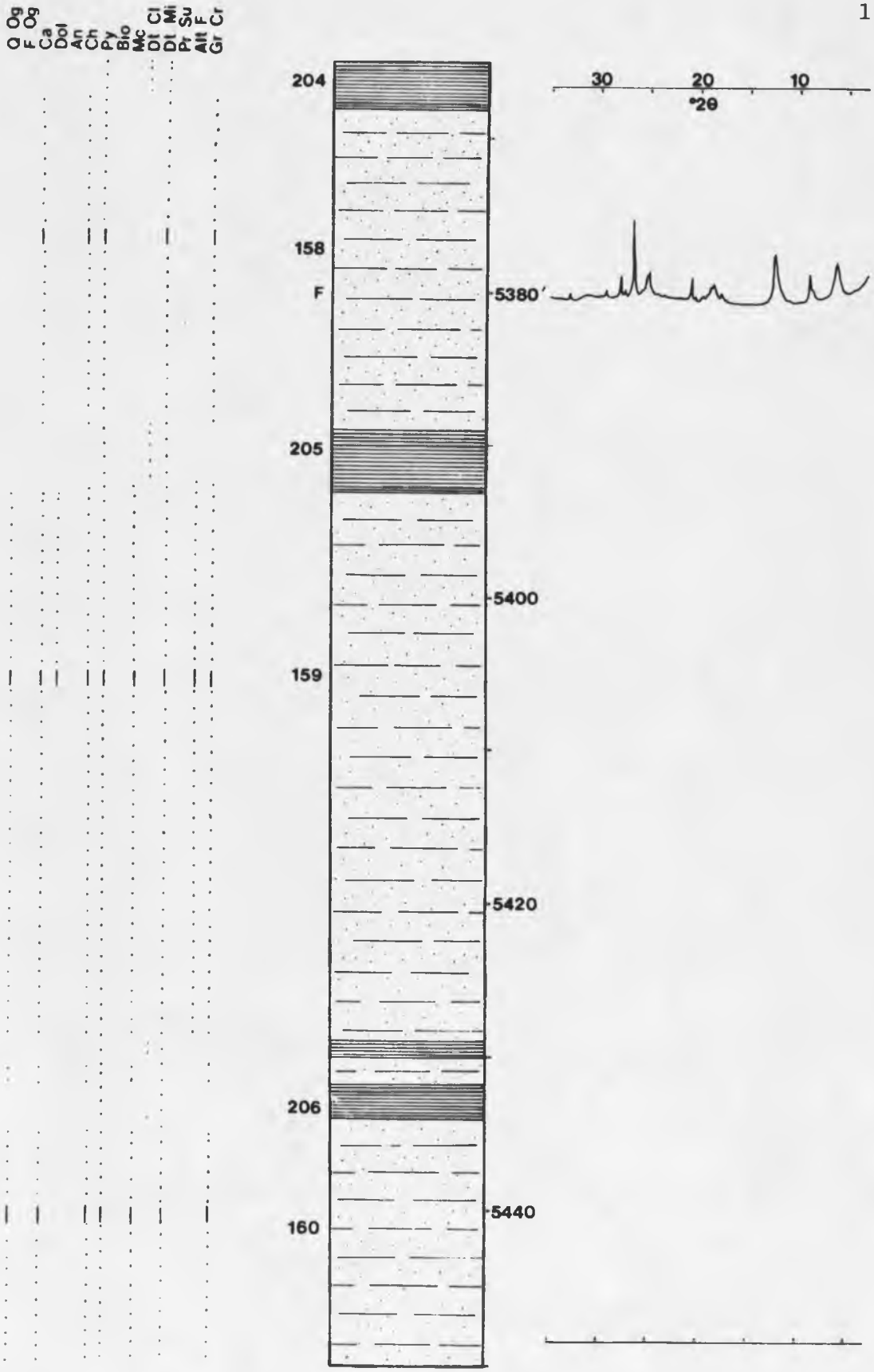
204
158
F
205
206
160
5380'
5400
5420
5440
30
20
10
°2θ

MOBIL

IVY B. WEATHERBY #4

Section 20 Block 48
Pecos County

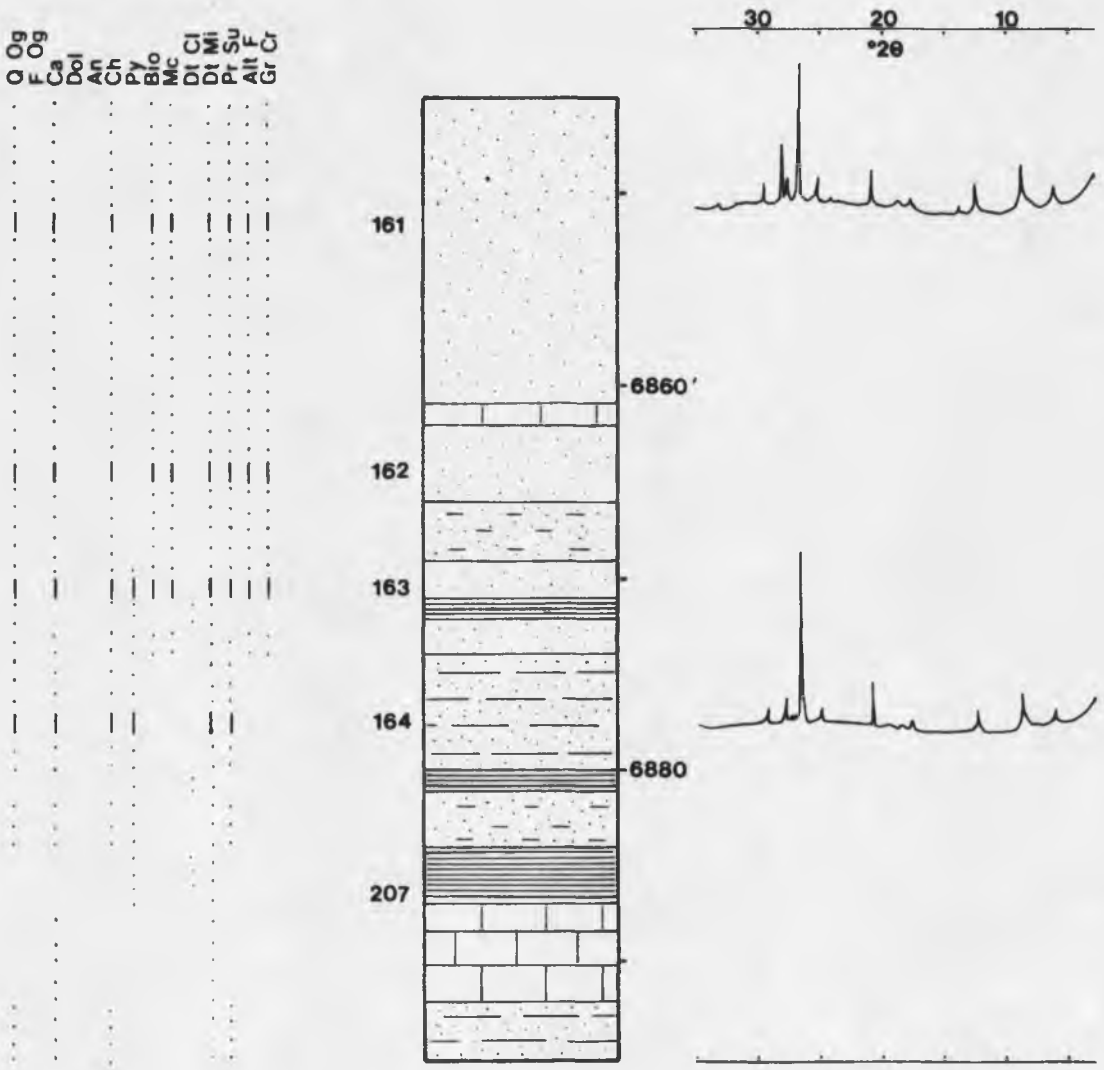

MOBIL

IVY B. WEATHERBY #1

Section 20 Block 48
Pecos County

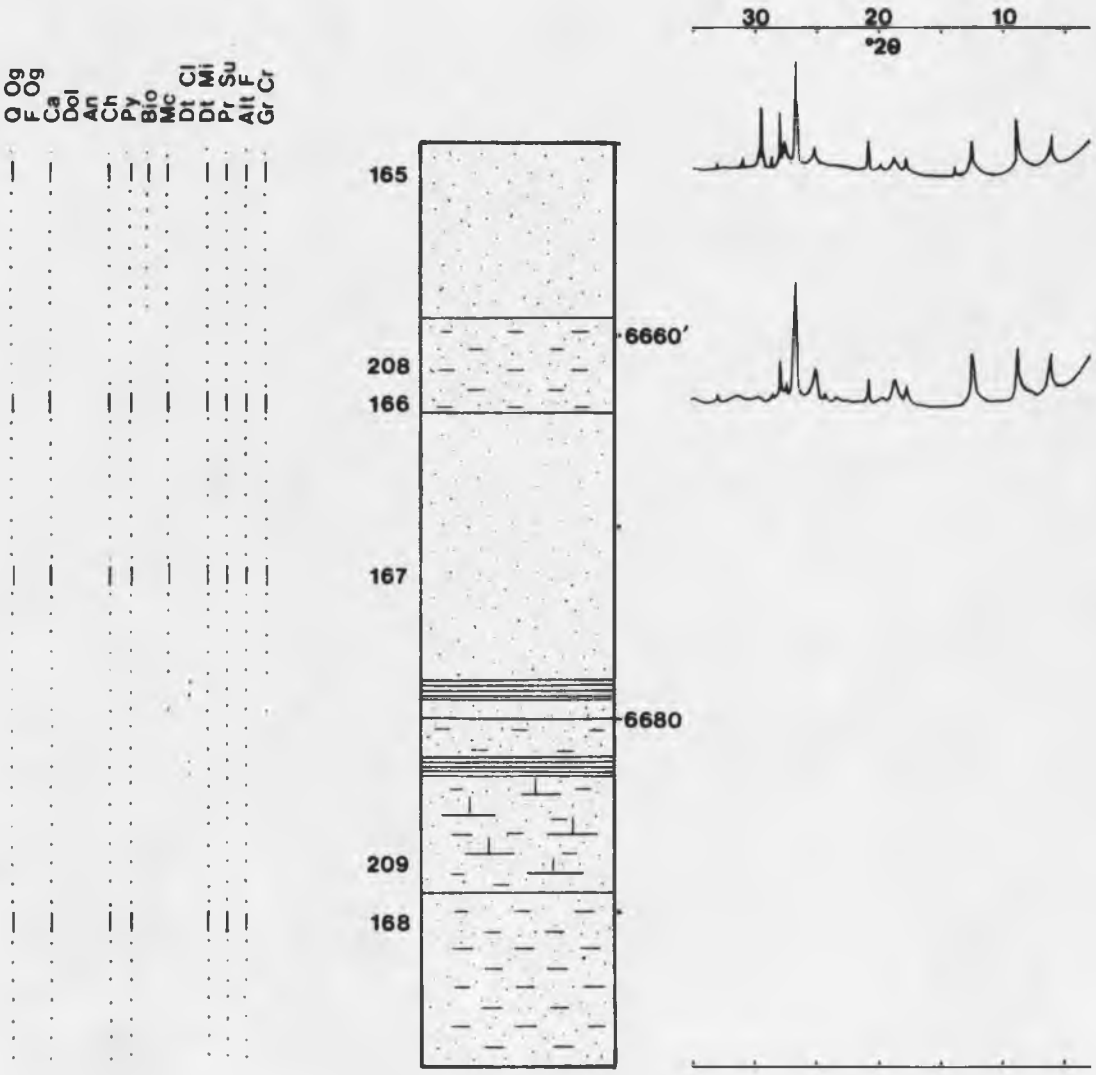

MOBIL

SIBLEY #B-1

Section 45 Block OW
Pecos County

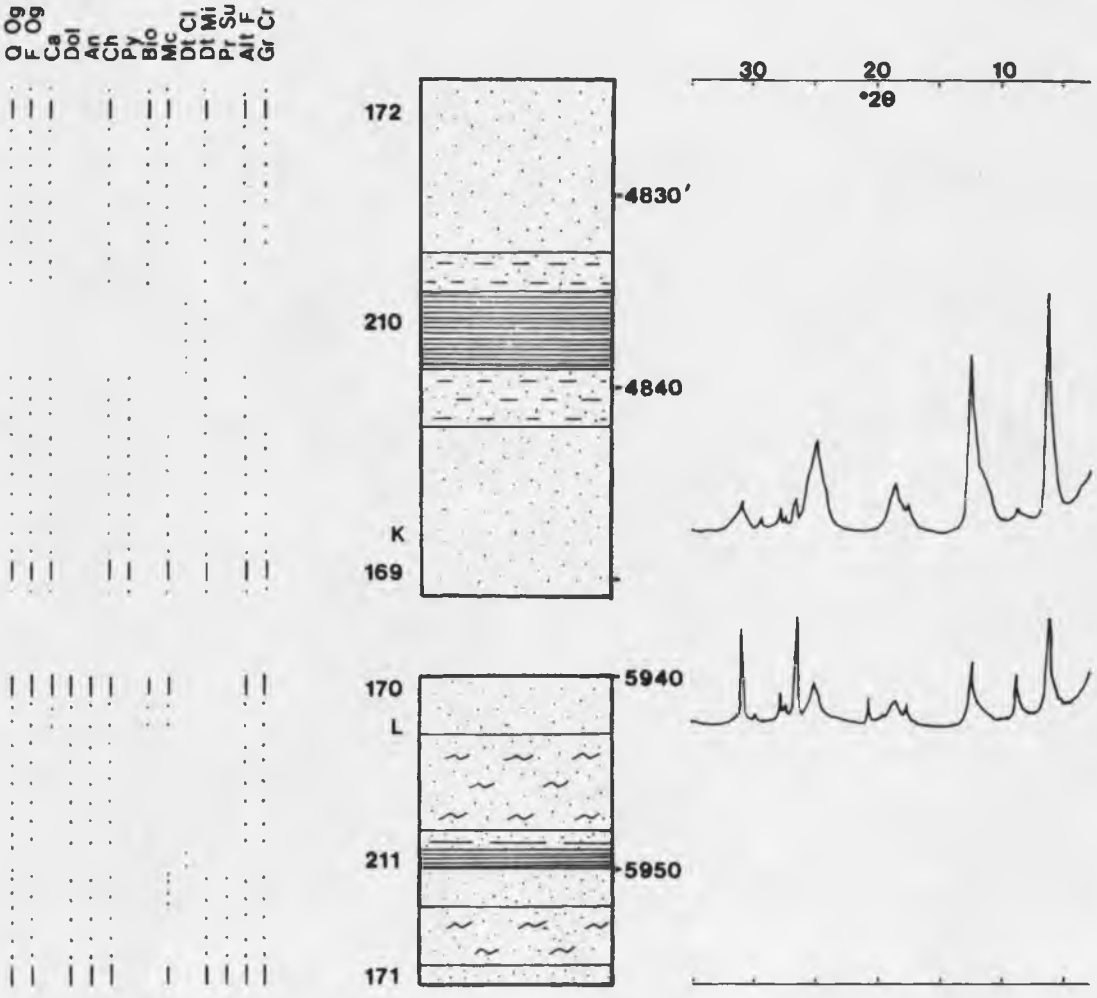

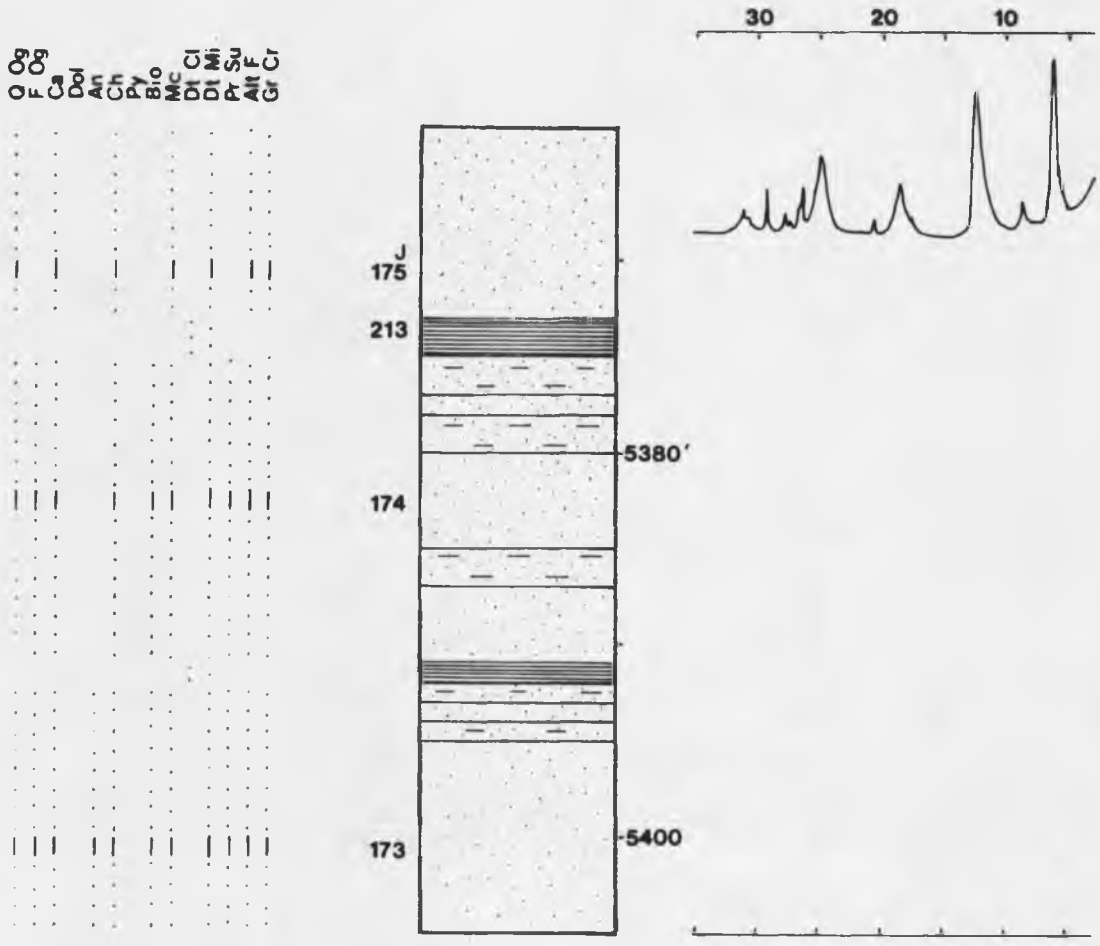
30
20
10
J
175
213
5380'
174
5400
173

PENNZOIL AND BROWN

WHISSELL #1

Section 12 Block 49
Pecos County

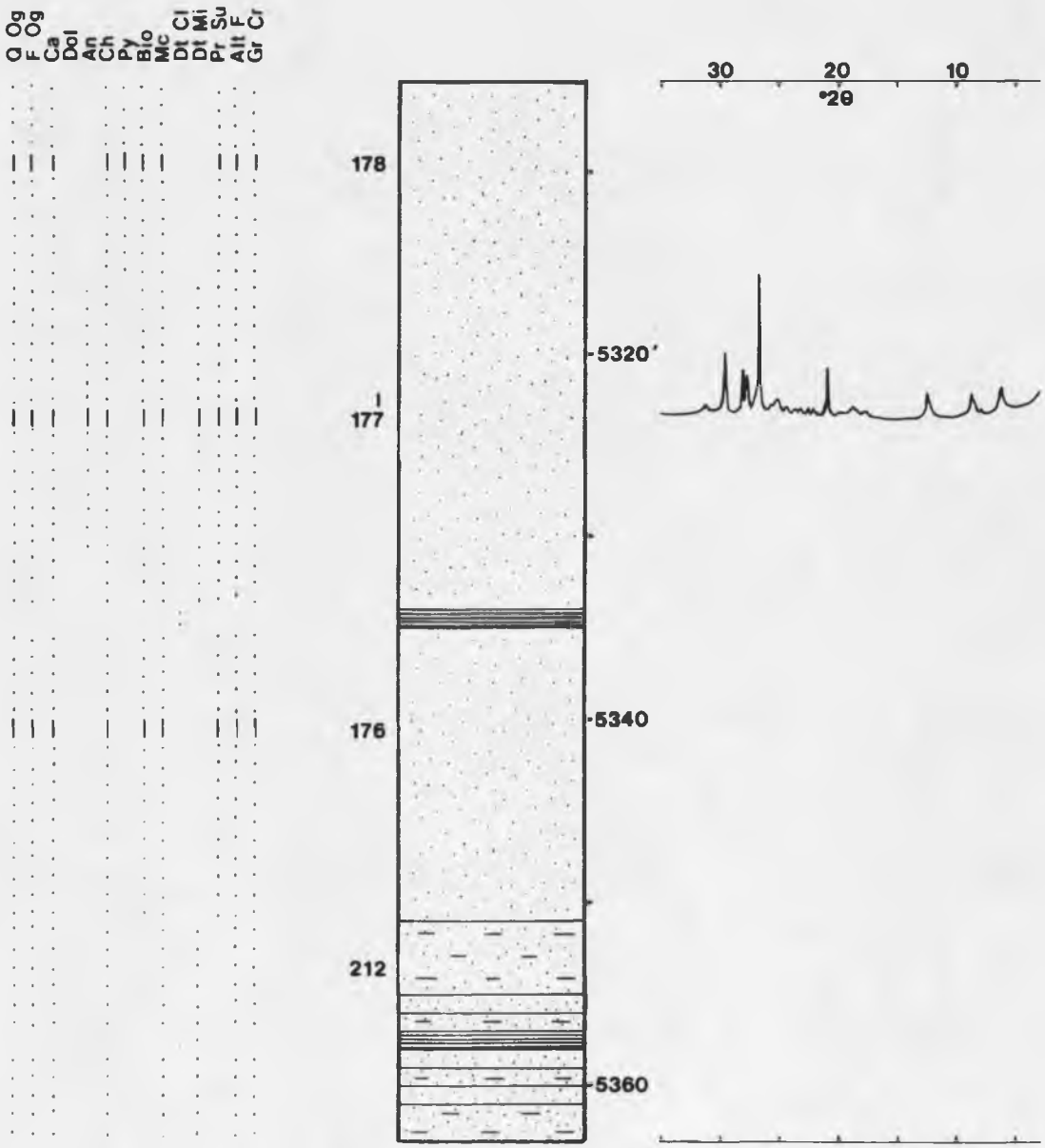

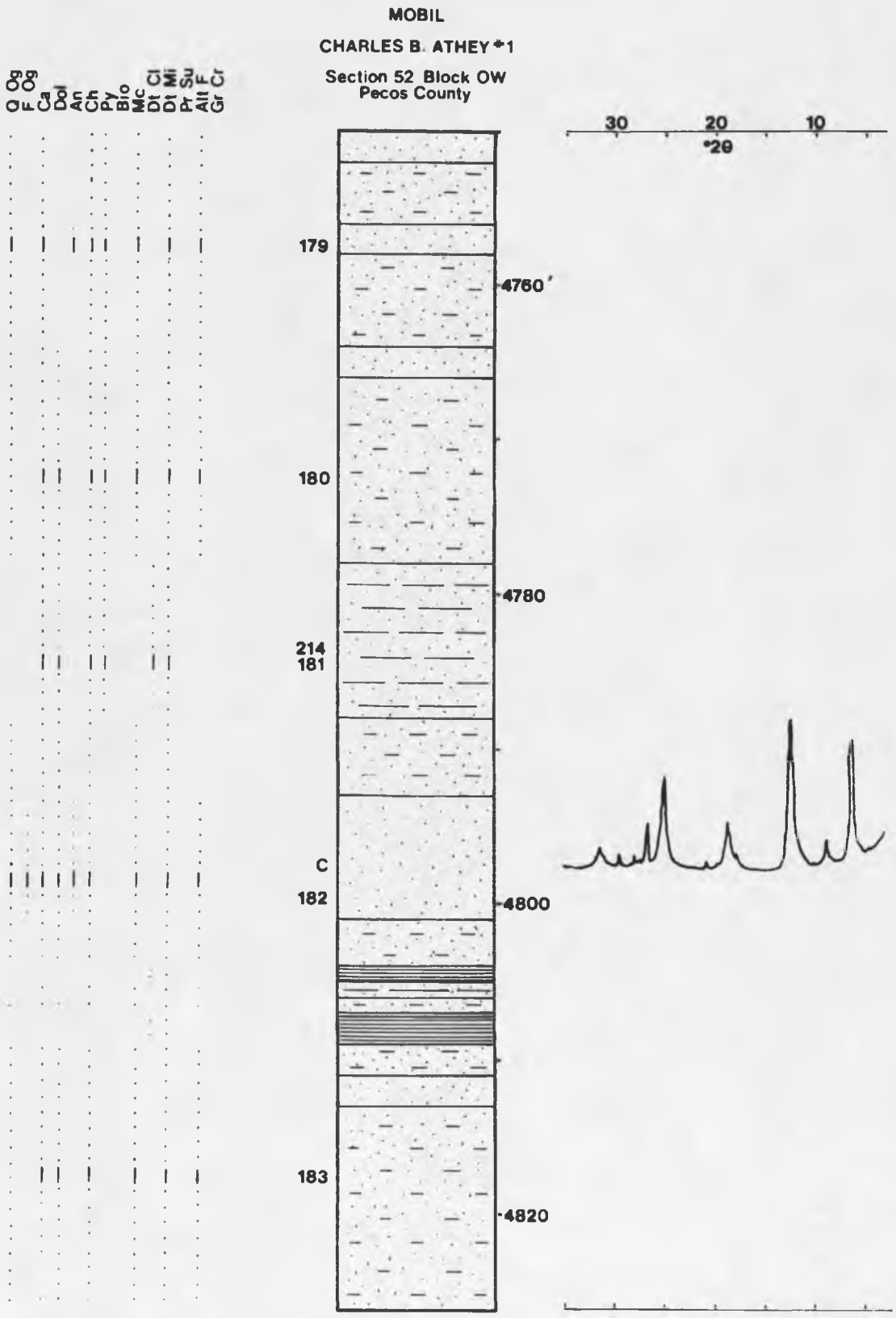
MOBIL
CHARLES B. ATHEY #1
Section 52 Block OW
Pecos County
Og
Og
Cf
Ca
Do
Ac
Cc
Py
Bio
Mc
Di
Di
Pr
All
Gr
30
20
10
°2θ
179
180
214
181
C
182
183
4760'
4780
4800
4820

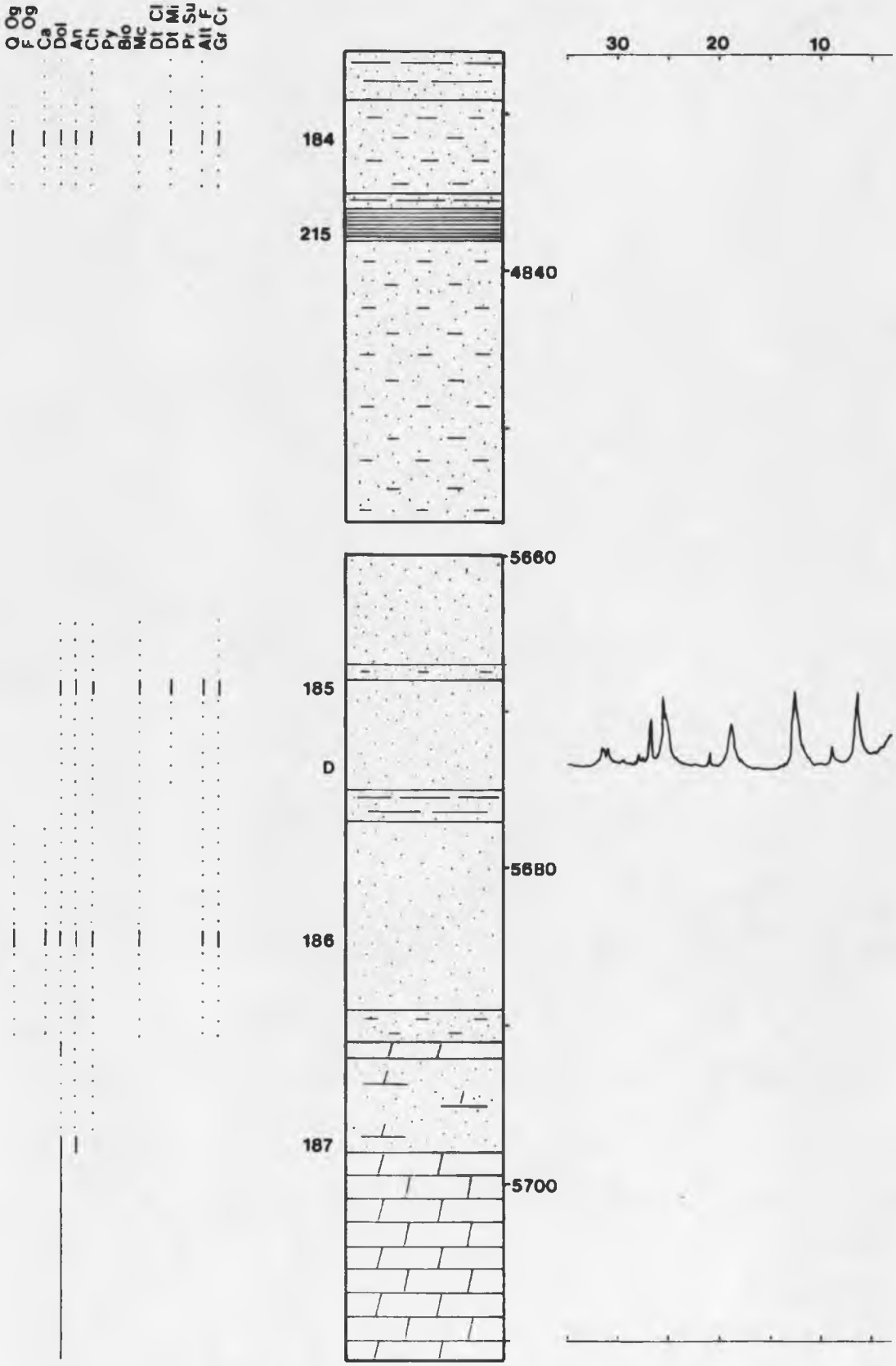
Og
Oo
Ca
Dol
Ac
Cl
Py
Bio
Mc
Cl
Di
Mi
Pr
Su
An
F
Gr
Cr
30
20
10
184
215
4840
5660
185
D
5680
186
187
5700

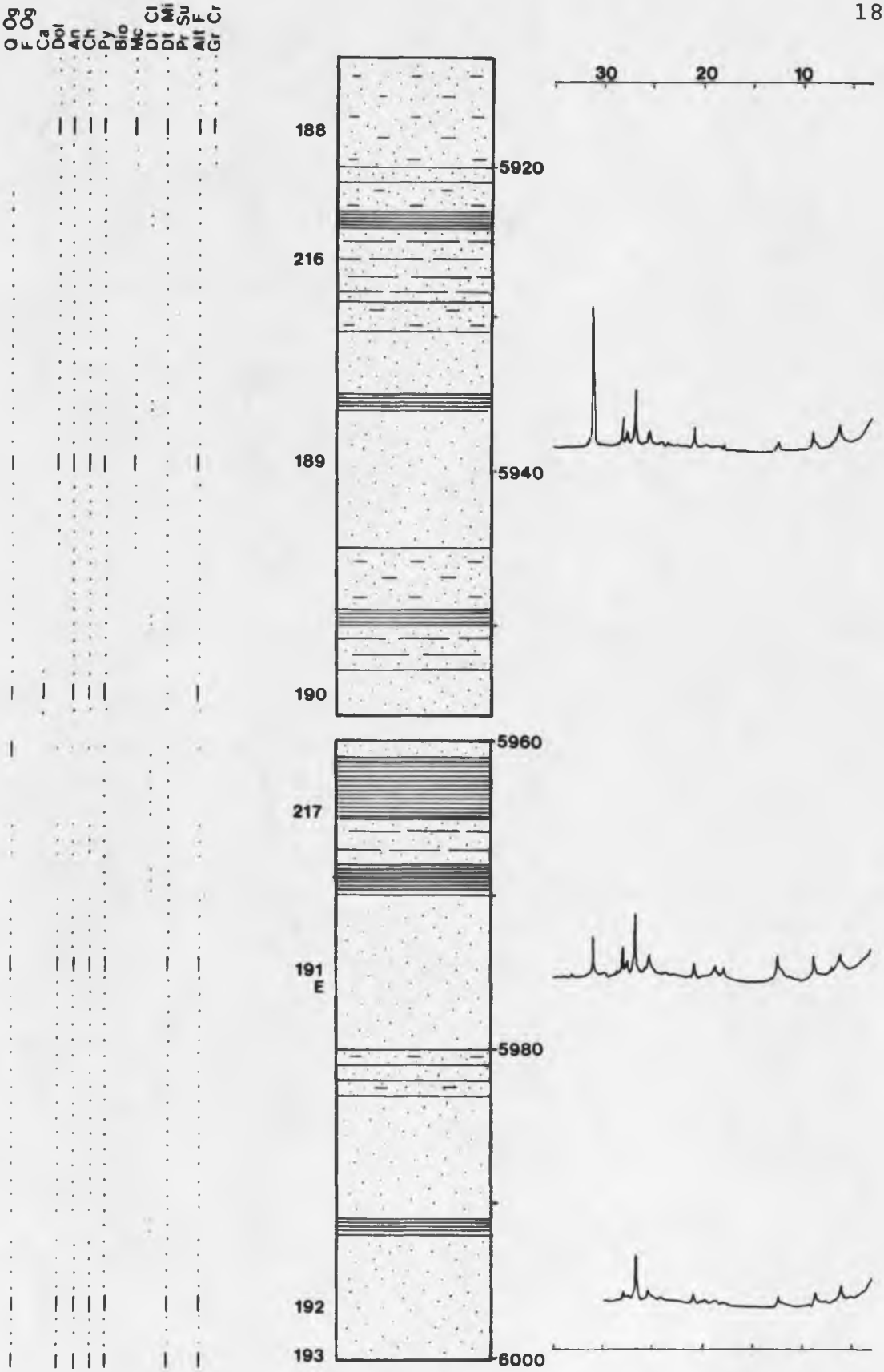
30
20
10
188
5920
216
189
5940
190
5960
217
191
E
5980
192
193
6000

REFERENCES

Adams, J.E., 1965, Stratigraphic-tectonic development of Delaware basin: Am. Assoc. Petroleum Geologists Bull., v. 49, p. 140-2148.

_____ and H.N. Frenzel, 1950, Capitan barrier reef, Texas and New Mexico: Jour. Geology, v. 58, p. 289-312.

Almon, W.R., 1979, Sandstone diagenesis: applications to exploration and exploitation: Am. Assoc. Petroleum Geologists Clastic Diagenesis School, Course Notes, 93 p.

Anderson, R.Y., W.E. Dean, Jr., D.W. Kirkland, and H.I. Snider, 1972, Permian Castile varved evaporite sequence, West Texas and New Mexico: Geol. Soc. America Bull., v. 83, p. 59-86.

Beck, R.H., 1967, Depositional mechanics of the Cherry Canyon Formation, Delaware basin, Texas: unpublished master's thesis, Texas Tech. University, 107 p.

Berg, R.R., 1975, Capillary pressures in stratigraphic traps: Am. Assoc. Petroleum Geologists Bull., v. 59, p. 939-956.

_____, 1979, Reservoir sandstones of the Delaware Mountain Group, southeast New Mexico in Guadalupian Delaware Mountain Group of West Texas and southeast New Mexico: Soc. Econ. Paleontologists Mineralogists, Permian Basin Section, Pub. 79-18, p. 75-95.

Bouma, A.H., 1962, Sedimentology of some flysch deposits: Elsevier, Amsterdam, 168 p.

Boyd, D.W., 1958, Permian sedimentary facies, central Guadalupe Mountain, New Mexico: New Mexico Bur. Mines and Mineral Resources Bull., v. 49, 100 p.

Bozanich, R.G., 1979, The Bell Canyon and Cherry Canyon Formations, eastern Delaware basin, Texas:

lithology, environments and mechanisms of deposition, in Guadalupian Delaware Mountain Group of West Texas and New Mexico: Soc. Econ. Paleontologists Mineralogists, Permian Basin Section, Pub. 79-18, p. 121-141.

Bradley, W.F., 1954, X-ray diffraction criteria for the characterization of chlorite material in sediments: Clays Clay Minerals, 2nd Natl. Conf. 1953, p. 324-334.

Brindley, G.W., and F.M. Gillery, 1956, X-ray identification of chlorite species: Am. Mineralogist, v. 41, p. 169-189.

Brown, G., 1955, The effects of isomorphous substitution on the intensities of (001) reflections of mica- and chlorite-type structures: Mineralogical Mag., v. 30, p. 657-665.

Collines, A.G., 1975, Geochemistry of oilfield waters: Elsevier, Amsterdam, 496 p.

Cromwell, D.W., 1979, Indian Draw Delaware field: a model for deeper Delaware sand exploration, in Guadalupian Delaware Mountain Group of West Texas and southeast New Mexico: Soc. Econ. Paleontologists Mineralogists, Permian Basin Section, Pub. 79-18, p. 142-152.

Dahl, H.M., 1965, Clay mineralogy of some Permian bentonites from the Delaware basin area, Texas: Am. Mineralogist, v. 50, p. 1637-1646.

Dickinson, W.R., 1981, unpublished research: University of Arizona, Dept. of Geosciences, Tucson.

Dickinson, W.R., and C.A. Suczek, 1979, Plate tectonics and sandstone compositions: Am. Assoc. Petroleum Geologists Bull., v. 64, p. 2164-2182.

Dodge, C.F., 1958, Delaware basin: what traps its oil?: Petroleum Engineer, v. 30, p. B48-B52.

Dunoyer de Segonzac, G., 1970, The transformation of clay minerals during diagenesis and low-grade metamorphism: a review: Sedimentology, v. 15, p. 281-346.

Elam, J.G., 1972, Tectonic style in the Permian basin and its relationship to cyclicity, in Cyclic

sedimentation in the Permian basin, (2nd ed.): West Texas Geol. Soc., Pub. 72-60, p. 55-80.

Faber, J.A., 1980, Submarine channel sands of the Cherry Canyon Formation, Delaware basin, West Texas: unpublished report, Mobil Producing Texas and New Mexico, Houston Exploration Division, 10 p.

Folk, R.L., 1974, Petrology of sedimentary rocks: Hemphill Pub. Co., Austin, 182 p.

Foscolos, R.E., and T.G. Powell, 1979, Categenesis in shales and occurrence of authigenic clays in sandstones, North Sabine, H-49 well, Canadian Artic islands: Canadian Jour. Earth Sci., v. 16, p. 1309-1314.

Friedman, G.M., 1958, Determination of sieve-size distribution from thin section data for sedimentary petrological studies: Jour. Geology, v. 66, p. 394-416.

Grauten, W.F., 1965, Fluid relationships in Delaware Mountain Sandstones, in Fluids in subsurface environments: Am. Assoc. Petroleum Geologists Mem. 4, p. 294-307.

Griffin, G.M., 1971, Interpretation of x-ray diffraction data, in Carver, R.E., ed., Procedures in sedimentary petrology: Wiley-Interscience, New York, p. 552-554.

Harms, J.C., 1974, Brushy Canyon Formation, Texas: a deep-water density current deposit: Geol. Soc. America Bull., v. 85, p. 1763-1784.

Harrison, S.C., 1966, Depositional mechanics of Cherry Canyon sandstone tongue: unpublished master's thesis, Texas Tech. Univ., 114 p.

Hayes, J.B., 1970, Polytypism of chlorite in sedimentary rocks: Clays Clay Minerals, v. 18, p. 285-306.

Hayes, P.T., 1964, Geology of the Guadalupe Mountains, New Mexico: U.S. Geological Survey Professional Paper 446, 69 p.

Heald, M.T., and R.E. Larese, 1974, Influence of coatings on quartz cementation: Jour. Sed. Petrology, v. 44, p. 1269-1274.

Hills, J.M., 1972, Late Paleozoic sedimentation in West Texas Permian basin: Am. Assoc. Petroleum Geologists Bull., v. 56, p. 2303-2322.

Horak, R.L., 1975, Tectonic relationship of the Permian basin to the Basin and Range province, in Exploration from the mountains to the basin: El Paso Geol. Soc. Field Guidebook 9, p. 61-94.

Hull, J.P.D., Jr., 1957, Petrogenesis of Permian Delaware Mountain Sandstone, Texas and New Mexico: Am. Assoc. Petroleum Geologists Bull., v. 41, p. 278-307.

Jacka, A.D., R.H. Beck, L.C. St. Germaine and S.C. Harrison, 1968, Permian deep-sea fans of the Delaware Mountian Group (Guadalupian), Delaware basin, in Guadalupian facies, Apache Mountain area, West Texas: Soc. Econ. Paleontologists Mineralogists, Permian Basin Section, Pub. 68-11, p. 49-90.

Jenkins, R.E., 1961, Characteristics of the Delaware Formation: Trans. Soc. Petrol. Engineers, AIME, v. 222, p. 1230-1236.

Jones, C.L., 1954, The occurrence and distribution of potassium minerals in southeastern New Mexico, in Guidebook of southeastern New Mexico: New Mexico Geol. Soc. Field Guidebook 5, p. 107-112.

Kerr, S.D., and A. Thomson, 1963, Origin of nodular and bedded anhydrite in Permian shelf sediments, Texas and New Mexico: Am. Assoc. Petroleum Geologists Bull., v. 47, p. 1726-1732.

King, P.B., 1934, Permian stratigraphy of Trans-pecos Texas: Geol. Soc. America Bull., v. 45, p. 697-798.

_____, 1942, Permian of West Texas and southeastern New Mexico: Am. Assoc. Petroleum Geologists Bull., v. 26, p. 535-763.

_____, 1948, Geology of the southern Guadalupe Mountains, Texas: U.S. Geological Survey Professional Paper 215, 183 p.

_____, 1965, Geology of the Sierra Diablo region, Texas: U.S. Geological Survey Professional Paper 480, 185 p.

_____, 1977, Tectonics and sedimentation of the Paleozoic rocks in the Marathon region, in Tectonics and Paleozoic facies of the Marathon geosyncline: Soc. Econ. Paleontologists Mineralogists, Permian Basin Section, Pub. 78-17, p. 5-37.

Kirkland, D.W., 1980, oral communication: Mobil Oil Corp., Research and Development Division, Dallas.

Kubler, B., 1962, Sur quelques interstratifies irreguliers mica-montmorillonite: Bull. Serv. Carte Geol. Als. Lorr., v. 14, p. 173-178.

LeRoy, L.W., and D.O. LeRoy, eds., 1977, Subsurface geology, (4th ed.): Colorado School of Mines, Golden, 941 p.

Levinson, A.A., 1955, Studies in the mica group: polymorphism among illite and hydrous micas: Am. Mineralogist, v. 40, p. 41-49.

Lucas, J., 1963, La transformation des mineraux argileux dans la sedimentation. Etudes sur les argiles du Trias: Mem. Carte Geol. Als. Lorr., v. 23, 202 p.

McBride, R.F., 1963, A classification of common sandstones: Jour. Sed. Petrology, v. 33, p. 644-669.

McGlasson, E.H., and W.L. Haseltine, 1971, Coyanosa gas field, Delaware basin, West Texas: unpublished report, Mobil Oil Corp., Houston Exploration and Production Division, 82 p.

McKee, E.D., S.S. Oriel, and others, 1967, Paleotectonic investigations of the Permian system in the United States: U.S. Geological Survey Professional Paper 515, 271 p.

McNeal, R.P. and T.D. Mooney, 1968, Relationships of oil composition and stratigraphy of Delaware reservoirs, in Basins of the southwest, vol. II: North Texas Geol. Soc., p. 68-75.

Marshall, W.S., 1954, Varve-like laminations in the Permian Bone Spring Limestone of western Texas: unpublished master's thesis, Columbia Univ., 48 p.

Meissner, F.F., 1972, Cyclic sedimentation in Middle Permian strata of the Permian basin, West Texas and New Mexico, in Cyclic sedimentation in the Permian

basin, (2nd ed.): West Texas Geol. Soc. Pub. 72-60, p. 203-232.

Montgomery, S., 1981, written comm.: Mobil Producing Texas and New Mexico, Midland Production Division.

Motts, W.S., 1972, Geology and paleoenvironments of the northern segment, Capitan shelf, New Mexico and West Texas: Geol. Soc. America Bull., v. 83, p. 701-722.

Nagtegaal, P.J.C., 1979, Relationship of facies and reservoir quality in Rotliegendes desert sandstones, southern North Sea region: Jour. Petroleum Geol., v. 2, p. 145-158.

Newell, N.D., and others, 1953, The Permian reef complex of the Guadalupe Mountains region, Texas and New Mexico: W.H. Freeman, San Francisco, 236 p.

Nottingham, M.W., 1960, Recent Bell Canyon exploration in the north Delaware basin (New Mexico-Texas): Southwestern Federation Geol. Socs. Trans., v. 1, p. 139-153.

Oriel, S.S., D.A. Myers, and E.J. Crosby, 1967, West Texas Permian basin region, in Paleotectonic investigations of the Permian System in the United States: U.S. Geological Survey Professional Paper 515, p. 21-64.

Payne, M.W., 1976, Basinal sandstone facies, Delaware basin, West Texas and southeast New Mexico: Am. Assoc. Petroleum Geologists Bull., v. 60, p. 517-527.

Perry, E.A., and J. Hower, 1972, Late-stage dehydration in deeply buried pelitic sediments: Am. Assoc. Petroleum Geologists Bull., v. 56, p. 2013-2021.

Pittman, E.D., and D.N. Lumsden, 1967, Relationship between chlorite coatings on quartz grains and porosity, Spiro Sand, Oklahoma: Jour. Sed. Petrology, v. 38, p. 668-671.

Randerson, L.W., 1980 written comm.: Mobil Producing Texas and New Mexico, Midland Production Division.

Richardson, G.B., 1904, Report of a reconnaissance in Trans-Pecos Texas north of the Texas and Pacific Railway: Univ. Texas Bull., v. 23, p. 38-45.

Sarkisan, S.G., 1972, Origin of authigenic clay minerals and their significance in petroleum geology: Sedimentary Geol., v. 7, p. 1-22.

Schoen, R., 1962, Semi-quantitative analysis of chlorites by x-ray diffraction: Am. Mineralogist, v. 47, p. 1384-1392.

Seemann, U., 1979, Diagenetically formed interstitial clay minerals as a factor in Rotliegend sandstone reservoir quality in the Dutch sector of the North Sea: Jour. Petroleum Geol., v. 1., p. 55-62.

Silver, B.A., and R.G. Todd, 1969, Permian cyclic strata, northern Midland and Delaware basins, West Texas and southeastern New Mexico: Am. Assoc. Petroleum Geologists Bull., v. 53, p. 2223-2251.

St. Germaine, L.C., 1966, Depositional dynamics of the Brushy Canyon Formation, Delaware basin, Texas: unpublished master's thesis, Texas Tech. Univ., 119 p.

Thoraz, J., 1976, Practical identification of clay minerals: a handbook for teachers and students in clay mineralogy, (G. Lelotte, ed.): Dison, Belgique, 90 p.

Vertrees, C.D., and others, 1964, Cross-section through Delaware and Val Verde basins from Lea County, New Mexico to Edwards County, Texas: West Texas Geol. Soc. Pub. 64-49.

Walper, J.L., 1976, Paleozoic tectonics of the southern margin of North America: Gulf Coast Assoc. Geol., Socs. Trans., 24th Ann. Conf. Proc., p. 230-241.

Watson, W.G., 1974, Inhomogeneities of the Ramsey Member of the Permian Bell Canyon Formation, Geraldine Ford Field, Culberson and Reeves Counties, Texas: unpublished master's thesis, Univ. of Texas, Arlington, 122 p.

White, J.L., 1962, X-ray diffraction studies on weathering of muscovite: Soil Sci., v. 93, p. 16-21.

Williamson, C.R., 1978, Depositional processes, diagenesis and reservoir properties of Permian deep-sea sandstones, Bell Canyon Formation, Texas - New Mexico: doctoral dissertation, Univ. of Texas, Austin, 276 p.

Wilson, M.D., and E.D. Pittman, 1977, Authigenic clays in sandstones: recognition and influence on reservoir properties and paleoenvironmental analysis: Jour. Sed. Petrology, v. 47, p. 3-31.